

**UNIVERSIDAD AUSTRAL DE CHILE**  
**FACULTAD DE CIENCIAS AGRARIAS**  
**ESCUELA DE INGENIERÍA EN ALIMENTOS**

Impacto de campos de pulsos eléctricos en enzimas y  
microorganismos - Rol del campo eléctrico y efectos térmicos  
acoplados, considerando la geometría de la cámara de tratamientos

Tesis presentada como parte de los  
requisitos para optar al grado de  
Licenciado en Ciencia de los Alimentos

**Nicolás Ismael Meneses Villalobos**

VALDIVIA - CHILE

2008

**Technischen Universität Berlin**

Fakultät III – Prozesswissenschaften  
Institut für Lebensmitteltechnologie und  
Lebensmittelchemie  
Fachgebiet Lebensmittelbiotechnologie  
und -prozesstechnik

**Universidad Austral de Chile**

Facultad de Ciencias Agrarias  
Escuela de Ingeniería en Alimentos

Impact of Pulsed Electric Fields on Enzymes and Microorganisms –  
role of electric field and coupled thermal effects with consideration of  
treatment chamber geometry

Prerequisite for the obtention of the  
academic degree of *Licenciado en  
Ciencia de los Alimentos*

Presented by:

**NICOLÁS ISMAEL MENESES VILLALOBOS**

Matr.-Nr. 312104 (TUB)

Berlin - Germany

Rol: 02053080 (UACH)

Valdivia - Chile

Berlin, den 25.2.2008

## **PROLOGE**

The present work, "Impact of Pulsed Electric Fields on Enzymes and Microorganisms – Role of Electric Field and Coupled Thermal Effects with Consideration of Treatment Chamber Geometry" was conducted entirely at Berlin University of Technology, Faculty III, School of Process Sciences and Engineering, Department of Food Biotechnology and Food Process Engineering under the supervision and responsibility of Prof. Dr. Dipl.-Ing. Dietrich Knorr. Experimental works were performed as of May 2007 to February 2008 under the assistance of research associate Mr. Henry Jäger.

The thesis is being presented by Nicolás Ismael Meneses Villalobos to the "Escuela de Ingeniería en Alimentos, Facultad de Ciencias Agrarias, Universidad Austral de Chile", as a prerequisite for the obtention of the academic degree "Licenciado en Ciencias de los Alimentos". For such purpose, Prof. Dr.-Ing. Kong Shun Ah-Hen and Prof. Erwin Carrasco acted as "Profesor Patrocinante" and "Profesor Informante" respectively, in accordance to the rules for submission of thesis at the "Universidad Austral de Chile".

**PROFESSOR SUPERVISOR UNIVERSIDAD AUSTRAL DE CHILE:**

Prof. Dr.-Ing. Kong Shun Ah-Hen .....  
Ingeniero en Alimentos, Dipl.-Ing., Dr.-Ing.  
Instituto de Ciencia y Tecnología de los Alimentos  
Universidad Austral de Chile

**PROFESSOR SUPERVISOR BERLIN UNIVERSITY OF TECHNOLOGY:**

Prof. Dr. Dietrich Knorr .....  
Food Technology Engineer, Dipl.-Ing., Dr.rer.nat.techn.  
Institute of Food Technology and Food Chemistry  
Berlin University of Technology

**PROFESSOR CO-SUPERVISOR UNIVERSIDAD AUSTRAL DE CHILE:**

Prof. Erwin Carrasco Ruiz .....  
Ingeniero Civil Químico  
Instituto de Ciencia y Tecnología de los Alimentos  
Universidad Austral de Chile

## **ACKNOWLEDGEMENTS**

I would like to express my sincere thanks to:

Prof. Dr. Dietrich Knorr, for putting into disposition the thesis theme and for his interest during the work.

Henry Jaeger, who was my thesis tutor, I thank him for his engagement, his great disposition and technical assistance during the work, which made my interest on this theme to grow.

Jeldrik Moritz, Nikolay and Antje for giving me opportunity for constructive discussions about my work during realization of the thesis.

I express my sincere thanks to all the former mates, workers and technicians of the Department of Food Process Engineering and Food Biotechnology of the Berlin University of Technology for creating the best working environment and providing a very agreeable atmosphere during my stay.

To my School director Prof. Marcia Costa for his great interest and guidance, Prof. Dr. Kong Shun and Prof. Carrasco for their interest and being my supervisor professors at the Universidad Austral de Chile. I like to show my appreciation to the Faculty of Agrarian Science, to the Institute of Science of Food and Technologie of the Universidad Austral de Chile and DAAD for their financial support during my stay.

Very affectionate and special thanks to my grandmother Teotista Villar, my family and Lucía for their support and confidence.

## INDEX

<b>Chapter</b>	<b>Page</b>
PROLOGUE	3
ACKNOWLEDGEMENTS	5
LISTE OF FIGURES	9
LIST OF TABLES	15
NOMENCLATURE	17
1 Introduction and Objective of the Work	21
2 Literature Review	23
2.1 PEF Equipment	23
2.1.2 High voltage repetitive pulser	23
2.1.2.1 Power supply	24
2.1.2.2 Capacitor	25
2.1.2.3 Switch	25
2.1.3 Treatment chamber	26
2.1.3.1 Parallel plate treatment chamber	28
2.1.3.2 Coaxial treatment chamber	28
2.1.3.3 Co- field treatment chamber	29
2.2 Processing Parameters	30
2.2.1 Electric field strength	30
2.2.2 Specific energy	33
2.2.3 Treatment temperature	34
2.2.3 Treatment time and frequency	35
2.2.4 Pulse geometry and pulse width	36
2.3 Product Factor	38
2.3.1 Conductivity, medium ionic strength and components	38
2.3.2 pH	39
2.3.3 Bubbles, presence of particles	40

2.4.1	Type of microorganisms	41
2.4.2	Growth phase	42
2.5	Mechanism of microbial inactivation	43
2.5.1	Kinetic models	47
2.6	Enzyme inactivation	47
2.6.1	Milk alkaline phosphatase inactivation	48
2.7	Electrochemical reactions	51
2.8	Mathematical modeling	52
3	Material and Methods	54
3.1	Experiment Equipment	55
3.1.1	PEF equipment	55
3.2.1.1	Rectangular pulse modulator in a continuous system	56
3.2.1.2	Exponential decay micro- pulse modulator in a batch system	56
3.2.1.3	Treatment chamber	58
3.2.2	Tempering equipment	60
3.2	Product and Microorganisms	60
3.3	Experimental Procedure	62
3.3.1	PEF treatment	62
3.3.1.1	Experiment to analyze the effect of PEF treatment on milk alkaline phosphatase	63
3.3.1.2	Experiment to determine the effect of the insulator geometry and the velocity effect on the microbiological inactivation	64
3.3.1.3	Experiment to determine the temperature distribution inside the treatment chamber and in the spiral heat exchangers	64
3.3.2	Thermal enzymatic inactivation by glass capillary method	67
3.4	Microbial Analysis	68
3.5	Determination of Phosphatase Activity in Milk	69
3.6	Computer Modeling	70
3.6.1	Required software	70
3.6.2	Governing equations	70

3.6.2.1	Fluid flow	70
3.6.2.2	Temperature field	73
3.6.2.3	Electric potential	74
3.6.3	Geometrics models and mesh	74
3.6.4	Boundary conditions	75
4	Result and Discussion	78
4.1	Enzyme Inactivation	78
4.1.1	Impact of PEF Treatment on Phosphatase Activity	79
4.1.1.1	Effect of electric field strength	80
4.1.1.2	Effect of energy input	81
4.1.1.3	Effect of pulse shape	84
4.1.1.4	Effect of temperature	86
4.1.2	Temperature – time profile of Milk in PEF Equipment	89
4.1.2	Thermal Inactivation of Phosphatase	93
3.1.4	Comparison between PEF and Thermal – effect in Phosphatase inactivation	96
4.2	Effect of chamber geometry in PEF treatments	98
4.2.1	Treatment chamber geometry	99
4.2.2	Effect of insulator geometry on the electric field strength	100
4.2.3	Effect of insulator geometry on the microbiological inactivation	101
4.2.4	Effect of pulse frequency on the microbiological inactivation in G1 and G2	104
4.2.5	Flow velocity in treatment chambers	109
4.2.5.1	Experimental velocity limitations	110
4.2.5.2	Velocity profile in the treatment chamber	111
4.2.5.3	Effect of the flow velocity on the microbiological inactivation	114
4.1.6	Homogenous PEF treatment	119
4.1.6.1	Insertion of devices in the treatment chamber	120
4.1.6.2	Impact on microbial inactivation due to the insertion of grids in the treatment chamber	124

4.1.6.3	Impact on enzyme inactivation due to the insertion of grids in the treatment chamber	129
4.1.7	Temperature distribution in the PEF treatment chamber	130
5	Conclusions and Outlook	136
	SUMMARY	138
	REFERENCES	140

## LISTE OF FIGURES

Figure		Page
2.1	High voltage pulse generator system	23
2.2	Block schematic of pulse modulator	24
2.3	Square wave pulses generator system	26
2.4	Configurations of treatment chambers for continuous PEF-treatment; (a) parallel plate, (b) coaxial and (c) co-linear configuration	30
2.5	Temperature-time-profile of a suggested PEF-treatment of apple juice at an initial treatment temperature of 55° C, and a specific energy input of 40kJ/kg compared to a HTST treatment 85°C, 30 s	35
2.6	Exponential and square shape pulses	37
2.7	A cell-size comparison	42
2.8	Cells of E coli harvested at different growth stages suspended in SMUF and subjected to an electric field of 36 KV/cm at 7°C	43
2.9	Surface polarization of a cell in presence of an electric field	45

2.10	Hydrophobic and hydrophilic pore	46
2.11	Effect of pH on the stability of milk. Milk held at indicated pH values for one hour (A) and two hours (B)	45
2.12	Scheme of coupling between the electrical and fluid analyses	52
2.13	Scheme to resolve a problem with software of FVM or FEM	53
3.1	Left; Pulse modulator (A) and oscilloscope (B). Right: Food Tank (C), pump (D), heating (E), treatment chamber (F), and cooling (G) and thermometer (H)	56
3.2	Micro-pulse modulator for batch system	57
3.3	Right: vertical adjustment of the electrodes. Left: field strength profile	58
3.4	Right: Electroporation cuvette. Left: Distribution of electrical field	59
3.5	Glass capillary	67
3.6	Phenol from disodium phenyl phosphate	69
3.7	Spiral geometry and mesh	74
3.8	Treatment chamber and mesh	75
4.1	Variation of ALP activity expressed as [ $\mu\text{g phenol/ ml}$ ] in raw and pasteurized milk and variation in the raw milk composition	78
4.2	ALP inactivation in function of the electric field strength and energy input	80
4.3	Inactivation in function of the energy input	82
4.4	Impact of the energy input on ALP activity	84
4.5	Effect of pulse form on the inactivation of ALP	85
4.6	Pulse number per volume in treatment zone. For a mass flow	

	of 5 kg/h and conductivity media of 4.6 mS/cm	87
4.7	Impact of the temperature treatment on the ALP activity	88
4.8	Temperature – time diagram in PEF system	89
4.9	Temperature contours for the spirally heat exchanger	91
4.10	Thermal inactivation of ALP in raw milk at different temperatures and residence time determined using a glass capillary method	94
4.11	Inactivation rate constant $k$ of thermal ALP inactivation in milk dependent on temperature (left). Inactivation of ALP dependent on temperature-time (right)	95
4.12	Diagram temperature-time during the PEF treatment (left). The figure (right) shows the phosphatase inactivation according to the temperature- time presented in the diagram of left side. This example was performed with an inlet temperature of 23 °C, energy input of 120 kJ/kg, energy per pulse of 4,1 J and a frequency of 35 Hz	96
4.13	Simulation of thermal phosphatase inactivation and PEF treatment and PEF treatment minus the thermal inactivation	98
4.14	Electric field strength distribution in treatment chamber with insulators with rounded edges, denominated G1	99
4.15	Electric field distribution in treatment chamber with convex insulators, denominated G2	100
4.16	Surface diagram of the electric field strength in treatment chamber G1	100
4.17	Surface diagram of the electric field strength in treatment chamber G2	101

4.18	Inactivation of <i>Lactobacillus rhamnosus</i> in Ringer solution adjusted at a conductivity of 4.7 mS/cm in G1 and G2 geometries	102
4.19	Inactivation of <i>Escherichia coli</i> in Ringer solution adjusted at conductivity of 4.7 mS/cm in G1 and G2 geometries	103
4.20	Needed frequency and energy input in a liquid of 2.4 and 4.7 mS/cm	104
4.21	Frequency Histogram in the G1 chamber (a) and G2 chamber (b)	105
4.22	Histogram of accumulative percent for G1 and G2	106
4.23	Inactivation rates of <i>Lactobacillus rhamnosus</i> by PEF treatment in Ringer solution at 2.3 mS/cm with a flow rate of 4.9 l/h	107
4.24	Inactivation rates of <i>Escherichia coli</i> by PEF treatment in Ringer solution at 2.3 mS/cm with a flow rate of 4.9 l/h	108
4.25	Inactivation of <i>Lactobacillus rhamnosus</i> by PEF treatment in Ringer solution at 2.3 and 4.7 mS/cm with a flow rate of 4.9 l/h. Geometry G1 was used	109
4.26	Velocity profile on the center line of the treatment chamber G1 at a flow rate of 20 l/h	111
4.27	Velocity profile on the center line of the treatment chamber G2 at a flow rate of 20 l/h	112
4.28	Zone of the treatment chamber where the intensity turbulence is computationally estimated	113
4.29	Turbulence Intensity in insulator zone for geometries G1 and G2 at a flow rate of 20 l/h and a Reynolds number of 1763	113
4.30	Comparison of turbulence intensity generated in the insulator	

	zone at 3, 10 and 20 l/h in G2 geometry	114
4.31	Inactivation of <i>Escherichia coli</i> in G1 geometry at 3, 10 and 20 l/h in Ringer solution adjusted at 4.65 mS/cm and inlet temperature of 30°C	115
4.32	Inactivation of <i>Escherichia coli</i> in G2 geometry at 3, 10 and 20 l/h in Ringer solution adjusted at 4.65 mS/cm and inlet temperature of 30°C	116
4.33	Inactivation of <i>Lactobacillus rhamnosus</i> in G1 and G2 geometries at 4.9 and 16 l/h, using Ringer solution adjusted at 2.3 mS/cm	117
4.34	Inactivation of <i>Escherichia coli</i> in geometry G2 at 3 and 10 l/h utilizing Ringer solutions adjusted at 2.3 and 4.7 mS/cm a inlet temperature of 30°C	118
4.35	Grid dimensions and location for models A and B	121
4.36	Comparison of the electric field strength on center line of insulator zone for the three models and the treatment chamber without grid	121
4.37	Comparison between the electric field strength generated in the case C (right) and an insulator without grid (left)	122
4.38	Turbulence intensity in the center of the insulator zone for the model B in comparison to a treatment chamber without grid	123
4.39	Electric field strength in treatment chamber for model A; insulator grid	124
4.40	Impact of grids on the inactivation of <i>E. coli</i> in ringer solution at 2.3 mS/cm in comparison to a treatment chamber without grid	125
4.41	Inactivation of <i>E.coli</i> using a treatment chamber with four	

	inserted grids in comparison with a treatment chamber without grid. Initial voltage of 15 (a) and 18 (b) kV. Ringer solution at 2.3 mS/cm at a inlet temperature of 30°C	127
4.42	Inactivation of <i>L. rhamnosus</i> using a treatment chamber with four inserted grids in comparison to a treatment chamber without grid. Initial voltage of 15 (a) and 18 (b) kV. Ringer solution at 2.3 mS/cm and inlet temperature 20°C	128
4.43	Impact of the grids insertion on the enzyme inactivation Experiment performed in row milk with a temperature inlet of 30°C	130
4.44	Electrical conductivity as function of the temperature	131
4.45	Temperature increment as function of the frequency and conductivity. Average temperature measured 3.5 cm after the 2 <sup>nd</sup> insulator	132
4.46	Temperatures as function of radial coordinate at 3.5 cm after the 2 <sup>nd</sup> insulator. Experiment with an initial voltage of 18 kV and a conductivity of 4.62 mS/cm as function of the temperature	133
4.47	Position of thermometer in treatment chamber	134
4.48	Temperature contour along the 2 <sup>nd</sup> insulator. Experiment with an initial voltage of 18 kV, frequency of 32 Hz and a conductivity (T) of 4.6 mS/cm	134
4.49	Temperature contour along the 2 <sup>nd</sup> insulator of the treatment chamber with inserted grids. Experiment with an initial voltage of 18 kV, frequency of 32 Hz and a conductivity (T) of 4.6 mS/cm	135

## LIST OF TABLES

Table		Page
2.1	Possible electrochemical reactions at the electrode/media interface and its respective problem in the PEF treatment (adapted from Toepfel 2002)	51
3.1	Range of the used parameters in the PEF treatments	62
3.2	Boundary conditions according to FLUENT and COMSOL	76
4.1	Parameters used to study the effect of electric field on ALP	80
4.2	Parameter used to study the impact of energy input on ALP	81
4.3	Parameter used to study the impact of BACTH system on ALP	83
4.4	Parameters used for batch and continuous system to study the effect on ALP activity	85
4.5	Parameter used to study the effect of the temperature on ALP activity	87
4.6	Parameters for heat exchanger (heating)	90
4.7	Parameters for heat exchanger (cooling)	92
4.8	Experimental and modeled temperatures and the prediction error	93
4.9	Parameters used to study the temperature and PEF effect on ALP	97
4.10	Parameters used to study the effect on G1 and G2 at 4.7 mS/cm on <i>Lactobacillus rhamnosus</i>	102
4.11	Parameters used to study the effect of G1 and G2 at 4.7	

	mS/cm on <i>Escherichia coli</i>	103
4.12	Parameters used to study the effect of G1 and G2 at 2.3 mS/cm on <i>Lactobacillus rhamnosus</i>	106
4.13	Parameters used to study the effect of G1 and G2 at 2.3 mS/cm on <i>Escherichia coli</i>	107
4.14	Parameters used to study the difference between 4.7 and 2.3 mS/cm on <i>Lactobacillus rhamnosus</i> using the G1 geometry	108
4.15	Parameters used to study the effect of flow velocity at 4.65 mS/cm on <i>Escherichia coli</i> using the G1 geometry	115
4.16	Parameters used to study the effect of flow velocity at 4.65 mS/cm on <i>Escherichia coli</i> using the G2 geometry	116
4.17	Parameters used to study the effect of flow velocity at 2.3 mS/cm on <i>Lactobacillus rhamnosus</i> using the geometries G1 and G2	117
4.18	Parameters used to study the effect of flow velocity at 2.3 and 4.7 mS/cm on <i>Escherichia coli</i> using the geometries G1 and G2	118
4.19	Average electric field strength	122
4.20	Parameter used study the impact of grids on <i>E. coli</i> using G1 and G2 at 2.3 mS/cm	125
4.21	Parameter used for a treatment chamber with four inserted grids in comparison with a treatment chamber without grid	126
4.22	Parameter used for a treatment chamber with four inserted grids in comparison with a treatment chamber without grid	128
4.23	Parameter used for a treatment chamber with four inserted grids, two insulator grids and a treatment chamber without grid	129

## NOMENCLATURE

A	heat transfer area ( $\text{m}^2$ )
ALP	alkaline phosphatase
C	capacity of the capacitor (F)
CAD	Computer Aided Design
CFD	Computational Fluid Dynamics
Cp	food heat capacity ( $\text{kJ kg}^{-1} \text{K}^{-1}$ )
$d$	interelectrode gap (m)
$\Delta T$	temperature increase ( $^{\circ}\text{C}$ )
$\Delta T_{\log}$	logarithmic temperature difference
D	flow rate ( $\text{m}^3\text{s}^{-1}$ )
DC	direct current
$D_e$	electrode diameter (m)
$D_i$	insulator diameter (m)
E	Electric field strength (V/m)
$E_{\text{aveg}}$	average electric field strength ( $\text{V cm}^{-1}$ )
$E_c$	critical electric field strength (V/m)
$E_i$	electric field strength in a volume element $V_i$
$E_{\text{SD}}$	electric field strength standard deviation
$f$	frequency (Hz)
$f_s$	shape factor for ellipsoidal cells
FEM	Finite Element Method
FVM	Finite Volume Method
g	shape factor for co-linear treatment chamber ( $\text{cm}^{-1}$ )
G	rate of generation of TKE
G1	treatment chamber geometry 1

G2	treatment chamber Geometry 2
HTST	High Temperature Short Time
HV	High Voltage
I	current (A)
IGBT	Insulated Gate Bipolar Transistor
L	inductor
$L_s$	cell length (m)
m	mass (kg)
$\dot{m}$	mass flow (kg/s)
n	pulse number
p	pressure ( $\text{kg m}^{-2}$ )
PEF	Pulsed Electric Field
Q	electrical charge (C)
$Q_j$	source of heat (W)
r	diameter where E is measured (m)
$R_0$	radius of the inner electrode surface (m)
$R_a$	treatment chamber resistance ( $\Omega$ )
$R_c$	resistance charge ( $\Omega$ )
Re	Reynolds number
$R_i$	radius of the outer electrode surface (m)
RelA	Relative enzyme activity ( $A/A_0$ )
RSM	Reynolds Stress Model
s	survival rate of microorganisms
S	available area for current flow ( $\text{m}^2$ )
SIMPLE	Semi-Implicit Method for Pressure-Linked Equations
t	pulsed electric field treatment time ( $\mu\text{s}$ )
$t_{\text{res}}$	residence time within the insulators (s)
$t_c$	pulsed electric field critical treatment time ( $\mu\text{s}$ )
T	temperature ( $^{\circ}\text{C}$ )
$T_{\infty}$	medium temperature ( $^{\circ}\text{C}$ )

$T_{in}$	temperature inflow ( $^{\circ}\text{C}$ )
TKE	Turbulence Kinetic Energy
$T_{out}$	temperature outflow ( $^{\circ}\text{C}$ )
TS	dry matter
TMP	transmembrane potential (V)
U	voltage (V)
$V_0$	Voltage supply (V)
$U_c$	maximum transmembrane potential (V)
$V_{gap}$	total volume of the treatment chamber ( $\text{cm}^3$ )
$V_i$	volume element of the treatment chamber ( $\text{cm}^3$ )
$W_{pulse}$	energy per pulse (J/pulse)
$W_{specific}$	specific energy input (kJ/kg)
$x_f$	fat content (%) in milk

## GREEK SYMBOLS

$\alpha_c$	orientation angle of the cell with respect to the electric field
$\delta_{ij}$	Kronecker's delta.
$\epsilon$	dielectric constant
$\epsilon_D$	dissipation rate
$\lambda$	milk thermal conductivity ( $\text{kJ kg}^{-1}\text{K}^{-1}$ )
$u_i$	velocity vector
$\mu_t$	turbulent eddy viscosity
$\eta_M$	milk viscosity ( $\text{kg m}^{-1}\text{s}^{-1}$ )
$\vec{\pi}$	viscous stress tensor
$\rho$	fluid density ( $\text{kg m}^{-3}$ )

$\rho_a$	food electrical resistivity ( $\Omega\text{m}$ )
$\rho_M$	milk density ( $\text{kg m}^{-3}$ )
$\sigma$	media conductivity ( $\text{S/m}$ )
$\sigma_k$	turbulent Prandtl number
$\tau$	pulse width ( $\mu\text{s}$ )

## 1 Introduction and Objective of the Work

The most commonly used method of food preservation today is thermal processing. In spite of achieving good inactivation of microorganisms and enzymes, thermal treatment leads to unwanted reactions in foodstuffs, involving the loss of flavor and nutrients. The increasing consumer demand for minimally processed food with high product safety can only partly be achieved with conventional thermal methods. Hence, the development of non-thermal techniques like pulsed electric fields (PEF) or high hydrostatic pressure has been stimulated (Mertens and Knorr, 1992).

Pulsed electric field (PEF) treatment can be an alternative to traditional thermal processes since it is capable of destroying microorganisms while maintaining fresh-like physical, chemical and nutritional characteristics of food products (Castro *et al.*, 1993, Barbosa-Cánovas *et al.*, 1999).

This processing technology consists of treatment with very short electric pulses (1 – 100  $\mu$ s) at high electric field intensities (10 – 50 kV/cm) at moderate temperatures to affect the integrity of cell membranes by electroporation. (Quin *et al.*, 1996).

The factors that affect microbial inactivation during the PEF treatment are process factors (electric field intensity, pulse width and shape, treatment time and temperature), microbial factors (type, concentration and growth stage of microorganism) and media factors (pH, antimicrobials and ionic compounds, conductivity and medium ionic strength) (Alkhafaiji *et al.*, 2006).

Continuous PEF treatment of liquid foods for microbial inactivation is realized by using treatment chambers for the application of the electric field to the food. This can be more or less effective, depending on treatment chamber design, which makes the latter one of the most important factors. An appropriate

design allows the implementation of a process at industrial scale (high flow rate) and a uniform treatment of food with a minimum increase in temperature.

The overall goal of this work was:

- The improvement of the effectiveness of microbial inactivation and the avoidance of a food over-processing by designing treatment chambers and simulating PEF process using computational tools.

The objectives to achieve the overall goal have been:

- To study the impact of the PEF treatment process parameters and temperature on the activity of heat sensitive milk alkaline phosphatase.
- To analyse the temperature distribution during a PEF treatment.
- To investigate the effect of the insulator geometry on the electric field strength distribution and on the microbial inactivation.
- To study the impact of the treatment flow rate on the microbial inactivation.
- To modify the electric field strength and to generate turbulences of the treated fluid by inserting devices in the treatment chamber.

## 2 Literature Review

### 2.1 PEF Equipment

Treatment of foods by pulsed electric fields (PEF) consists of the application of short duration pulses (1 – 10  $\mu$ s) of high electric field strength (10 – 50 kV/cm) to a food placed between two electrodes. The pulsed electric field can be generated with equipment that includes a number of components, which can be summarized in the following figure, as described in Figure 2.1, according to Barsotti *et al.* (1999a).

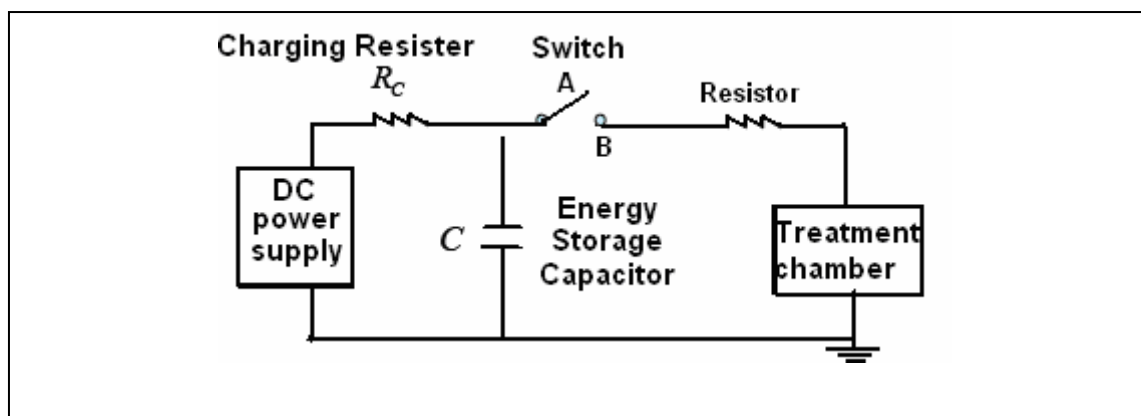


**Figure 2.1** High voltage pulse generator system.

#### 2.1.2 High voltage repetitive pulser

The most important components of a high voltage repetitive pulser include:

- A power supply
- An energy storage element
- A switch

in Figure 2.2 one of the technologies of a Pulse Modulator (or High voltage repetitive pulser) can be seen schematically. The DCPS is the main power source of the system. It converts the 3- phase line voltage to a regulated DC

voltage. It charges up all the IGBT Modules to a primary voltage around 1000V. An external trigger pulse enters the modulator, gating all the IGBT Modules and discharging some of the stored energy. The IGBT's are high power solid-state switches, which can be turned on and off electronically, responding to the trigger pulse. All parts of the modulator are located inside a common enclosure, but only the pulse transformer and the load HV-interface are surrounded by transformer oil. The DCPS, Switching Modules and Control interface are all in air.

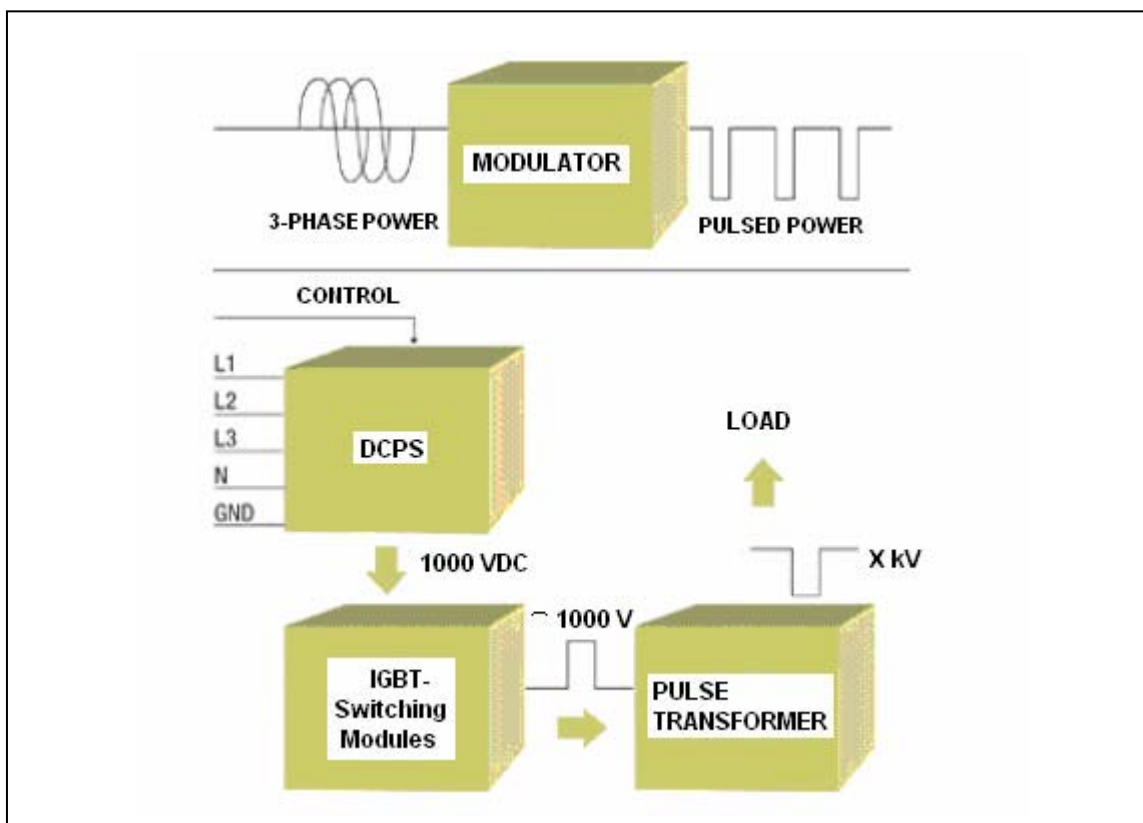


**Figure 2.2** Block schematic of pulse modulator.

### 2.1.2.1 Power supply

Pulsed power refers to the general technology of accumulating energy on a relative long time scale (pulse charging, slow systems) and then compressing

that energy in time and space to deliver large power pulses (pulse discharging, high speed system) to a desired load (Ho and Mittal, 2000).

The accumulation of energy takes place in a capacitor, that's why it is essential to provide it with a power of a determined voltage.

Fast pulsed power machines are characterized by charging time scales around 1  $\mu$ s. Slower charged machines are characterized by charging time scales from 2 to 100  $\mu$ s (Ho and Mittal, 2000).

Once the energy is charged in the capacitor, it must be delivered in the form of high voltage electric pulses with a controllable rate of repetition.

### 2.1.2.2 Capacitor

PEF equipment can have one or more capacitors, connected in parallel, which temporarily store electrical energy. The maximum voltage across the capacitors is equal to that across the generator, and by means of a switch the stored energy is discharged. The capacity of a capacitor is given by:

$$C = \frac{Q}{U} \quad (2.1)$$

Where C is the capacity in Farad, Q is the electrical charge in Coulomb and U the voltage across the capacitor in volts.

### 2.1.2.3 S witch

The major function of the switch is to deliver the energy stored in the capacitor.

When the high voltage switch is in position "b" (Fig 2.1), the capacitor(s) discharge into the treatment chamber, sending an electric pulse through the food sample. This may take less than a microsecond.

A switch is mainly characterized by its switching times, the maximum voltage that it is able to resist, the maximum intensity of current crossing it, and its operative frequency (Pataro, 2004) Furthermore, according to the type of switch, it is possible to produce different kinds of pulse shapes.

. A classification of the switch is that in “on” and “off” switches and those that provide only “on” function. In an electric circuit with an “on” and “off” switch, the partial discharge of a capacitor results in a square-like wave-shape pulses. Only “on” switches are needed for the full discharge of capacitors and pulse – forming networks to generate exponentially decaying pulses, but these type of switches can be also used to generate square wave pulses in a more complex circuit (Barbosa-Cánovas *et al.*, 1999) (see Figure 2.3).

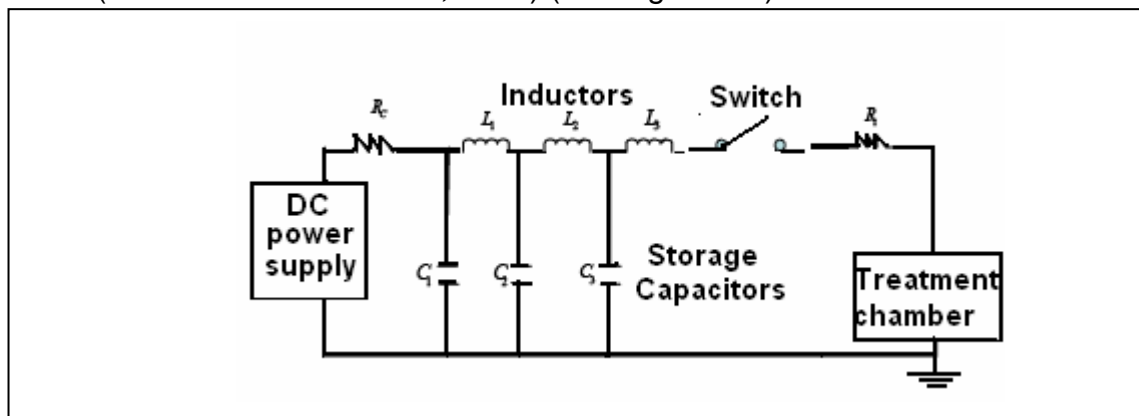


**Figure 2.3** Square wave pulses generator system.

In general, the firing rate (frequency) and the service life (number of pulses) have an inverse relationship with the current and voltage.

In order to protect the switch from a power overload or a dielectric breakdown in the treatment chamber, it is recommended to install a protective resistance between the switch and the treatment chamber.

### 2.1.3 Treatment chamber

The treatment chamber consists of at least two electrodes (made of carbon or metal) one on high voltage (HV) and the other on ground potential (free potential), separated by insulating material in different geometric configurations (Toepfl, 2006).

The high voltage electrode is charged with a voltage between 20 – 40 kV and a current intensity around of 10 – 100 amperes by connecting it with the

capacitor bank. A current thus flows through the liquid food, which is situated in contact between the two electrodes. The voltage is distributed all throughout the volume that covers the treatment chamber. To define the voltage across the treatment chamber, the parameter known as electric field strength,  $E$ , is used and it is measured in volts per unit length (V/m). The electric field strength can be either homogenous or not, depending on the geometry of the electrodes and/or isolators.

Different types of electrode arrangements have been proposed, the most commonly used are: plate – plate (parallel plates), coaxial cylindrical electrodes and co – field configuration. The chamber may be of continuous type (a fluid food flowing through at a flow rate  $D$  in  $\text{m}^3\text{s}^{-1}$ ) or batch type. (Barsotti *et al.*, 1999a)

In chamber design of treatment there are factors that can be controlled regardless of the electrode arrangement and its material. They are:

- the interelectrode gap
- electrode surface

Both factors have a direct impact on the effective resistance of the treatment chamber. In accordance to the following equation, the previously mentioned parameters can related:

$$R_a = \rho_a \cdot \frac{d}{S} \quad (2.2)$$

Where  $R_a$  is the resistance (in  $\Omega$ ) of the treatment chamber  $\rho_a$  is the electrical resistivity (in  $\Omega\text{m}$ ) of the food sample,  $d$  is the interelectrode gap (in m) and  $S$  the available area for current flow (in  $\text{m}^2$ ). The cross sectional area of the food sample is assumed to remain constant in the gap between the two electrodes. (Barsotti *et al.*, 1999a)

### **2.1.3.1 Parallel plate treatment chamber**

Parallel plates are the simplest in design and produce the most uniform distribution of electric field (Jeyamkondan *et al.*, 1999)

The geometry consists of a rectangular duct of insulating material with two limited electrodes on opposite sides. Only the electrode length and distance determine the electric field distribution. The disadvantage of this chamber type is that they have a low resistance. Therefore, they are not appropriate for the use for big quantities of food. This type of geometry is commonly used on a laboratory scale and batch system (Jaeger, 2006).

Plate electrodes with rounded edge can minimize the local increment of the electric field strength and so, the dielectric breakdown event of fluid food.

### **2.1.3.2 Coaxial treatment chamber**

In this chamber design, the food is placed between two cylinders, one internal cylinder as high voltage electrode and an external cylinder that works as a ground. The food is situated inbetween both cylinders.

The electric field is not homogeneous in a chamber of this type, because it is distributed in ascendant order, from the central cylinder towards the external cylinder. One of the major advantages of this type of chambers is that the peaks of local electric field strenght are minimized or eliminated.

Generally, this chamber type is used in a continuous process. The liquid food must flow through the thin gap that exists between the two cylinders, for which reason it is restrained for the work with low flow velocity and with liquid food of a low viscosity. Furthermore, the effective area of the electrodes is very big, causing a low resistance in the chamber, as can be seen in equation 2.2.

### 2.1.3.3 Co- field treatment chamber

This geometry is one of the most utilized recently to operate in continuous systems. Basically this geometry consists of two metal tubes that function as electrodes separated from each other by another tube, whereas the latter is made of insulated material. These three tubes are placed in a vertical position. In these types of chambers the electric field strength is not homogeneous as in the co-axial chambers, and it depends strongly on the insulator geometry that is placed between the two electrodes. By deformations of insulator geometry, it is possible to obtain different electric field strength distributions, which can be modeled with finite element programs. The most common design is a chamber of three electrodes with the same diameter  $D_e$ , one in the center (working as high voltage electrode) and the other two on the sides (working as ground). The central electrode is separated from the other two electrodes by two insulated tubes (one at each side of central electrode) with a diameter  $D_i$ . Usually the diameter  $D_i$  is smaller than the diameter  $D_e$ , therefore it can also obtain appropriate electric field strength distribution, namely more homogeneous. The electric field is located in the volume that is included by the tubes of insulated material of diameter  $D_i$ .

The major advantage presented by this geometry type is the possibility to utilize electrodes with a relatively big diameter in comparison to the interelectrode gap in parallel and co-axial geometries. Therefore the liquid food can flow easily, allowing hence an industrial use. Furthermore, the area where the electric field is generated is small, that means that the resistance of the treatment chamber is higher.

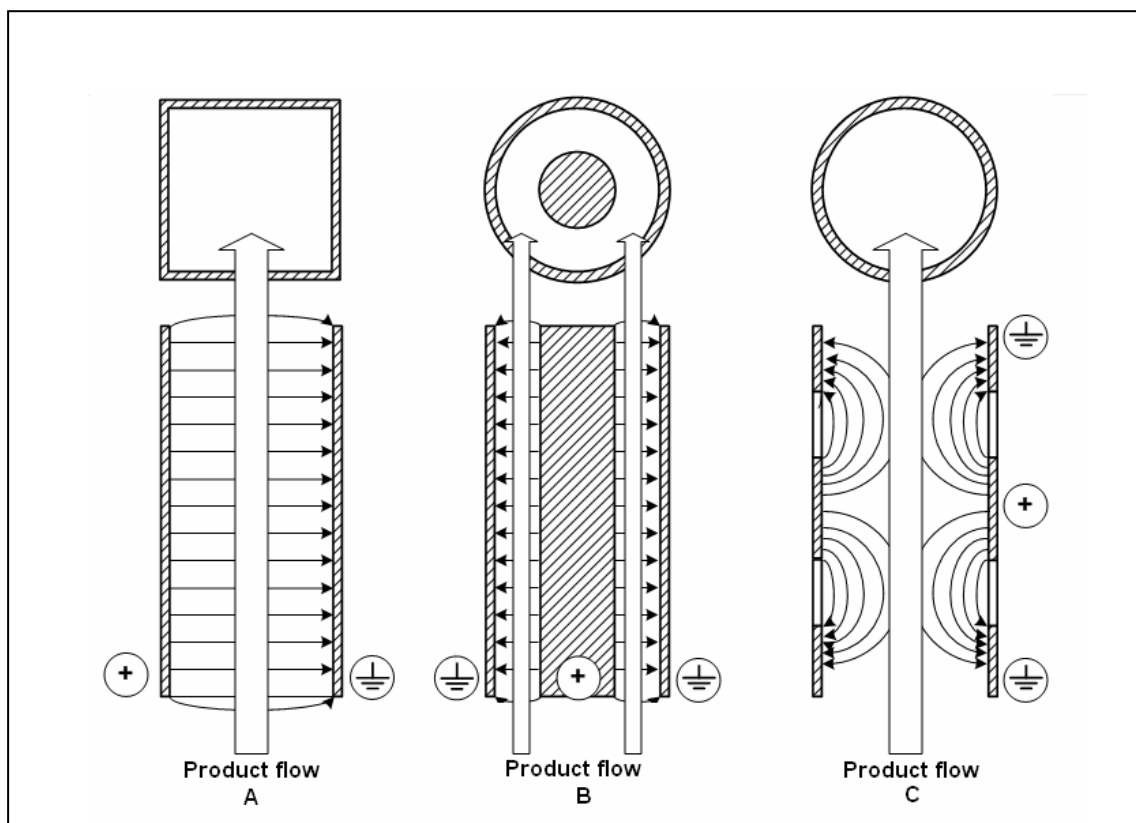


**Figure 2.4** Configurations of treatment chambers for continuous PEF-treatment; (a) parallel plate, (b) coaxial and (c) co-linear configuration.

## 2.2 Processing Parameters

### 2.2.1 Electric field strength

Basically, the electric field strength can be defined as the difference of voltage between two points and is generated in the treatment chamber where the food sample is located.

As described in section 2.4, the microbiological inactivation occurs by electroporation. To generate a cellular membrane damage it is necessary to achieve a critical value of the voltage, which is between 4.7 – 14.2 kV/cm for many microorganisms (Grahl & Märkl, 1996). The local electric field strength variations in the treatment chamber must be avoided in order to prevent

dielectric breakdown of liquid foods due to local increase of the electric field and also to ensure that each cell within the microbial population receives the same treatment (Pataro, 2004)

The electric field strength  $E$  depends on the voltage  $U$ , the geometry of the electrodes and the distance between them. In case of parallel plates the electric field strength is calculated using the following equation (Zhang *et al.*, 1995):

$$E = \frac{U}{d} \quad (2.3)$$

Where  $U$  is the voltage across the electrodes (in V) and  $d$  the interelectrode gap (in m). The uniformity of the electric field is improved by utilizing electrodes with rounded edges.

In case of coaxial geometry the electric field strength is calculated using the following equation:

$$E = \frac{U}{r \ln\left(\frac{R_0}{R_i}\right)} \quad (2.4)$$

Where  $r$  is the radius at which  $E$  is measured,  $R_0$  and  $R_i$  are the radius of the inner and outer electrode surface respectively (Bushnell *et al.*, 1993) The electric field in coaxial chamber is, therefore, not uniform and depends on the location in the chamber. The uniformity of the electric field is improved when the difference between the inner and outer radius of the electrode surfaces is negligible compared to the inner radius,  $(R_0 - R_i) \ll R_i$ .

The electric field strength calculation in treatment chamber with a co-linear geometry is still under discussion. It is possible to obtain an approximation according to the following equation:

$$E_{avg} = U \cdot g \quad (2.5)$$

Where  $g$  (in  $\text{cm}^{-1}$ ) is a shape factor that depend on the chamber geometry (normally this factor is between 1 and 2). The  $g$  factor can be obtained calculating the average electric field strength that is generated in the treatment chamber; this is possible through finite element method.

The average electric field strength can be calculated according to the following equations:

$$E_{aveg} = \frac{1}{V_{gap}} \sum_{i=1}^N E_i \delta V_i \quad (2.6)$$

$$V_{gap} = \sum_{i=1}^N \delta V_i \quad (2.7)$$

Where  $E_{avg}$  is the average field strength,  $E_i$  is the electric field strength in an volume element  $\delta V_i$  and  $V_{gap}$  is the total volume considered.

As previously described, the electric field strength in this type of chambers is not homogeneous, and its uniformity is possible to obtain by changing the insulator geometry until a minimal electric field strength standard deviation is achieved.

The standard deviation  $E_{SD}$  can be obtained according to:

$$E_{SD} = \sqrt{\frac{1}{V_{gap}} \sum_{i=1}^N (E_i - E_{avg})^2 \delta V_i} \quad (2.8)$$

This parameter is very useful when designing this type of chambers , because it gives us an idea of how homogeneous the electric field strength inside the treatment chamber is (Lindgren *et al.*, 2002, Gerlach *et al.*, 2008).

### 2.2.2 Specific energy

In a PEF process, the food, upon receiving an electric pulse, receives a quantity of electric energy that was stored in the capacitors. The electric energy delivered by this pulse can also be measured per kilogram of food. This parameter is called specific energy and it is very useful in describing a PEF process and to compare energy consumption with traditional processes.

The specific energy is related to the energy per pulse, the repetition rate of the pulses and the mass flow. It is defined as:

$$W_{specific} = W_{pulse} \frac{f}{\dot{m}} \quad (2.9)$$

where  $W_{specific}$  is the specific energy input (kJ/kg),  $W_{pulse}$  is the energy per pulse (J/pulse),  $f$  the frequency (Hz) and  $\dot{m}$  the mass flow rate (kg/s). For batch system the term  $f/\dot{m}$  can it easily replaced by  $n/m$ , where  $n$  is the pulse number and  $m$  is the mass in the treatment chamber.

For exponential decay pulses the energy per pulse can be estimated by the energy stored in the capacitor bank:

$$W_{pulse} = \frac{1}{2} \cdot C \cdot U^2 \quad (2.10)$$

Where  $C$  is the capacity of the capacitor(s) and  $U$  is the initial charge voltage.

In square-wave shaped pulses, the energy per pulse can be determined by the current intensity, according to:

$$W_{pulse} = U \cdot I \cdot \tau \quad (2.11)$$

Where  $I$  is the current in amperes flowing through the media during the pulse width  $\tau$  ( $\mu$ s) as a result of the applied voltage  $U$  in volts (Zhang *et al.*, 1995).

Based on media conductivity  $\sigma$  and electric field strength  $E$  measured the specific energy input for exponential decay and rectangular pulses can also be calculated by (Toepfel, 2006):

$$w_{specific} = f \frac{1}{\dot{m}_0} \int_0^{\infty} \sigma(T) \cdot E(t)^2 dt \quad (2.12)$$

### 2.2.3 Treatment temperature

The electrical pulse energy is discharged into the food as a Joule type heating. Therefore, the temperature of the food will increase in relation to the amount of energy that it receives. This temperature increase can be calculated according to the following equation, where heat transfer to the surrounding is not considered:

$$\Delta T = \frac{W_{specific}}{C_p} \quad (2.13)$$

Where  $C_p$  is the specific heat capacity of the food and  $\Delta T$  the temperature increase.

This is why one must bear in mind the initial treatment temperature. Normally the temperature may grow up to 25 – 30 °C, if the specific energy is 100 kJ/kg and the heat capacity is 4 kJ/ kg K. Figure 2.5 shows graphically a comparison of the temperature-time profile of a PEF treatment with the temperature-time profile of a HTST treatment.

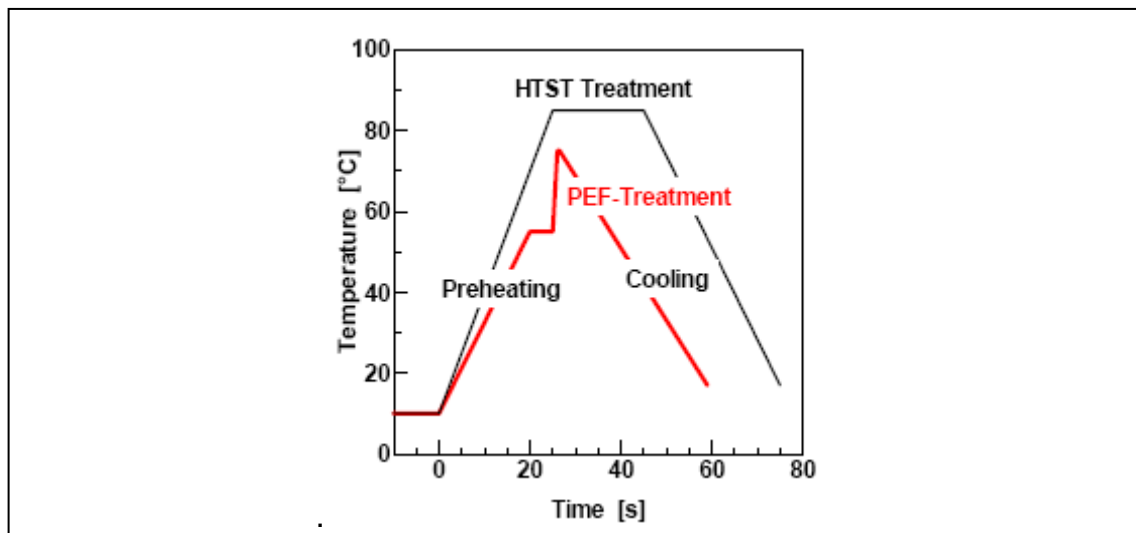


**Figure 2.5** Temperature-time-profile of a suggested PEF-treatment of apple juice at an initial treatment temperature of 55°C, and a specific energy input of 40kJ/kg compared to a HTST treatment 85°C, 30 s.

**Source:** adapted from Toepfl (2006).

It is not recommended to work at low initial temperatures, because the microbiological inactivation done by PEF is based on pore formation, and this is strongly encouraged with increased temperature, this synergic effect between temperature and PEF is based on variation of membrane fluidity with temperature. At low temperatures the phospholipid structure is packed in a gel-like structure and their order decreases with increasing temperature. The temperature dependent phase shifts from gel to a liquid crystalline structure, affecting cell membrane stability and susceptibility to PEF (Stanley, 1991).

## 2.2.4 Treatment time and frequency

The treatment time is an important parameter which should be controlled in order to avoid an over- or under-processing.

Treatment time is defined as the product of a number of pulses ( $n$ ) and pulse duration ( $\tau$ ):

$$\tau = n \cdot \tau \quad (2.14)$$

The frequency is defined as the number of pulses delivered per second. It is measured in Hz. This parameter can be regulated with the PEF equipment in order to obtain a desired energy input per kilogram of food.

In a continuous process it is important to consider the mass flow in order to always obtain the same number of pulses per unit volume. If mass flow is faster, frequency must also be consequently higher. The maximum applicable energy input value must be chosen so as to avoid any excessive increase of temperature of the treatment medium, that may be lethal to microorganisms as well as promoting bubble formation, and thereafter, arc discharge inside the treatment chamber.

### **2.2.5 Pulse geometry and pulse width**

When the high voltage switch is set to position A (open), current will flow into the capacitor (see Figure 2.1). The electric field within the dielectric is displaced and the bound electric charges are polarized from their normal position of equilibrium. Then, as the switch is thrown to position B (closed), current will flow out of the capacitor and an electric pulse is thus induced into the treatment chamber.

Depending on the specific system, pulses may be of constant polarity with an exponential decay, or with a square-wave shape or with alternating polarity (bipolar pulse), for example, in a sinusoidal or triangular sinusoidal manner.

Use of bipolar pulses and very short duration pulses reduces the risk of undesirable electrochemical reactions, as well as formation of deposits, at the electrodes.

Moreover, the most commonly used waveform in the PEF application are the exponentially decaying and the square-wave, where the former are easier to generate. (Pataro, 2006).

The square-wave pulses can be obtained by using a switch with on-off function or an adequate network. The pulse-forming network necessary for producing square-wave pulses is more complex and costly than for exponential decay pulses, but generally they save more energy and require a lower effort of cooling than the circuits in order to produce exponential decay pulses. (Martín *et al.*, 1994). The main advantage of square-wave pulses is that it delivers electrical energy at the maximum voltage during most of the pulse width.

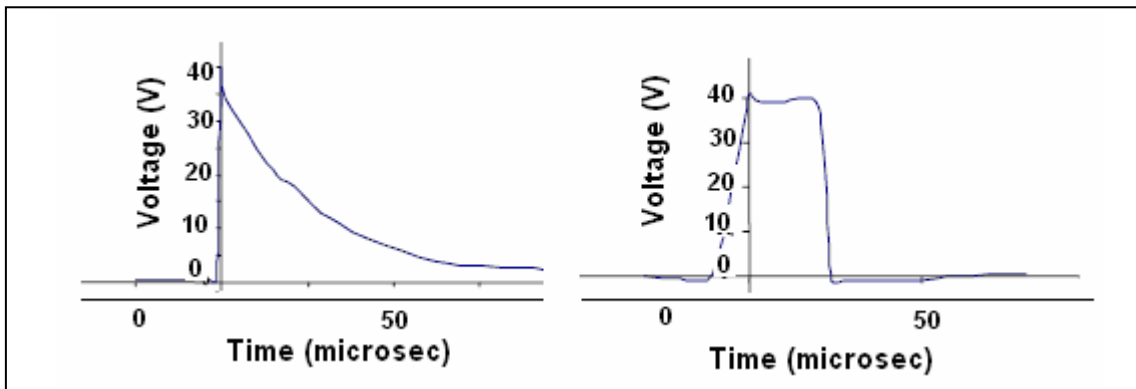


**Figure 2.6** Exponential and square shape pulses.

In the case of an exponential decay pulse, the delivered voltage is related to the capacity of the capacitor(s) and the resistance, in accordance to the following equation (Ho & Mittal, 2000):

$$U(t) = U_0 \cdot e^{-\frac{t}{R_c \cdot C}} \quad (2.15)$$

Where  $U(t)$  is the voltage across the resistor at any time  $t$  (s),  $V_0$  is the voltage supply,  $R_c$  is the resistance and  $C$  the capacitance.

The pulse width for exponential decay pulse is defined as the length of the time at which the electric field strength is reduced to 37% of the initial value or

$$\tau = R \cdot C \quad (2.16)$$

## 2.3 Product Factor

Microbial inactivation by pulsed electric fields also depends on the characteristics of the microorganism-containing medium or food. Factors such as the resistivity, ionic strength, pH, water activity, viscosity, presence of solid particles, bubbles or oil droplets. (Jayaram *et al.*, 1993; Vega-Mercado *et al.*, 1996a) have an impact on PEF effectiveness.

### 2.3.1 Conductivity, medium ionic strength and components

The conductivity of a medium, defined as the ability to conduct electric current, is an important variable in PEF technology. In general, conductivity is symbolically defined by  $\sigma$  in siemens per meter. It is the inverse of resistivity,  $\rho$  (in  $\Omega\cdot\text{m}$ ).

Foods resistivity ranges from 0.4  $\Omega\text{m}$  ( $\sigma = 2.5 \text{ S/m}$ ) for foods with high salts and water contents, to values in excess of 100  $\Omega\text{cm}$  ( $\sigma = 0.01 \text{ S/m}$ ) for pure fats and oils that are electrical insulators (Barsotti *et al.*, 1999).

Treatment chambers with high conductivity foods have a poor resistance and it is necessary to produce higher voltage to achieve the same effect of microbiological inactivation that is achieved when it processes the food with a low conductivity (where less current flows due to its high resistance). However, it is more difficult to build sufficient field strength when the conductivity is too high (Wouters 2001). To obtain the same degree of microbiological inactivation in foods with very different conductivity, the conditions of treatment, such as: the interelectrode gap in the treatment chamber, the pulse width and the voltage intensity must be changed.

On the other hand, the presence of ions appears to be necessary to increase the transmembrane potential (Bruhn *et al.*, 1998). The membrane will be weakened and more susceptible to an electric pulse in media with higher ionic strength, causing higher permeability and structural changes (Toepfl 2006),

but in general, the bactericidal effect of PEF is inversely proportional to the ionic strength of the suspension material, namely, the inactivation is generally enhanced when the medium has a high electric resistivity (Huelsheger *et al.*, 1981, Mizuno and Hori, 1988). Due to the presence of ionic charge in foods, conductivity shows a considerable increase with a raising temperatures (Pataro 2004) and the impact of temperature on conductivity can be approximated by a linear function (Heinz *et al.*, 2002).

The behavior of the food components in the PEF treatments is very different. The ions in a liquid food are responsible for the conductivity. On the other hand, the proteins, polysaccharides, macromolecules or lipids also have a subordinated effect on the conductivity. An increase in the concentration of protein, lipid or xanthan appears to increase microbial resistance to electric pulses (Jaeger 2007, Bruhn *et al.*, 1998; Martín *et al.*, 1997, Grahl and Maerk, 1996; Ho *et al.*, 1995).

The divalent cations such as  $\text{Ca}^{++}$  and  $\text{Mg}^{++}$  play an important role in the integrity of the bacterial membrane. Their presence in liquid food protects cell membranes during electric treatment (Huelsheger *et al.*, 1981).

### **2.3.2 pH**

The influence of pH on the microbial inactivation by PEF treatment is unclear. Several authors (Sale and Hamilton, 1967; Huelsheger *et al.*, 1981; Heinz and Knorr, 2000) observed that the pH has no effect on the inactivation of microorganisms by PEF. However, other authors (Jeanet *et al.*, 1999; Vega-Mercado *et al.*, 1996c) found that pH plays an important role in the inactivation kinetics by PEF. Both acidic and alkaline pH values induce additional stress to cells, and consequently increases their susceptibility to physical and chemical treatments (Pataro 2004).

The membrane is relatively impermeable to  $\text{H}^+$  and  $\text{OH}^-$  ions, and the membrane permeability increases due to the formation of pores in the cell wall

during the PEF treatment. Thereby the rate of transportation of  $H^+/OH^-$  increases and results in a change in the cytoplasmic pH value.

The change of pH within the cells may produce chemical modifications in fundamental compounds such as DNA or ATP (Vega-Mercado *et al.*, 1996b).

### **2.3.3 Bubbles, presence of particles**

The dielectric breakdown must happen in the membrane of the microorganism, but it should not happen in the food itself.

When the temperature increases, the solubility of gases in the liquid decreases producing a gas bubble and the local heating could make a part of the liquid to evaporate, giving a bubble. An air bubble has a dielectric strength much lower than the one of the food and then is easy that occur a local dielectric breakdown in a liquid food. This dielectric breakdown will increase the size of the present bubbles, and the further applications of the electric pulses could make a spark.

In order to remove the air, a degassing can be used before the PEF treatment, working under pressure and some precautions should be considered, such as: avoiding the formation of unhomogenous electric fields, and to prevent that their intensity does not exceed the dielectric capacity of the liquid food under the working conditions.

When a liquid food has impurities, the dielectric breakdown can be attributed to their presence. The impurities can significantly change the strength of the local electric field due to the differences of the dielectric properties. Such impurities can be agglomerations of microorganisms or fat globules that are present in the food (Toepfl 2006).

## 2.4 Microbiological factors

### 2.4.1 Type of microorganisms

Principally, the effect of the electric pulses on the cell membrane is given by the membrane potential theory. This theory assumes that the potential led across the membrane (transmembrane potential TMP) depends on the cell size, according to equation 2.19 or to equation 2.17 given by Grahl & Märkl (1996); the latter adds the orientation angle  $\alpha$  of the cell with respect to the electric field.

$$U_c = f_s \cdot a_0 E \cdot \cos \alpha_c \quad (2.17)$$

For example, the factor  $f$  for non spherical particles, supposing that they have a form of cylinder, with a hemisphere on each side, is obtained according to Zimmermann *et al.* (1974) as:

$$f_s = \frac{L_s}{(L_s - 0.33 \cdot d)} \quad (2.18)$$

Where  $L$  is the particle length (m) and  $d$  the diameter (m).

In other words, the particle size has an inverse relationship to the external electric field strength necessary to induce a specific TMP. It has been demonstrated by many authors that for the smaller particles, a higher electric field strength is necessary in order to threshold the critical membrane potential. Furthermore, Sitzmann (1995) affirms that it is impossible to kill endospores and ascospores with a PEF treatment and that yeast cells are more sensitive than vegetative bacteria, and the Gram-negative bacteria are more susceptible than Gram-positive. This leads to deduce that the microbiological inactivation by PEF depends on the intrinsic properties of the microbial cell, such as electric resistance and membrane potential (Zimmermann *et al.*, 1976; Kinosita and Tsong, 1979).

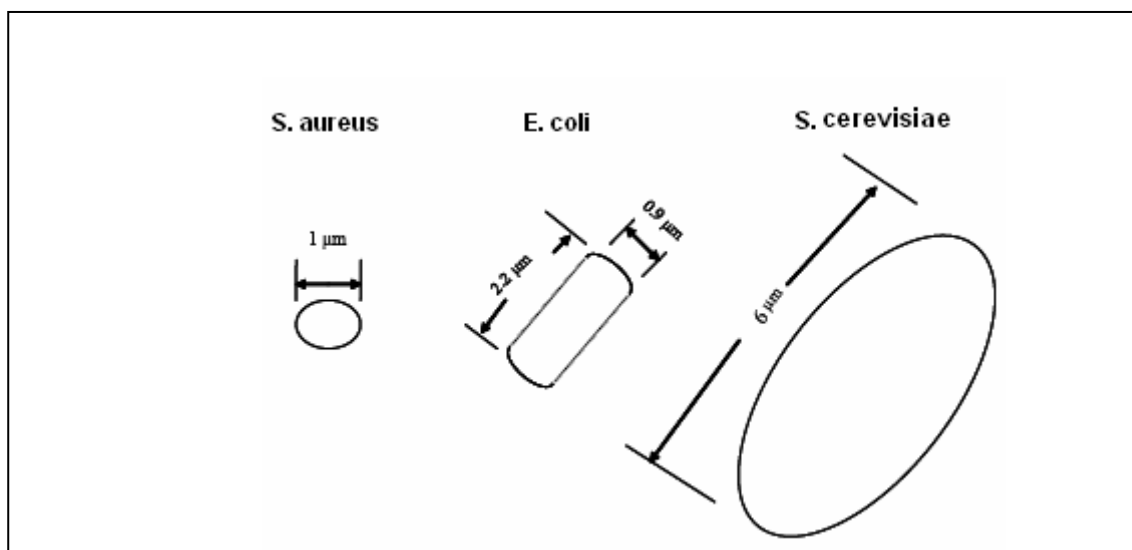


**Figure 2.7** A cell-size comparison (adapted from Alkahafali 2006).

### 2.4.2 Growth phase

The cells in the logarithmic growth phase are more sensible to inactivation by PEF, because that part of the membrane, where cell division is produced, is especially sensible to electric pulses, and in this phase the number of dividing cell is also very great. Inactivation by PEF is therefore better in the logarithmic phase than in the stationary phase (Jacob *et al.*, 1981; Huelshager *et al.*, 1983, Pothakamury *et al.*, 1996). Furthermore, based on measurements of mechanical properties, Smith *et al.* (2000) demonstrated that yeast cell populations strengthen as they enter the stationary phase, whereby wall thickness increases without alteration of average elastic properties of the cell-wall material (Pataro, 2004).

The growth phase impact on results of inactivation by PEF has been demonstrated by many authors; for example, Jacob *et al.*, (1981) performed experiments with *Saccharomyces cerevisiae* in logarithmic and stationary phases, while Wouters *et al.*, (2001) performed the same experiments with *L. plantarum*. Inactivation was found to be better in the logarithmic phase in both cases. This has to be taken into account when conducting experiments on microbial inactivation of model microorganisms by PEF.

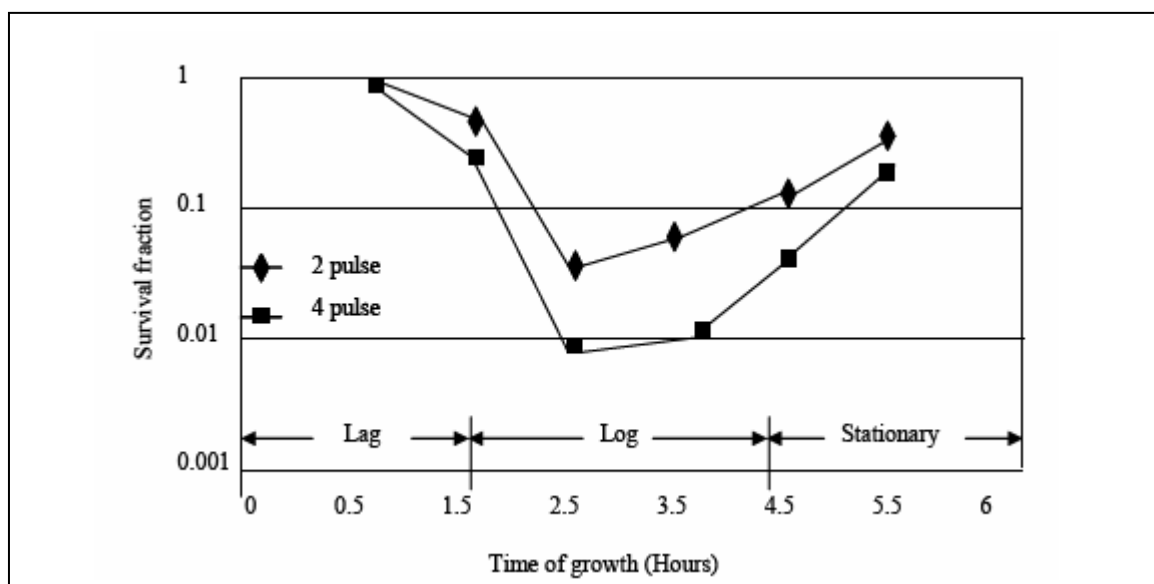


**Figure 2.8** Cells of *E. coli* harvested at different growth stages, suspended in SMUF and subjected to an electric field of 36 kV/cm at 7 °C

**Source:** Pothakamury *et al.*, 1996.

## 2.5 Mechanism of microbial inactivation

The membrane of the cells is one of the most important components because it has different functions such as (Rogers *et al.*, 1980):

- Acts as a semipermeable barrier
- Extrudes extracellular enzymes and cell wall materials
- Is the site of many complex activities as RNA, protein and cell wall synthesis and control of DNA synthesis
- Realises electron transport and oxidative phosphorylation

In a cell subject to no stress, the membrane acts as a semipermeable barrier. Any damage to the membrane affects its functions and may lead to the inhibition of cell reproduction or may lead to cellular death (Barbosa-Cánovas *et al.*, 1999).

The main reason for microbiological inactivation produced by PEF is given to the lysis of the cellular membrane (Sale and Hamilton, 1967), and can be partly explained by electroporation.

Electroporation is the phenomenon whereby a cell exposed to a high-voltage electric field suffers a temporary destabilization of the lipid bilayer and the proteins of their membrane (Chang *et al.*, 1992), so that it loses its semi permeable properties. The result is the formation of pores in the membrane, so that it is partially or completely damaged (Tsong, 1990a).

The damage may be reversible if the cell regains membrane structure when the electric field is turned off. If not, the cell membrane is structurally damaged and microbial inactivation results (Barbosa-Cánovas *et al.*, 1999)

Zimmermann *et al.* (1976) described the dielectric breakdown effect, as one theory of electroporation. To explain this effect, the following must be considered:

The double lipid layer of the cell membrane acts as an insulator shell to the cytoplasm, since it separates the cytoplasm of the environment.

The conductivity of the cytoplasm is six to eight orders greater than that of the membrane (Chen and Lee, 1994), so the membrane can be considered as a capacitor with a low dielectric constant ( $\epsilon \approx 2$ ) in comparison to the dielectric constant of the water ( $\epsilon \approx 80$ ) and also, on both sides of the cell membrane there are free loaded particles, being responsible for the naturally occurring transmembrane potential (Figure 2.9).

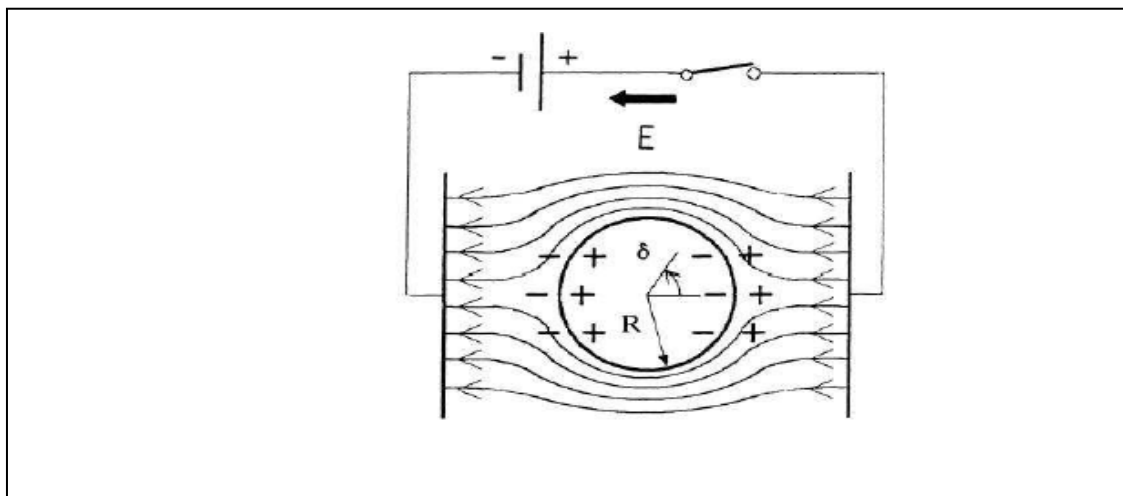


**Figure 2.9** Surface polarization of a cell in presence of an electric field

**Source:** Adapted from Dimitrov (1995).

The maximum transmembrane potential ( $U_c$ ) generated by an external field is given by Schoenbach *et al.* (1997) as:

$$U_c = f \cdot a_0 E_c \quad (2.19)$$

Where  $a_0$  is the outer radius of the cell,  $E_c$  is the critical field strength and  $f$  is a form factor that depends on each microorganism.

According to Zimmermann (1986) when a cell suspension is exposed to an electric field, the loaded particles on the membrane surfaces are of opposite charge and attract each other, leading to an increase of the transmembrane potential (TMP) and the electromechanical stress. This attraction gives rise to a compression pressure that causes the membrane thickness to decrease (Barbosa-Cánovas *et al.*, 1999) ending in the formation of pores.

Pores formation involves a two-step mechanism, an initial perforation that takes place when the critical TMP, a value of approx. 1 V, is reached. This is followed by pore expansion that produces an irreversible loss of the membrane structure. Depending on intensity of the electric field strength, on treatment time and temperature as well as on others factors, like pH and conductivity, the pore formation can be reversible or irreversible.

It is important to emphasize that the critical breakdown value decreases with increasing temperature (Hofmann and Evans 1986, Zimmermann 1986).

Other explanations for pore formation phenomena are based on the induction of pores in membrane protein channels. The cell membrane naturally contains protein channels, pores and bubbles (Vassilev and Tien, 1985), and the aperture and closure of different protein channels depends on the electric membrane potential (Tsong, 1990a). This can occur by achieving a threshold potential of approx. 50 mV. This potential is lower than the dielectric capacity of the lipid bilayer. Therefore, when electric pulses of 150 – 500 mV are applied, much protein channels sensible to the voltage will be opened before the electric potential across the membrane achieves the breakdown potential of the lipid bilayer.

On the other hand, the lipid bilayers are sensible to the application of electric pulses due to the electric charge of the lipid molecules. In a lipid bilayer two types of pores can be formed, hydrophobic and hydrophilic pores (Weaber, 2000) The formation of little cylindrical pores in the hydrophobic wall requires relative low energy in comparison to the energy necessary to induce pores in the hydrophilic area.

When the hydrophobic pore diameter achieves a size of 0.3 – 0.5 nm, the energy is enough to induce the formation of hydrophilic pores. The damage can be reversible when the size of the new pores is between 0.6 -1.0 nm, but by exceeding this value, an irreversible mechanical breakdown of the membrane results.

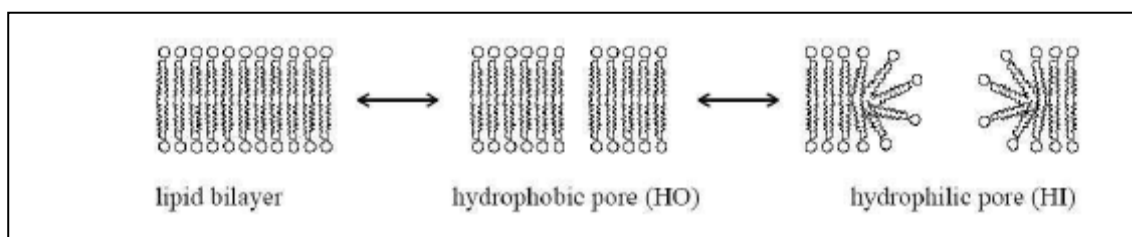


**Figure 2.10** Hydrophobic and hydrophilic pore

**Source:** Adapted from Waschipky & Zschörnig (2005).

### 2.5.1 Kinetic models

The mathematical models that describe the microbiological inactivation kinetic are based on experimental results.

Two models often used to describe inactivation kinetics are the following: The Huelsheger model (1981, 1983) described the kinetics of survival curves assuming a linear relationship between the logarithm of survival fraction, electric field strength and treatment time

$$s = \left( \frac{\tau}{\tau_c} \right)^{\frac{-(E-E_c)}{K}} \quad (2.20)$$

Where  $s$  is the survival rate,  $\tau$  the treatment time,  $\tau_c$  the critical treatment time,  $E$  the electric field strength,  $E_c$  the electric field strength at the extrapolated survival fraction of 100%, and  $K$  is a constant. This equation shows that an increase in electric field strength is much more profitable than an increase in treatment time (Hulsheger *et al.*, 1981; Jayaram *et al.*, 1992).

The Peleg model (1995) described the percentage of survivors as a function of the electric field and number of pulses.

$$s = \frac{1}{1 + e^{\frac{E-E_c(n)}{k(n)}}} \quad (2.21)$$

$E_c(n)$  is the electric field strength where the survival level is 50% and  $k(n)$  is a kinetic constant that describes the steepness of the sigmoid curve.  $E_c(n)$  and  $k(n)$  depend both on the number of pulses or treatment time.

### 2.6 Enzyme inactivation

Food spoilage can be caused by enzymes naturally present in the food or by the enzymes produced from certain microorganisms. On the other hand, some

enzymes bring desirable changes such as flavor and odor in foods (Ho & Mittal, 2000).

Due to the application of PEF, changes in the conformational state of proteins might cause changes in enzyme structure (Bendicho *et al.*, 2003 and Tsong, 1990b).

In general, the mechanisms involved in the inactivation of enzymes by PEF are not fully understood (Ohshima *et al.*, 2006)

Possible mechanisms are proposed by Castro *et al.* (2001a) and Perez and Pilosof (2004).

If the duration of the pulse is long enough, the effects of pulsed electric fields on proteins could entail:

- Polarization of the protein molecule
- Dissociation of non-covalently linked protein sub-units involved in quaternary structures
- Changes in the protein conformation so that buried hydrophobic amino acid or sulfhydryl groups are exposed
- Attraction of polarized structures by electrostatic forces, and
- Hydrophobic interactions or covalent bonds forming aggregates.

The observed effects of PEF on enzymes by different research groups appear to depend, besides the enzyme, on the characteristics of the PEF system used and on the electric process parameters.

### **2.6.1 Milk alkaline phosphatase inactivation**

Alkaline phosphatase (ALP) (EC 3.1.3.1) is a dimeric, membrane-derived glycoprotein (Hsu, 1985 and Fosset, 1974) that contains two  $Zn^{++}$  ions and one  $Mg^{++}$  ion at the active center. Zn ions at all three sites also produce a maximally active enzyme. These metal ions have center-to-center distances of 3.9 Å (Zn1-Zn2), 4.9 Å (Zn2-Mg3), and 7.1 Å (Zn1-Mg3). The alkaline phosphatase is a

hydrolase enzyme responsible for removing phosphate groups from many types of molecules, including nucleotides, proteins and alkaloids.

The enzyme is most stable in the pH range 7.5–9.5 and its optimum pH for enzymatic activity is between 8 and 10 (Fosset, 1974). The optimum pH will change depending upon substrate, substrate concentration and ionic concentration (Latner, 1970). In publications of different authors it is possible to observe that the pH changes could affect the enzyme activity up to 60% (see Figure 2.11).

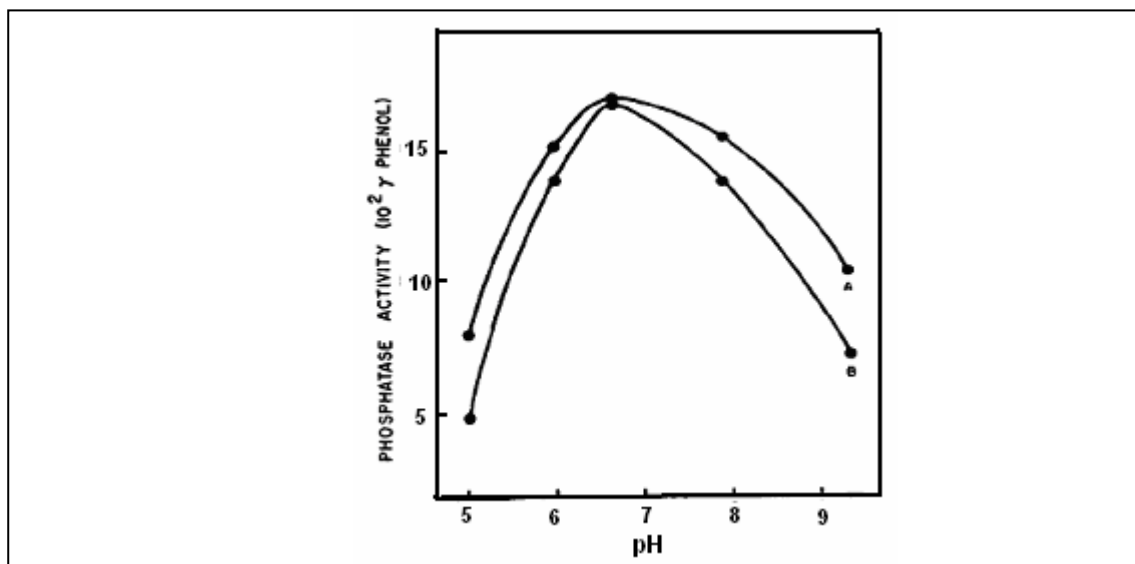


**Figure 2.11** Effect of pH on the stability of milk, held at indicated pH values for one hour (A) and two hours (B)

**Source:** Adapted from Haab and Smith (1980)

Due to its thermal sensibility this enzyme is of great interest to determine the effectiveness of pasteurization of milk and dairy products (Sanders *et al.*, 1947). ALP denatures when subjected to temperatures of approximately 72 °C for at least 15 seconds or at 62 °C for 15 min.

A possible inactivation mechanism of this enzyme in a thermal treatment was proposed by Poltorak *et al.* (1999). He proposed a denaturation mechanism

of this enzyme based on the structural data. The mechanism contained several steps imparting no loss of enzyme activity. These steps were explained by a sequential destruction of enzyme, leading to the dissociation of the protein into inactive monomers. The thermal inactivation of ALP follows first-order kinetics (Claeys *et al.*, 2001) and Castro *et al.* (2004) investigated the differences between the effect of conventional and ohmic heating on the inactivation kinetics of ALP, which was described with a first-order model.

On the other hand, the PEF treatments appeared not to cause inactivation of endogenous alkaline phosphatase. But different experiments shows very different results, for example the activity of alkaline phosphatase was reduced by 60% in raw milk with 2 % fat and by 65% in non-fat milk after 70 pulses of 400  $\mu$ s, and 18.8 kV/cm at 22°C. Bovine alkaline phosphatase, dissolved in a buffer containing 1M diethanolamine and 0.5 mM magnesiumchloride (pH 9.8) was subjected to 30 pulses of 40, 60 and 80 kV/cm and under all conditions tested, a slight 5% reduction could be noticed (Van Loey *et al.*, 2002).

According to Castro *et al.*, (2002a), the inactivation mechanism consists of the degradation of the secondary structure of the enzyme and it was found that PEF altered the entire globular configuration of ALP. Van loey *et al.*, (2002) using polyacrylamide gel electrophoresis of untreated and PEF treated alkaline phosphatase samples demonstrated that PEF does not hydrolyze alkaline phosphatase.

However, electric pulses appear to be able to inactivate some enzymes that are detrimental for food quality and storage, for example: an exogenous protease produced by *Pseudomonas fluorescens* present in milk, that increases the risk of coagulation and enhances the bitterness of refrigerated milk, and plasmin, an endogenous milk protease with detrimental effects for milk quality; both enzymes were demonstrated to be inactivated by PEF treatment (Vega-Mercado *et al.* 1995b).

## 2.7 Electrochemical reactions

In pulsed electric field system for preservation of liquid food, electrochemical reactions can occur in the treatment chamber at the electrode surface. This may result in a partial electrolysis of the solution, in corrosion of the electrode material and in introduction of small particles of electrode material in the liquid. (Morren *et al.*, 2003).

When an electrode is placed in an electrolyte, immediately a so-called double layer will develop, even if no external voltage is applied to the electrode. When the applied voltage is below a certain threshold voltage, no electrochemical reactions occur, except some low-level reactions due to the exchange current. When the potential difference that is applied to the cell is increased above the threshold voltage, two independent electrochemical half-reactions will occur at the electrodes. The amount of reaction is proportional to the charge (i.e. electrons) that is transferred across the metal–solution interface (Lelieveld *et al.*, 2007). An overview of possible electrochemical reactions is shown in Table 2.1.

**Table 2.1** Possible electrochemical reactions at the electrode/media interface and its respective problem in the PEF treatment (adapted from Toepfel 2002).

Anode (oxidation)	Cathode (reduction)	Problem
$2 \text{H}_2\text{O} \longrightarrow \text{H}^+ + \text{OH}^-$	$2\text{H}^+ + 2\text{e}^- \longrightarrow \text{H}_2(\text{g})$	Local pH changes, which affect enzymatic activity.
$2 \text{OH}^- \longrightarrow \text{H}_2\text{O}_2$		Reactive substance, formation of undesired components.
$4 \text{OH}^- \longrightarrow \text{O}_2(\text{g}) + 2 \text{H}_2\text{O} + 4\text{e}^-$		Gas formation, which facilitates the formation of dielectric breakdowns.
$2 \text{Cl}^- (\text{aq}) \longrightarrow \text{Cl}_2(\text{g}) + 2\text{e}^-$		
$\text{Fe}(\text{s}) \longrightarrow \text{Fe}^{2+}(\text{aq}) + 2\text{e}^-$		Releases of metal particles in the food.

## 2.8 Mathematical modeling

The resolution of complex mathematical problems requires computational techniques. Numerous software exists to carry out this process, for example; FLUENT (Fluent, Inc.), COMSOL (COMSOL, Inc.), ANSYS (ANSYS, Inc), ALGOR (ALGOR, Inc.), etc. These programs use Finite Volume Method (FVM) or Finite Element Method (FEM) to resolve a set of partial differential equations. The partial differential equations describe the change of a phenomenon or entity as an independent variable is changed, e.g. a space coordinate or time.

The FVM and FEM technique are widely used as general approximation method in the area of computational fluid dynamics. Computational fluid dynamics is a computer-based methodology for the solution of the fundamental equations of fluid flow, heat transfer, and chemical reactions. It is also possible to resolve many other physical problems and it is also possible to couple physical problems, for example, electrical problems coupled with fluid dynamics and heat transfer.

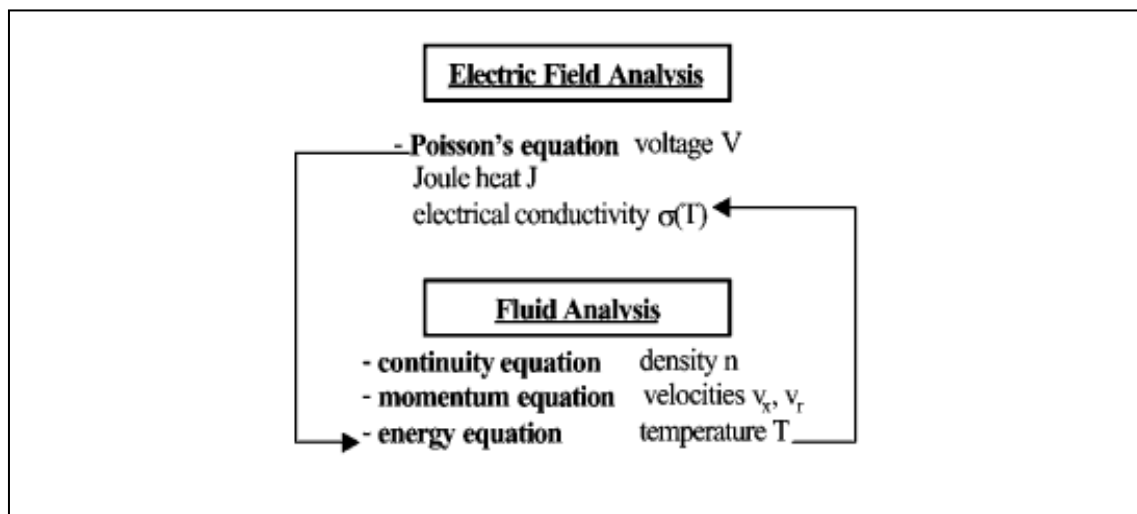


**Figure 2.12** Scheme of coupling between the electrical and fluid analyses

**Source:** Adapted from Fiala *et al.*, 2001.

The fundamental steps to resolve a mathematical problem with software of FVM or FEM technique are summarized below:

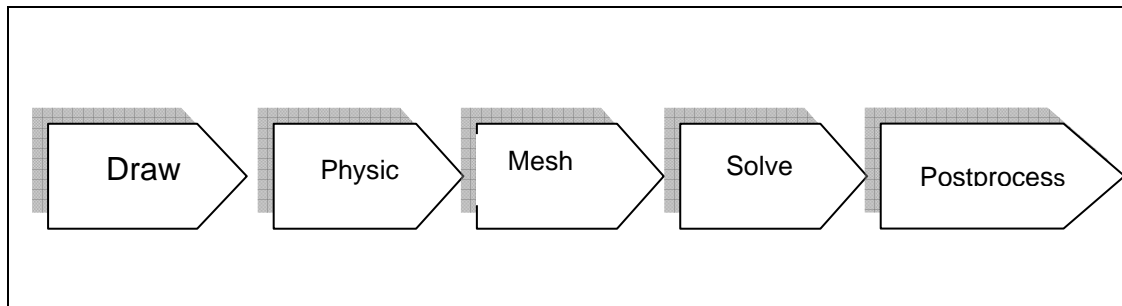


**Figure 2.13** Scheme to resolve a problem with software of FVM or FEM.

The first step is to draw the geometry, which is possible using CAD (Computer Aided Design) tools, some software provide it, such as; GAMBIT (Fluent, Inc.), AutoCAD (Autodesk, Inc.), Rhinoceros (Robert McNeel & Associates) or some FEM/VEM software have inclusive CAD tools. The geometry is a digital model of a physical system, which would be interesting to study, and can be real (drawing of existent models; food, pipes, treatment chamber, etc), but does not necessarily exist (for developing new designs).

Then, the definition of physical equations for the specific problem and their respective boundary conditions are needed. In some softwares the step to mesh can be before the definition of physical equations.

The mesh divides the drawn geometry into small sections. A proper mesh distribution is important for solution accuracy and for making the best use of the available computational resources. The integral of the governing equations is applied to each control volume, or cell, in the computational domain and discretized.

The Solve step consists in resolving the previously selected set of governing equations by means of an adequate algorithm, a most common algorithm for CFD problems is the SIMPLE algorithm (Semi-Implicit Method for Pressure-Linked Equations) (FLUENT 2003). Finally, it is possible to make the

visualization settings as well as perform various postprocessing of the analysis results. Several solution properties can be visualized at the same time using colored surfaces, contours, streamlines and vector fields.

### **3 Materials and Methods**

The present work can be separated in 3 sections.

**Section I:** Comparison between the impact of the PEF treatment on inactivation of milk alkaline phosphatase (ALP) and thermal inactivation.

The factors of special interest to be studied on the PEF treatment are the following:

- The effect produced by the intensity of the electrical field.
- The effect produced by the shape of the pulse
- The effect produced by frequency and consequent change of the energy input.
- The effect produced by temperature increase as a result of the dissipation of electrical energy.

**Section II:** Study on the design of treatment chambers.

The factors that have been studied are:

- The effect produced by geometry on the distribution of the electrical field and its effectiveness for microbiological inactivation
- The effect produced by the flow of the fluid to be treated and the effect of the turbulence caused by the increase of velocity after the insertion of devices to alter the flow order and the electric field strength distribution and intensity.

**Section III** : Study on the distribution of temperature inside the treatment chamber during the PEF process.

A detailed explanation of the equipment and parameters used to fulfill the objectives listed above is described next.

### **3.1 Experimental Equipment**

Basically, the system used to conduct the experiments can be summarized as followed:

- A feed tank, where the fluid food to be processed is located, in this case milk or saline solution. This fluid is transported using a peristaltic pump to a heat exchanger to adjust the desired inlet temperature. Then the fluid is transported to the PEF treatment chamber, after the treatment the fluid must be cooled down in a second heat exchanger before a sample is taken for analyses. See figure 3.1
- A batch system with electroporation cuvettes is used. The fluid must be previously heated to the desired treatment temperature prior to be filled into the cuvette and immediately cooled after treatment. See figure 3.2.

#### **3.1.1 PEF equipment**

The generation of electrical pulses is carried out by a mechanism described in section 2.1 (PEF Equipment).

For this work 2 different pulse modulators have been used, one to generate square wave pulses and another one to generate exponentially decaying pulses.

The following paragraphs summarize the main characteristics of each pulse modulator.

### 3.1.1.1 Rectangular pulse modulator in a continuous system.

The pulse modulator for rectangular pulse shape (A) (ScandiNova Systems, Uppsala, Sweden) was used (Figure 3.5). The modulator consists of a high voltage power supply with 1 kV maximum voltage, six energy storage capacitor banks and six parallel IGBT units for rectangular pulse generation. Using a 1:50 pulse transformer at the secondary side up to 50 kV pulses can be achieved, the maximum current is limited to 200 A, the maximum repetition rate is 400 Hz, subjected to average power. Pulse width is adjustable between 3 and 8  $\mu$ s.

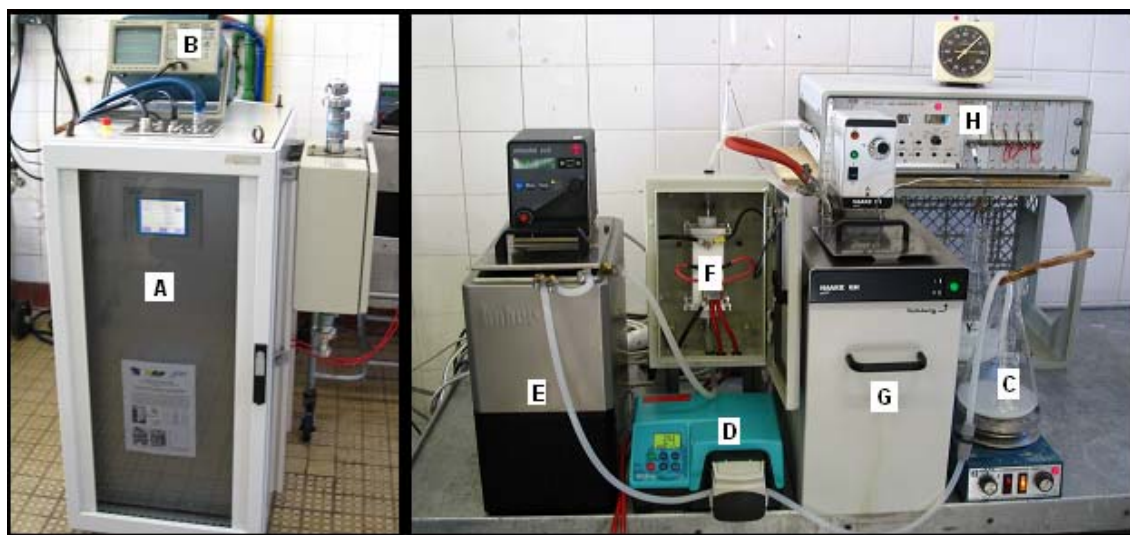


**Figure 3.1** Equipment for continuous pulsed electric field treatment. Left: Pulse modulator (A) and oscilloscope (B). Right: Food Tank (C), pump (D), heating (E), treatment chamber (F), and cooling (G) and thermometer (H).

### 3.1.1.2 Exponential decay micro- pulse modulator in a batch system

A power supply FUG HCK 800M-20000, 20 kV, 80 mA (FUG, Rosenheim, Germany) was used to deliver the electrical energy to a capacitor bank (see Figure 2.1). This consisted of a setup of Ceramite Y5U 6800Z (Behlke,

Kronberg, Germany) capacitors, with 3 capacitors of 4.5 nF each, that could be placed in parallel to obtain a capacity up to 13.5 nF (A).

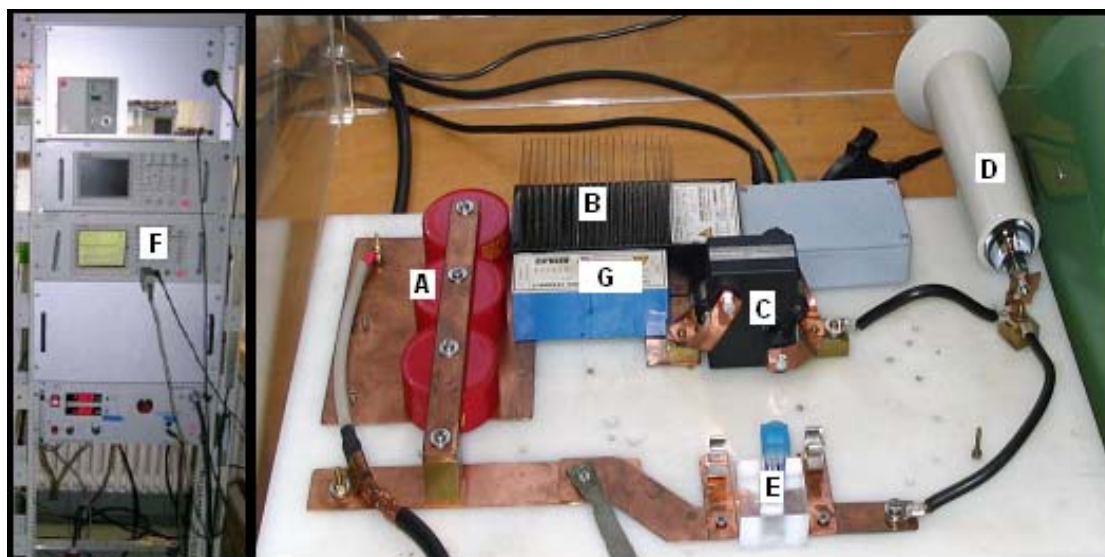


**Figure 3.2** Micro-pulse modulator for batch system.

A HTS 160-500 SCR, 16 kV, 5 kA, 2 kHz (Behlke, Kronberg, Germany) was used as switching unit (B), connected in series to the storage capacitors and a protective resistor (C) with 2.5 ohm (Stervice, France). The switch was protected against current reversal by a free wheeling diode (G): FDA 150-200, 20 kV, 1.5 kA (Behlke, Kronberg, Germany) and triggered by a TTL signal from a frequency generator (AFG 320 Sony Tektronix, Beaverton, US).

Pulse parameters were controlled by a high voltage and a current probe (D), connected to a TDS220 (Sony Tektronix, Beaverton, US) oscilloscope (F). Data acquisition and control were performed on a PC connected by GPIB, using software developed based on TestPoint (Keithley Instruments, Cleveland, USA). The unit was used to supply pulsed power to micro batch cuvettes (E).

The treatment voltages given in the results and discussion section for cuvette treatments refer to the applied treatment chamber voltage. The circuit voltage was higher (as the protective) because a voltage drop was also observed along the protective resistor. The ratio of treatment chamber resistivity

(depending on the conductivity of the treated media) and resistivity of the protective resistor determined this voltage division.

### 3.1.1.3 Treatment chamber

As treatment chamber for the continuous PEF treatment a co-linear type was used. The two chambers used in this work consist of 2 stainless steel electrodes of 85 mm length and 6 mm diameter, both working as ground. They are placed in a vertical position. Between these two electrodes there is another electrode of stainless steel material with diameter like the previous ones, but a length of 35 mm, this one works as a high voltage (HV) electrode. This HV - electrode is separated from the others by an insulator (made of Teflon) of 4 mm diameter and 4 mm length. For a better visualization of the electrodes position see Figure 3.3 below:

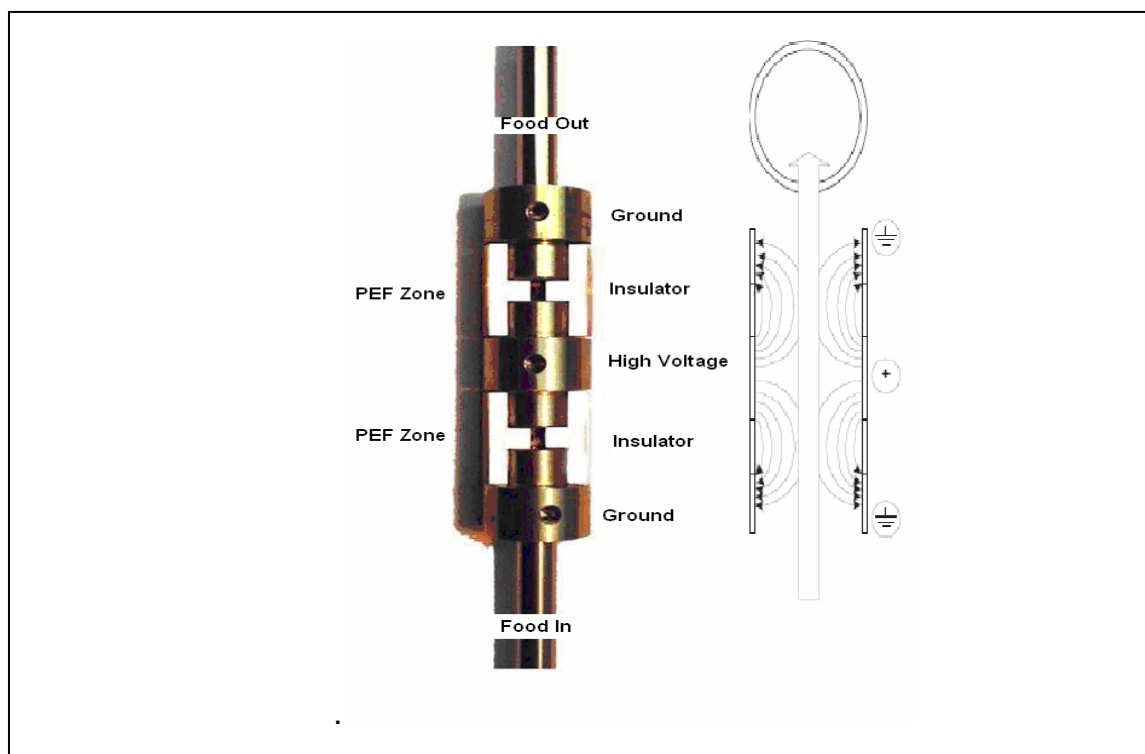


**Figure 3.3** Vertical adjustment of the electrodes and field strength profile

According to this geometry, a fluid volume of 1.1 ml is obtained within the treatment chamber. And a volume of 0.2 ml stays 0.1 second on each insulator, when the pump is regulated to a flow rate of 5 l/h.

The average electrical field generated inside the treatment chamber (specifically on the insulators) is obtained by multiplying the initial voltage by 1.7. This value depends of the insulator geometry. For more information on how to obtained this value, section 4.1.2, Effect of insulator geometry on the electric field strength, should be consulted.

The PEF treatment chamber for batch treatment is of parallel plate type. For this, an electroporation cuvette was used (Eppendorf AG, Hamburg, Germany (4307 000.59) or VWR International GmbH, Darmstadt, Germany (732-0021)). Each electrode has an area of  $2 \text{ cm}^2$  and is separated from each other by a distance of 2 mm, which provides a liquid volume of  $400 \text{ }\mu\text{l}$ . See the Figure 3.4 below:

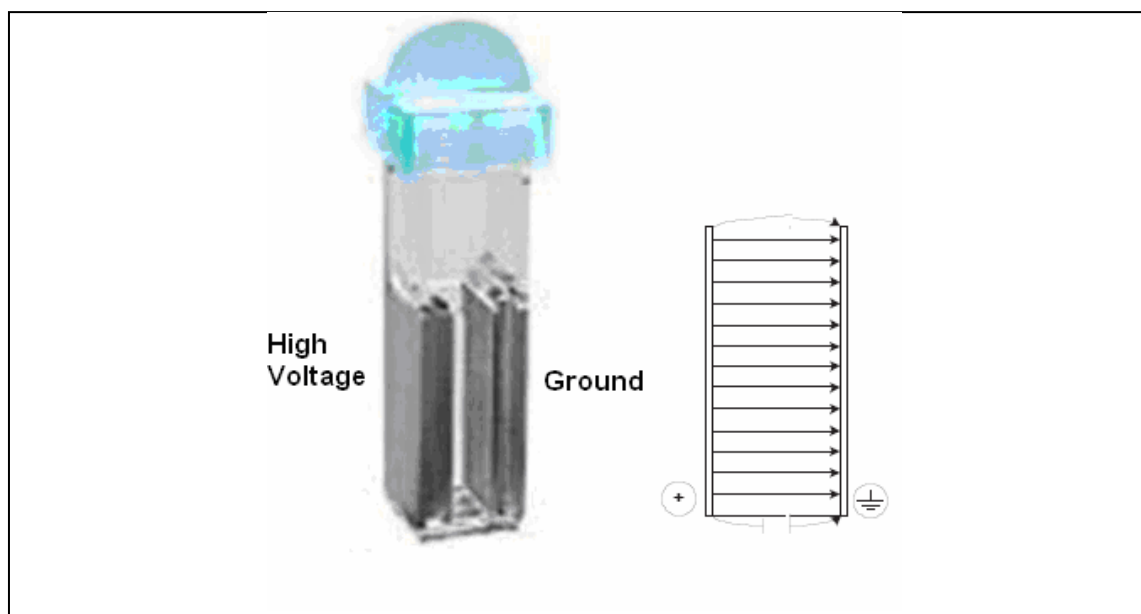


**Figure 3.4** Electroporation cuvette and distribution of electrical field.

### **3.1.2 Tempering equipment**

The temperature-leveling equipment is used for heating and cooling the fluid at the desired temperature before and after the electric treatment. To achieve this, a pump of adjustable velocity was used (Watson Marlow sci323, Falmouth Cornwall, UK) to transport the fluid to the heat exchanger. A velocity between 3 and 20 l/h was used in experiments). This heat exchanger consists of a stainless steel spiral tube of 2.10 m of total length and 2 mm of diameter and is immersed into a tempering bath of adjustable temperature (Polystat cc3, Fa. Huber, Offenburg, D), normally this temperature is adjusted between 22 and 32 °C, to heat the fluid up to 20 and 30 °C respectively (the temperature of the tempering bath is adjusted depending on the flow velocity that is used; in some cases the bath temperature can be adjusted to 50 °C in order to increase the fluid temperature to 30 °C when the flow velocity is approx. 20 l/h ).

After the fluid is heated to the desired temperature, the PEF treatment takes place. A fiber optic thermometer is used (TAKAOKA Fiber Thermometer 1110, Tokyo, Japan) for temperature measurement, which is not altered by the presence of the electric field. After the electrical treatment, the cooling phase begins. For this purpose a heat exchanger like the previous one described before is used, but in this case the bath temperature is adjusted between 5 and 15 °C to obtain a product with a temperature of 13 °C, depending on the flow velocity.

## **3.2 Product and Microorganisms**

For the investigation of the impact of the PEF treatment on alkaline milk phosphatase, raw milk was obtained from a local farming institute.

For the investigations related to the geometry of the insulators and its effect on the microbiological inactivation, Ringer solution was used (adjusted at a conductivity of 2.3 and 4.6 mS/cm).

In order to conduct the investigation of the distribution of temperature inside the treatment chamber (Ohmic heating), saline solutions of NaCl adjusted at conductivity of 2.3, 3.5 and 4.7 mS/cm were used. NaCl was also used to start up PEF treatment before product inlet.

The microorganisms used for the investigation of the lethal effect of the PEF treatment were obtained from the collection of the Department of Food Biotechnology and Food Process Engineering as frozen cultivation at -80 °C in pellets using Roti-Store cryo-vials (Carl Roth GmbH, Kalsruhe, Germany). These pellets must be inoculated before its use as is summarized below:

- *Lactobacillus rhamnosus E522* (VTT Biotechnology, Espoo, Finland). The initial inoculation of a pellet was done in 9 ml MRS Bouillon, and incubated under anaerobic conditions, without shaking at 37 °C for 24 h, then 90 µl of this solution were diluted in 9 ml of Ringer solution, from which 50 µl were transferred into 50 ml of MRS Bouillon and finally incubated like the first inoculation step. The final concentration of microorganisms in this medium was 10<sup>9</sup> CFU/ml.
- *Escherichia coli K12 DH5α* (Hygiene Institute, Hamburg). The inoculation of a pellet is made in 20 ml ST1-Bouillon, and incubated under aerobic conditions, on a shaker at 120 U/min at 30 °C for 24 h, then 90 µl from this solution were diluted into 9 ml of Ringer solution, from which 50 µl were deposited in 50 ml of ST1-Bouillon and incubated like before. The final concentration of *E. coli* was 10<sup>10</sup> CFU/ml.

With this procedure it can be assured that microorganisms are in a stable growth phase, which is suitable to perform the PEF treatment

### 3.3 Experimental Procedure

In this section the experimental procedure is described.

#### 3.3.1 PEF treatment

The PEF equipment used in the present work can be adjusted to different levels of the following parameters: applied voltage, frequency and pulse width. Additionally temperature and flow velocity can be regulated. When these parameters are modified, the energy input is changed as depending parameter.

The following table summarizes the main sublevels of each parameter:

**Table 3.1** Range of the used parameters in the PEF treatments.

Parameter	Parameter range	
	Continuous treatment, co-linear electrode	Batch treatment, parallel electrode
Voltage (kV)	16 – 20	5.4– 6.8
Field strength (kV/cm)	27 – 34	27 – 34
Pulse shape	Square wave	Exponential decaying
Pulse width ( $\mu$ s)	3 – 4.2	2 – 2.5
Frequency (Hz)	25 – 46	30
Conductivity fluid (S/m)	0.23 – 0.47	0.46
Velocity fluid (m/s)	0.45 – 2	0
Temperature input ( $^{\circ}$ C)	10 – 30	20
Energy per pulse (J/puls)	2.2 – 3.4	0.28 – 0.44
Energy input (kJ/kg)	40 – 220	40 – 220

Before each PEF treatment, where the microbiological inactivation was studied, the broth containing the microorganisms was centrifugated at 4000 rpm for 10 min and the pellet was resuspended in the treatment media. For *Lactobacillus rhamnosus*, 10 ml are needed to be centrifugated and then resuspended in 1 liter of the treatment media, with the purpose to obtain an initial concentration of  $10^6$  CFU/ml. For the case of *Escherichia coli K12 DH5 $\alpha$* , 1 ml was centrifugated and then resuspended in 1 liter of treatment media, for an initial concentration of  $10^6$  CFU/ml.

After finishing any experiment, the equipment must be cleaned as follow: at first it must be rinsed with circulating water, and a caustic solution of 3 % Ronalin (Tensid Chemie), which is followed by a second rinse with water, and an acid solution of 1% Weicod (Tensid Chemie). The washing is finished by rinsing with water again.

### **3.3.1.1 Experiment to analyze the effect of PEF treatment on milk alkaline phosphatase**

Raw milk was used and the determination of phosphatase activity was performed according to section 3.6 (Determination of Phosphatase Activity in Milk).

For this experiment, continuous and batch treatment chambers with square decay pulse and exponential wave pulse were respectively used.

The experiments consisted in fixing each parameter of the previous table to specific levels in order to study the following factors (in section 4.1.1 Impact of PEF treatment on phosphatase activity, the exact values for each parameter are presented):

- Effect of energy input
- Effect of field strength

- Effect of pulse shape
- Effect of temperature

### **3.3.1.2 Experiment to determine the effect of the insulator geometry and the velocity effect on the microbiological inactivation**

For the experiments *Lactobacillus rhamnosus* and *Escherichia coli* K12 DH5 $\alpha$  resuspended in Ringer solution were used.

The effect produced by the geometry 1 and 2 at different levels of energy input and frequency and conductivity of the media were compared. Section 4.2.2 describes in detail the values used for each parameter.

To study the effect of the flow velocity, the parameters were adjusted so as to conduct the experiments between velocities of 3 and 20 l/h.

To study the effect of turbulence and some changes of intensity of the electric field strength, a grid was inserted inside the treatment chambers, exactly before the insulators.

### **3.3.1.2 Experiment to determine the temperature distribution inside the treatment chamber and in the spiral heat exchangers**

The temperature distribution inside the treatment chamber is too difficult to obtain experimentally. An easier way is to use mathematical models, that deliver the temperature profile of the electrodes, which can be compared with experimental measurements, but it has the disadvantage that the temperatures cannot be measured exactly at different places where the electric field is.

The parameters needed to resolve the mathematical model are the following:

- Medium conductivity measured as temperature function and then

adjusted to 1<sup>st</sup> order.

- Density, viscosity, thermal conductivity and thermal capacity of the media
- Flow velocity.
- Input and output temperature in the treatment chamber and heat exchanger.

Mathematical models were also used to obtain the temperature profile in the heat exchangers, but in this case, this model can be compared with the experimental results, and measured temperatures using raw milk as the medium to be heated.

The parameters that were utilized to solve the mathematical model are:

- Heat transfer coefficient  $\alpha$ . This parameter can be calculated experimentally according the following equation:

$$\dot{m} \cdot Cp \cdot (T_{in} - T_{out}) = \alpha \cdot A \cdot \Delta T_{log} \quad (3.1)$$

where  $\dot{m}$  is the fluid flow in  $kg/s$ ,  $Cp$  the fluid specific heat capacity in  $J/kg \cdot K$ ,  $T_{in}$  the inflow temperature,  $T_{out}$  the outflow temperature,  $\alpha$  the heat transfer coefficient in  $W/K \cdot m^2$ ,  $A$  the area, where the heat transfer takes place in  $m^2$  and  $\Delta T_{log}$  the logarithmic temperature difference (Equation 3.2) and  $T_{\infty}$  the medium temperature.

$$\Delta T_{log} = \frac{(T_{in} - T_{\infty}) - (T_{out} - T_{\infty})}{\ln \frac{T_{in} - T_{\infty}}{T_{out} - T_{\infty}}} \quad (3.2)$$

The milk properties were calculated according to Bertsch (1983):

- Milk density in  $\left[ \frac{kg}{m^3} \right]$ : according to Equation 3.3:

$$\rho_M = -2,3 \cdot 10^{-3} T^2 - 2,665 \cdot 10^{-1} T + 1040,7$$

$$- x_f (-4,81 \cdot 10^{-5} + 9,76 \cdot 10^{-3} + 1,011) \quad (3.3)$$

where  $x_f$  is the fat content in %

- Milk viscosity in  $\left[ \frac{kg}{m \cdot s} \right]$ : according to Equation 3.4:

$$\ln \eta_M = 3,03 \cdot 10^{-5} T^2 - 1,813 \cdot 10^{-2} T + 0,609 + x_f (-2,3 \cdot 10^{-6} T^2 + 5,49 \cdot 10^{-4} T + 2,06 \cdot 10^{-3})$$

$$+ x_f^2 (2,5 \cdot 10^{-7} T^2 + 6,29 \cdot 10^{-5} T + 5,42 \cdot 10^{-3}) \quad (3.4)$$

- Milk heat capacity in  $\left[ \frac{kJ}{kg \cdot K} \right]$ : according to Equation 3.5:

$$C_p = (1 - TS)c_w + 0,534 \cdot TS \cdot 1,4 + 0,381 \cdot TS \cdot 1,6 + 0,083 \cdot TS \cdot 0,8 \quad (3.5)$$

where TS is dry matter content in % and

$c_w$  specific heat capacity of water  $\left[ \frac{kJ}{kg \cdot K} \right]$  according to equation 3.6

$$c_w = 4,214 - 2,153 \cdot 10^{-3} T + 3,646 \cdot 10^{-5} T^2 - 1,4948 \cdot 10^{-7} T^3 \quad (3.6)$$

- Milk thermal conductivity in  $\left[ \frac{W}{m \cdot K} \right]$  according to Equation 3.7:

$$\lambda_M = 0,5406 - 0,0055 x_f \quad (3.7)$$

- Milk flow velocity: measured as described in the previous section.
- Temperature inflow and temperature outflow of the heat exchanger.

### 3.3.2 Thermal enzymatic inactivation by glass capillary method

Glass capillary was used for the thermal treatments, with a length of 10 mm, a inner diameter of 1 mm and a external diameter of 1.3 mm (see Figure 3.7). The volume of milk within the capillary is just 100  $\mu$ l, and the small wall thickness ensures a quick heat transfer between the milk and the medium.

To compare the effect of the PEF treatment with the thermal effect on microbial inactivation, thermal experiments between 60 and 70 °C with residence times between 2 and 25 s were performed. This is the time in which the milk remains at constant temperature after the PEF treatment before it is cooled. This time depends on the tube length that connects the PEF equipment to the heat exchanger and on the flow velocity.

In each PEF treatment, as described in section 2.2.3 (Treatment temperature), the temperature of the product increases owing to ohmic heating. That is why thermal behavior of the enzyme should be analyzed.

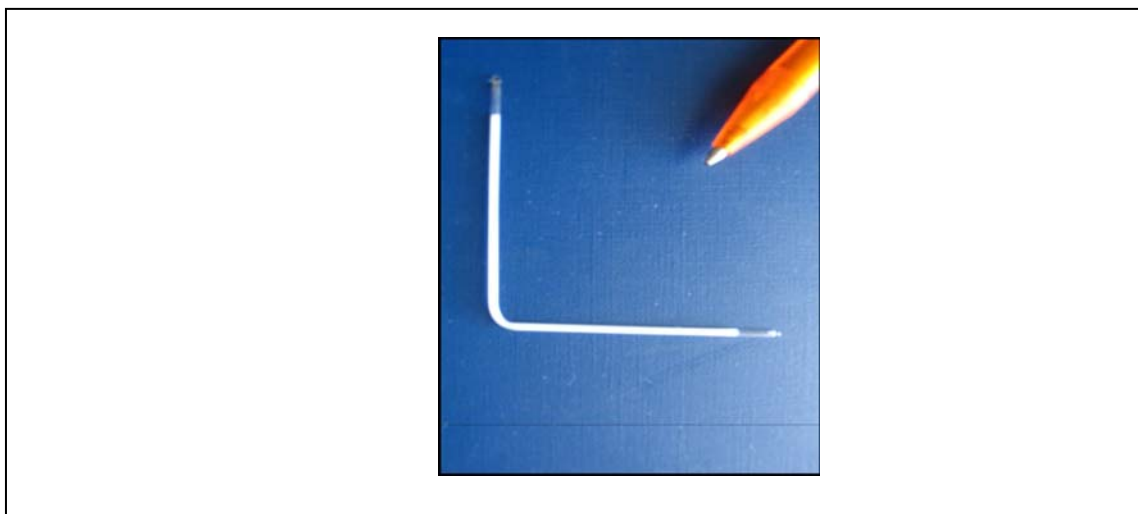


**Figure 3.5** Glass capillary.

90 µl were pipetted into the glass capillary, and the edges of the capillary were sealed with flame; for which the capillary was submerged into an ice water bed, so as to prevent a possible overheating of the milk

The capillary was then submerged in a water bath, which is adjusted at the desired temperature of inactivation. Afterwards the capillary is quickly cooled to stop any enzymatic inactivation; this was achieved by introducing the capillary in ice water.

For analysis of the sample, the capillary was broken and the milk extracted.

The results were processed to obtain relationship between temperature, processing time and the rate of inactivation, using the softwares Table Curve 2D Version 4 and Table Curve 3D (SPSS Inc, Chicago, USA) and MathCad 2001i Professional (MathSoft Engineering and Education, Inc., Cambridge, USA).

### **3.4 Microbial Analysis**

At the outflow of the complete PEF treatment equipment, as well as at the outlet of the final heat exchanger for cooling, the sample was collected in an Eppendorf – tube and placed on ice to avoid posterior inactivation.

The analytical method consisted of a plating of 100 µl of the sample on a nutrient media utilizing the drop plating method, a posterior incubation and finally a viable cell count.

Before plating the 100 µl sample, it must be diluted until the number of microorganisms is enough to count. The dilution of each sample was realized on microtiter – plates, which was filled with a multichannel pipette with 270 µl of Ringer solution and 30 µl of the sample. From this procedure, successive dilution were prepared using Ringer solutions, until microorganism concentrations between 10 of  $10^{-5}$  CFU/ml are obtained; this is then plated and carried to incubation.

The incubation of *Lactobacillus rhamnosus* was on MRS-Agar, under anaerobic conditions at 37 °C during 72 h.

The incubation of *Escherichia coli* was on Endo-Agar at 30°C during 24 h.

The inactivation of microorganisms was evaluated by calculating the log reduction in viable cell counts compared to the untreated sample.

### 3.5 Determination of Phosphatase Activity in Milk

Alkaline phosphatase (ALP) is a hydrolase enzyme responsible for removing phosphate groups from many types of molecules, including nucleotides, proteins, and alkaloids; this process of removing the phosphate group is called dephosphorylation.

This principle is used to determine the phosphatase activity, according to the Sanders and Sager's method (BVL, 1980). Under well-defined conditions, the enzyme produces phenol from disodium phenyl phosphate (see Figure 3.6). The phenol reacts with dibromochinoclorimid to dibromoindophenol, which is blue and measured photometrically in macro dispensable cuvettes at a wavelength of 610 nm. The absorbance obtained was compared with a phenol calibration curve, which is a relation between the phenol concentration and absorbance. The phosphatase activity is expressed in µg phenol per ml of sample.

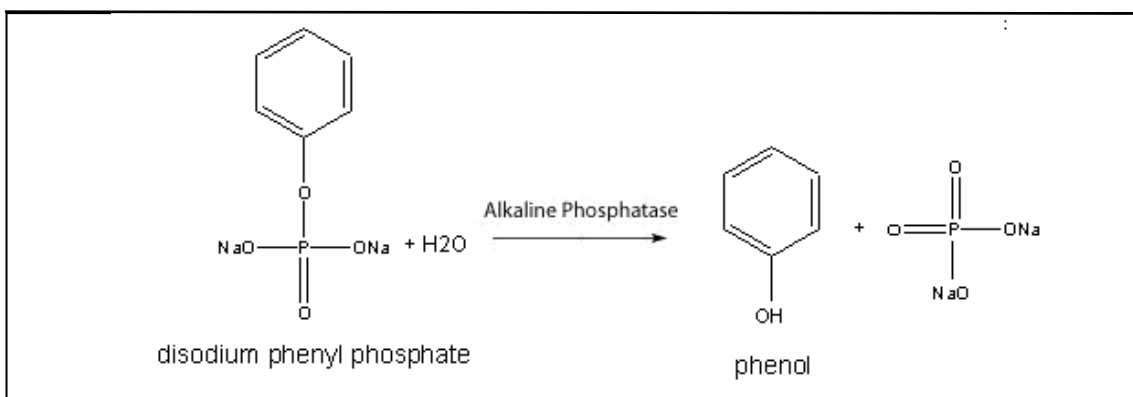


**Figure 3.6** Phenol from disodium phenyl phosphate.

## 3.6 Computer Modelling

### 3.6.1 Required software

The two programs used to resolve complex mathematical equations are:

**FLUENT:** This is a computer program based on a finite volume technique to convert the governing equations to algebraic equations that can be solved numerically. This commercial software is appropriate for solving fluid flow and heat transfer problems.

**COMSOL multiphysics:** This is a finite element analysis and solver software package for various physics and engineering applications, especially for coupled phenomena.

### 3.6.2 Governing equations

The governing equations for fluid dynamics are adapted from Hämäläinen (2001).

#### 3.6.2.1 Fluid flow

The continuity equation simply states that the mass must be conserved. In the cartesian coordinates  $x_i$  this equation can be written as:

$$\frac{\partial \rho}{\partial t} + \frac{\partial(\rho u_i)}{\partial x_i} = 0 \quad (3.8)$$

where  $\rho$  is the density of the fluid,  $t$  time and  $u_i$  the velocity vector. The second equation, conservation of momentum, states that momentum must be conserved. It can be written in the cartesian coordinates as

$$\frac{\partial(\rho u_i)}{\partial t} + \frac{\partial(\rho u_i u_j)}{\partial x_j} = \rho f_i - \frac{\partial p}{\partial x_i} + \frac{\partial \vec{\pi}}{\partial x_j} \quad (3.9)$$

where  $f_i$  is a body force,  $p$  the pressure.  $\vec{\pi}$  is the viscous stress tensor. For laminar flow it is as given by Equation 3.10:

$$\vec{\pi} = \mu \left[ \left( \frac{\partial u_i}{\partial x_j} + \frac{\partial u_j}{\partial x_i} \right) - \frac{2}{3} \delta_{ij} \frac{\partial u_k}{\partial x_k} \right] \quad (3.10)$$

where  $\mu$  is the molecular viscosity and  $\delta_{ij}$  the Kronecker's delta.

For a turbulent flow the stress tensor  $\vec{\pi}$  is resolved according to the standard  $k$ - $\varepsilon$  model. This one relates the turbulent eddy viscosity with the turbulence kinetic energy (TKE)  $k$  and the dissipation rate  $\varepsilon$  through Boussinesq's approximation.

$$\vec{\pi} = \mu \left[ \left( \frac{\partial u_i}{\partial x_j} + \frac{\partial u_j}{\partial x_i} \right) - \frac{2}{3} \delta_{ij} (\rho k) + \mu_t \left( \frac{\partial u_i}{\partial x_j} + \frac{\partial u_j}{\partial x_i} \right) \right] \quad (3.11)$$

$$\mu_t = \frac{\rho C_\mu k^2}{\varepsilon} \quad (3.12)$$

where  $\mu_t$  is the turbulent eddy viscosity and  $\varepsilon$  is the dissipation rate of TKE. The modelled equation of the TKE  $k$  is given by:

$$\frac{\partial}{\partial x_j} (\rho u_j k) = \frac{\partial}{\partial x_j} \left( \frac{\mu_e}{\sigma_k} \frac{\partial k}{\partial x_j} \right) + G - \rho \varepsilon \quad (3.13)$$

In which  $\mu_e = \mu_t + \mu$  is effective viscosity and  $\sigma_k$  and  $\sigma_\varepsilon$  are the turbulent Prandtl numbers for  $k$  and  $\varepsilon$ . Similarly the dissipation rate of TKE is given by the following equation:

$$\frac{\partial}{\partial x_j}(\rho u_j \varepsilon) = \frac{\partial}{\partial x_j} \left( \frac{\mu_e}{\sigma_\varepsilon} \frac{\partial \varepsilon}{\partial x_j} \right) + \frac{\varepsilon}{k} (C_{\varepsilon 1} G - C_{\varepsilon 2} \rho \varepsilon) \quad (3.14)$$

where  $G$  is the rate of generation of the TKE, while  $\rho \varepsilon$  is its destruction rate.  $G$  is given by:

$$G = \mu_e \left[ \left( \frac{\partial u_i}{\partial x_j} + \frac{\partial u_j}{\partial x_i} \right) \frac{\partial u_i}{\partial x_j} \right] \quad (3.15)$$

$C_\mu$ ,  $C_{\varepsilon 2}$ ,  $\sigma_k$  and  $\sigma_\varepsilon$  are empirical constants in the turbulence transport equations.

The turbulence equations are diverse and it is suitable to choose one according to the presented problem. As previously stated; the tempering equipment consists of a spiral submerged into a cold or hot water bath. Due to its geometry, there is a turbulent flow that does not follow the turbulence laws of  $k - \epsilon$  model. A model which would be appropriate for this kind of problem is called the Reynolds Stress Model (RSM), which was found to provide a very precise result when dealing with flows that contain streamline curvature, rotation, and swirl.

The model is anisotropic, that is, the deformation rates are not the same in all of the directions; this model proposes the following reformulation of the equation 3.9:

$$\begin{aligned} \frac{D \overline{u_i u_j}}{dt} = & - \left( \overline{u_i u_k} \frac{\partial u_j}{\partial x_k} + \overline{u_j u_k} \frac{\partial u_i}{\partial x_k} \right) \text{ Term I and II} \\ & - \frac{\partial}{\partial x_k} \left[ \overline{u_i u_j u_k} + \frac{1}{\rho} \left( \overline{p u_i} \delta_{jk} + \overline{p u_j} \delta_{ik} \right) - \nu \frac{\partial \overline{u_i u_j}}{\partial x_k} \right] \text{ Term III} \end{aligned}$$

$$+ \frac{p}{\rho} \left( \frac{\partial u_i}{\partial x_j} + \frac{\partial u_j}{\partial x_i} \right) - 2\nu \left( \frac{\partial u_i}{\partial x_k} \frac{\partial u_j}{\partial x_k} \right) \quad \text{Term IV and V} \quad (3.16)$$

The term I represents the rate of change of  $\overline{u_i u_j}$  along a streamline.

The term II represents the rate of production of  $\overline{u_i u_j}$  by mean shear, which is the reason for turbulence.

The term III represents the rate of spatial transport of  $\overline{u_i u_j}$  by the action of turbulence fluctuations, pressure fluctuation and molecular diffusion.

The term IV represents the redistribution of the available turbulent kinetic energy amongst the fluctuating velocity components. The redistribution term just drives turbulence towards isotropy by redistributing energy.

The term V represents the dissipation rate of  $\overline{u_i u_j}$  due to molecular viscous action.

### 3.6.2.2 Temperature field

The third equation, conservation of energy, states that the energy must be conserved. It can be written as (FLUENT 2003):

$$\frac{\partial(\rho C_p T)}{\partial t} + \frac{\partial}{\partial x_j} (\rho C_p T u_j) = \frac{\partial}{\partial x_j} \left( \lambda \frac{\partial T}{\partial x_j} \right) + Q_j \quad (3.17)$$

where  $Q_j$  is an external source of heat (like in the case of electrical problems where there is a joule heating), that can be expressed as (Fiala *et al.*, 2001):

$$Q_j = \sigma(T) E^2 \quad (3.18)$$

### 3.6.2.3 Electrical potential

The equations to resolve the electrical potential are based on charge conservation (Fiala *et al.*, 2001):

$$\frac{\partial(J)}{\partial x_i} = \frac{\partial}{\partial x_i} \left[ \sigma(T) \frac{\partial U}{\partial x_i} \right] = 0 \quad (3.19)$$

where  $\sigma$  represents the conductivity,  $U$  is the electric potential and  $J$  is the current density.

It is assumed that the pulsating electric field does not induce a time varying magnetic field, thus  $\frac{\partial(E)}{\partial x_i} = 0$  (Gerlach *et al.*, 2008). In consequence, the electric

field vector  $E$  can be written as the gradient of the electrical potential  $U$  .

$$E = - \frac{\partial U}{\partial x_i} \quad (3.20)$$

### 3.6.3 Geometrics models and mesh

The models used are illustrated in Figure 3.7 and 3.8. Figure 3.8 shows the spiral geometry and mesh, while Figure shows the treatment chamber and mesh.

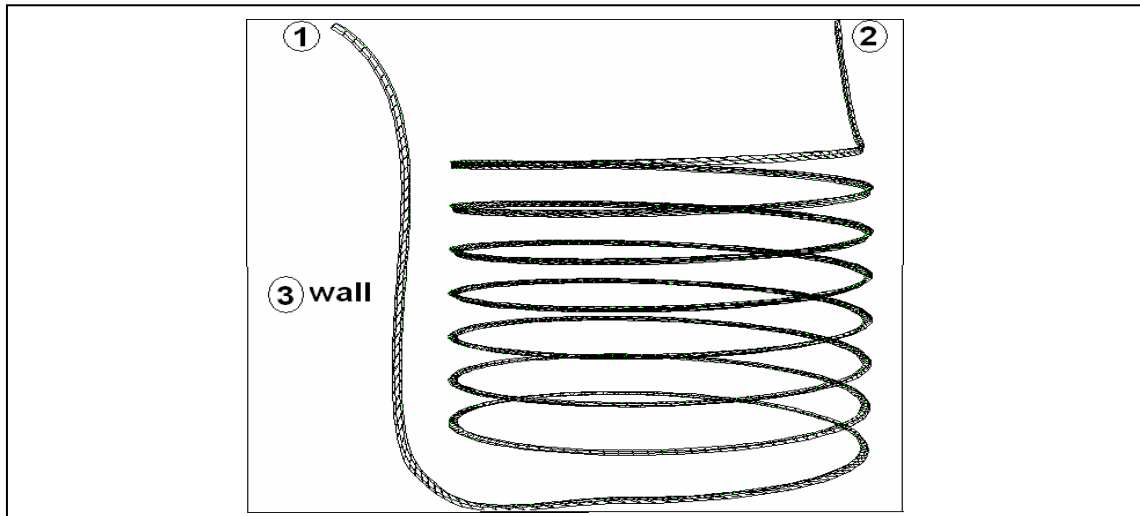


**Figure 3.7** Spiral geometry and mesh.

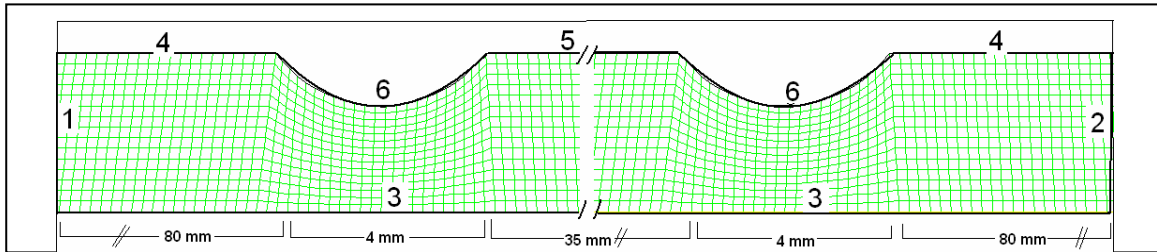


**Figure 3.8** Treatment chamber and mesh.

### 3.6.4 Boundary conditions

The equations for each thermophysical variable were incorporated into the model as functions of the temperature.

In the case of the spiral heat exchanger, the thermophysical properties are the ones presented in section 3.3.1.2

In case of the velocity profiles in the treatment chamber, the thermophysical properties are considered to be constant.

In the case of the temperature profile in accordance with Joule heating, the thermophysical properties are considered to be constant, with the exception of conductivity.

The variable  $Q_j$  (external source of energy in the heat transfer equation) was multiplied by the factor  $f\tau$ , where  $f$  is the applied pulses frequency and  $\tau$  the pulse width. In this way, it is considered that only relevant quantity is emitted in the PEF treatment.

The advantage of carrying out this operation lays in the fact that problems can be resolved in a stationary state, which means less calculation time.

All boundary conditions according to FLUENT (2003) and COMSOL (2005) are summarized in Table 3.2.

**Table 3.2** Boundary conditions according to FLUENT and COMSOL .

Boundary and number	Expression
<p><b>Spiral heat exchanger (Figure 1)</b></p> <ul style="list-style-type: none"> <li>• Thermal model <ul style="list-style-type: none"> <li>○ Inflow (1)</li> <li>○ Wall (3)</li> </ul> </li> <li>• Flow model <ul style="list-style-type: none"> <li>○ Inflow (1)</li> <li>○ Outflow (2)</li> </ul> </li> </ul>	$T = T_0$ $n \cdot \lambda \nabla T = \alpha (T_\infty - T_0)$ $k = \frac{3}{2} (v_0 I)^2; I \cong 0,16 (\text{Re}_{DH})^{-1/8} \quad \varepsilon \cong 2,35 \frac{k^{3/2}}{D}$ $v = 0, \quad p = 0$
<p><b>Velocity profile on chambers (Figure 2)</b></p> <ul style="list-style-type: none"> <li>• Flow model <ul style="list-style-type: none"> <li>○ Inflow (1)</li> <li>○ Outflow (2)</li> <li>○ Symmetry axis (3)</li> </ul> </li> </ul>	$k = \frac{3}{2} (v_0 I)^2; I \cong 0,16 (\text{Re}_{DH})^{-1/8} \quad \varepsilon \cong 2,35 \frac{k^{3/2}}{D}$ $v = 0, \quad p = 0$ $v = 0$
<p><b>Joule heating in PEF chamber (Figure 2)</b></p> <ul style="list-style-type: none"> <li>• Electrostatic model</li> </ul>	

<ul style="list-style-type: none"> <li>○ HV electrode (4)</li> <li>○ Ground electrode (5)</li> <li>○ Insulator (6)</li> <li>• Thermal model <ul style="list-style-type: none"> <li>○ Inflow (1)</li> <li>○ Outflow (2)</li> <li>○ Wall (2 – 6 all)</li> </ul> </li> <li>• Flow model <ul style="list-style-type: none"> <li>○ Inflow (1)</li> <li>○ Outflow (2)</li> <li>○ Wall (4,5,6)</li> <li>○ Symmetry axis (3)</li> </ul> </li> </ul>	$U = U_0$ $U = 0$ $n \cdot \sigma \cdot \nabla U = 0$ $T = T_0$ $n \cdot q = 0, \quad q = -k \nabla T$ $n \cdot k \nabla T = 0$ $v = 2v_0 \left(1 - (r/R)^2\right)$ $v = 0, \quad p = 0$ $v = 0$ $v = 0$
---	--

## 4 Result and Discussion

### 4.1 Enzyme Inactivation

The study of the phosphatase inactivation with pulsed electric field was performed in raw milk.

The variation of the ALP activity of all analysed samples is shown in Figure 4.1 together with the variations in raw milk composition during the whole experimental time (June 07 - February 08).

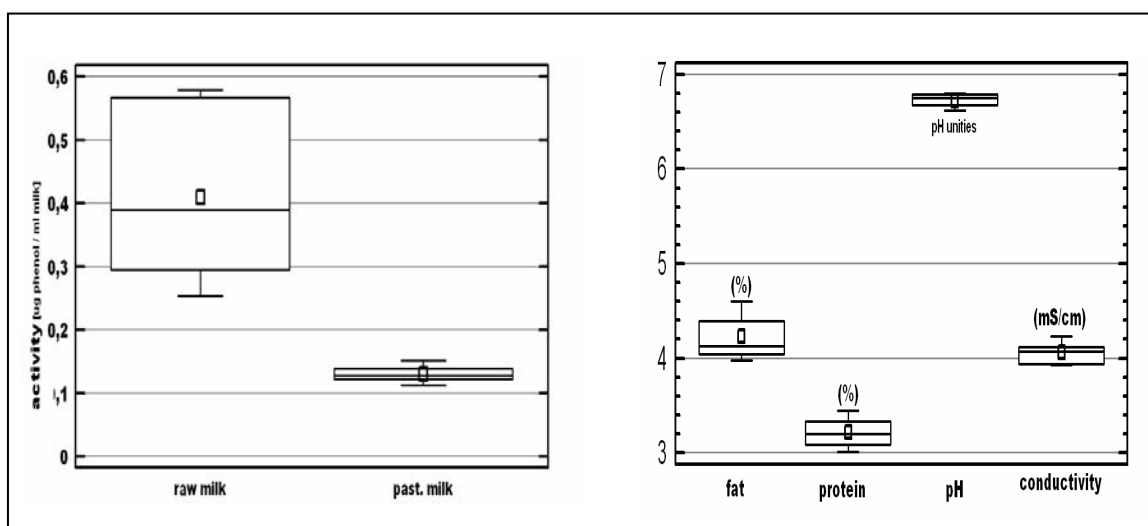


**Figure 4.1** Variation of ALP activity expressed as  $\mu\text{g phenol} / \text{ml milk}$  in raw and pasteurized milk together with variation in the raw milk composition

In the Figure 4.1 (left) the variation of the enzyme activity in raw and pasteurized ( $100^{\circ}\text{C} / 2 \text{ min}$ ) milk is shown, with an average value of  $0.409 \pm 0.12$  and  $0.130 \pm 0.012$  respectively.

The variation in raw milk could be due to intrinsic factors, such as: feed of the cattle, differences in the amount of the components where the enzyme is found (fat and proteins), etc. On the other hand, in the pasteurized milk, there is no significant difference in the enzyme activity, since it concerned a thermo

sensible enzyme, which after a thermal treatment, as expected, will be completely inactivated.

Figure 4.1 (right) shows differences in milk composition and physicochemical properties. This enzyme is found principally in the fat and protein fraction, and as observed, the range for the amount of these components varies between 3.98 – 4.6 % and 3.01 – 3.45 respectively, so it can be said that more phosphatase is found in the samples that have more fat and protein. As fluctuations of composition were distributed randomly over the whole period and ALP activity was always referred to the corresponding untreated raw milk sample, a systematic influence can be neglected.

Furthermore, it is important to analyze how the pH and the conductivity vary, since PEF treatment is related with both parameters. Moreover, the pH value has a strong impact on the enzyme stability. As observed, no variations are found within both factors.

#### **4.1.1 Impact of PEF Treatment on Phosphatase Activity**

The experiment of the PEF impact on phosphatase activity was performed in the treatment chamber with co-linear electrodes and in the treatment chamber with parallel electrodes.

It is important to note that PEF treatments were carried out reaching levels of energy input up to 300 kJ / kg, this means that the increase of temperature in the sample could be up to 75 K (with a heat capacity of approx. 4 kJ/kg K). To avoid this, the treatment was separated into 3 cycles. In each cycle a maximum of 100 kJ / kg was used, thus obtaining a maximum increase in temperature of 25 K. After each cycle, the milk was carried to its initial temperature. Temperature increase in bath treatment with parallel plate electrodes was only in the range of 20 – 29 K and therefore negligible. Energy input could then be applied in one cycle.

#### 4.1.1.1 Effect of electric field strength

In order to study the effect of the electric field on the phosphatase inactivation, experiments were performed at 3 different voltage levels which are relevant for microbial inactivation. The parameters used are summarized below:

**Table 4.1** Parameters used to study the effect of electric field on ALP.

Parameter			
Flow [l/h]	5	5	5
T input [°C]	20	20	10
T output [°C]	36	37	31
voltage [kV]	16	20	22.5
Freq [Hz]	46	30	35
Epulse [J/pulse]	2.16	3.3	4.2
Energy input [kJ/kg]			
1st cycle	71.539	71.28	105.84
2nd cycle	143.078	142.56	211.68
3th cycle	214.618	213.84	317.52

The figure below shows the enzymatic inactivation at three different levels of electric field strength and three levels of energy input

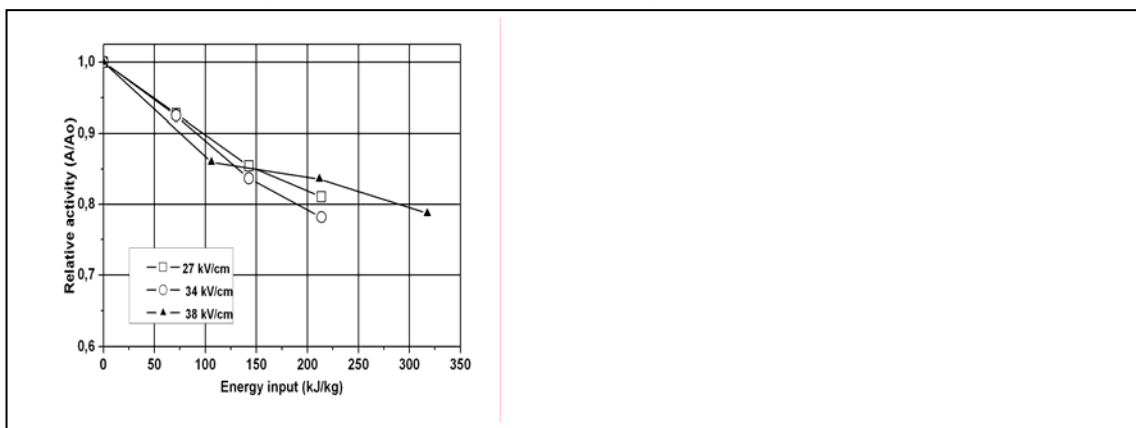


**Figure 4.2** ALP inactivation in function of the electric field strength and energy input.

Analysis of variance at a 95% confidence with  $p = 0.522$  confirms that there are no significant differences in the enzyme inactivation produced by the electric field. The ANOVA was applied for each level of energy input. However, it is clear that there is a downward trend in the inactivation curve with increasing energy input.

#### 4.1.1.2 Effect of energy input

As it was confirmed, that the intensity of the electric field in the range of 27 to 38 kV/cm does not have any affect on phosphatase inactivation by PEF and that there is no dependence between this electric field strength and the energy input concerning inactivation, the samples can be treated at different levels of electric field strength for the analysis. Summarized below are the parameters used.

**Table 4.2** Parameter used to study the impact of energy input on ALP.

Parameter	Continuous/square wave pulse	
	Mass flow [kg/h]	5
T input [°C]	10	20
T output [°C]	31	37
Freq [Hz]	35	30
Pulse number per volume in treatment zones per cycle	5	4.6
Residence time in treatment zones per cycle [s]	0.154	0.154
Voltage [kV]	22.5	20
Elec. field strength [kV/cm]	38	34
Epulse [J/pulse]	4.2	3.3
Energy input [kJ/kg]		
1st cycle	105.84	71.28
2nd cycle		142.56
3th cycle	317.52	213.84

The residence time was calculated considering the zone corresponding to the two insulators (each insulator 4 mm in diameter and 4 mm in length) and 1 mm before and after each insulator (6 mm in diameter and 1 mm in length)

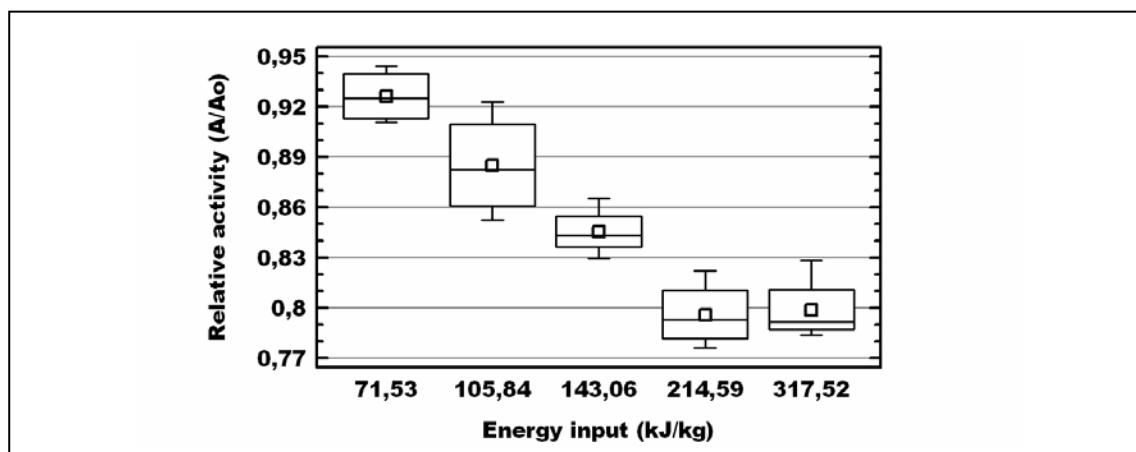


**Figure 4.3** Inactivation in function of the energy input.

Analysis of variance at a 95% confidence with  $p = 0.000$  confirms that there are significant differences in enzyme inactivation produced by different levels of energy input. The differences, according to the ANOVA were found between all levels, except between the last two (214 and 317 kJ / kg).

The phosphatase inactivation is closely related with temperature and pH. The effect of temperature on this analysis can be discarded, since the maximum temperature reached was 37 °C, and the enzyme does not present any level of inactivation at this temperature.

Although the samples used have a very narrow variation among its pH values, the local pH change that occurs on the electrodes surface cannot be controlled.

As known, the enzyme is very sensitive to pH changes. In each treatment there are electrochemical reactions on the electrode surface, and therefore local pH changes occur. This local change in pH value can be very large, if the electrodes surface and the residence time of the sample on the electrodes

surface are large, but this does not occur in the type of treatment chamber used, because the contact time with the electrodes does not exceed 0.2 s.

As previously mentioned, the treatment was performed in 3 cycles to achieve the desired higher energy input, i.e., the time of contact between the sample and the electrode increases with the cycles. The enzyme inactivation could then be related with the contact and the time that the sample has with the electrodes and not with the energy input.

To dismiss or confirm this fact, experiments were performed in a chamber of parallel electrodes, with an electrode surface of 2 cm<sup>2</sup>, an electrode gap of 2 mm and a treatment time up to 3 s. Summarized below are the parameters used.

**Table 4.3** Parameter used to study the impact of BACTH system on ALP.

Parameter	BACTH /exponential pulse	
	Mass [g]	0.4
T input [°C]	19	19
T output [°C]	26	29
Freq [Hz]	30	30
Pulse number per volume in treatment zones per treatment step	102	65
Residence time per treatment step [s]	3.4	2.167
Voltage [kV]	5.44	6.8
Elec. field strength [kV/cm]	27.2	34
Epulse [J/pulse] (Equation 2.12)	0.278	0.438
Energy input [kJ/kg]		
1st step	70.89	71.175
2nd step	141.78	142.35
3th step	212.67	213.525

Figure 4.4 shows the effect of the energy input on the phosphatase inactivation in a treatment chamber with parallel electrodes.

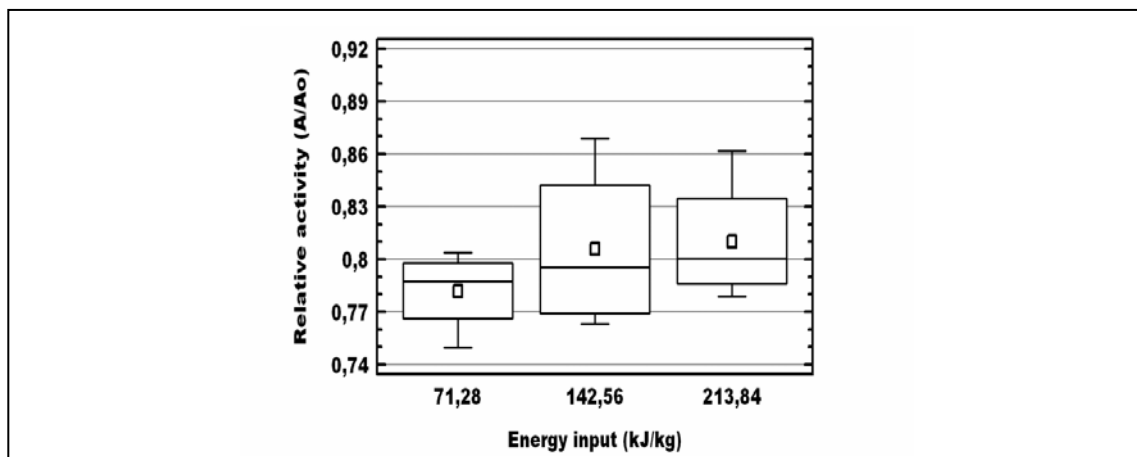


**Figure 4.4** Impact of energy input on ALP activity.

As observed, the energy input has no impact on the enzymatic inactivation.

ANOVA at a 95% confidence with  $p = 0.530$  confirmed it. The reason for the enzymatic inactivation could be the electrochemical reactions and also their related local pH-value change. However, in both cases (co-linear and parallel electrodes) the same maximum level of enzyme inactivation around 20% was found, independent from the treatment chamber and the pulse shape. In case of cuvette treatment there is a large electrode area and nearly all the sample is in contact with the electrodes. Therefore the impact of electrochemical reactions on the sample is much higher than in the case of continuous treatment in co-linear geometry.

In cuvette treatment inactivation is already obtained at low energy input (residence time) whereas for co-linear chamber multiple cycles of passing the small electrode surface are needed for the same inactivation.

#### 4.1.1.3 Effect of pulse shape

The following section presents the parameters of the previous section in order to perform a comparison between the pulse shape and the enzyme inactivation.

**Table 4.4** Parameters used for batch and continuous system to study the effect on ALP activity.

Parameter	BACTH /exponential pulse		CONTINUOUS/square pulse	
	mass [g]	0.4	0.4	5
T input [°C]	19	19	20	20
T output [°C]	26	29	36	37
Freq [Hz]	30	30	46	30
Pulse number per volume in treatment zones	102	65	7	4.6
Residence time (sec)	3.4	2.167	0.154	0.154
voltage (kV)	5.17	6.67	16	20
Elec. field strength [kV/cm]	27.2	34	27.2	34
Epuls [J/puls]	0.278	0.438	2.16	3.3
Energy input [kJ/kg]				
1st cycle	70.89	71.175	71.539	71.28
2nd cycle	141.78	142.35	143.078	142.560
3th cycle	212.67	213.525	214.618	213.840

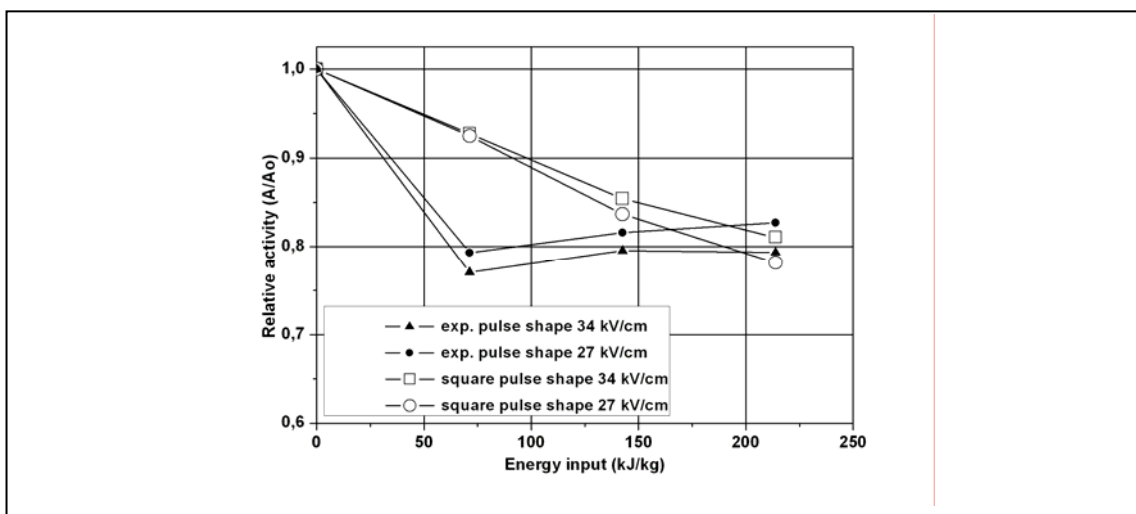


**Figure 4.5** Effect of pulse form on the inactivation of ALP.

As previously mentioned, the maximum of 20% of enzymatic inactivation found, is independent of the treatment chamber type and the pulse shape. This fact can be observed between the energy levels of 140 kJ/kg and 240 kJ/kg; at this level of energy input a significant difference, at a 95% confidence with  $p = 0.2052$ , among the enzymatic inactivation was not found. Here the residence time and the electrode contact time in both chambers is large enough to produce the same effect on the enzyme inactivation.

A difference is observed in the first cycle (70 kJ/kg). Here, the chamber with parallel electrodes already reaches the 20% of enzymatic inactivation, because the residence time and electrode contact in the chamber with parallel electrodes is higher in comparison with the chamber with co-linear electrodes. This confirms that the chemical reactions and the electrode media contact surface of the sample have an influence on the enzymatic inactivation.

#### **4.1.1.4 Effect of temperature**

In this section the effect of the temperature on a PEF enzyme inactivation was investigated.

The PEF treatments were performed at three different energy input levels. As said in section 2.2.2, for square shape pulses, the energy input is the product of the maximum voltage, the current intensity and the pulse width.

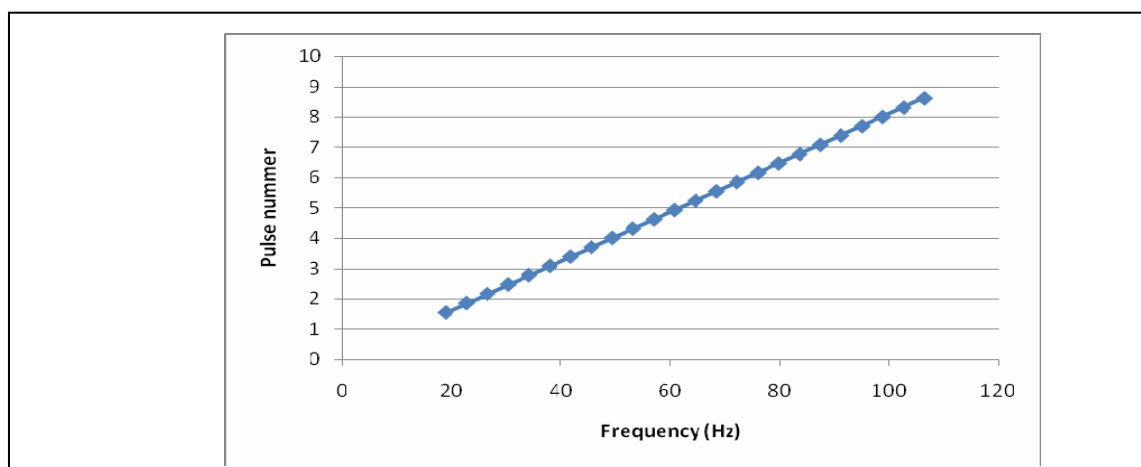
The current can easily flow across the liquid food sample when a larger amount of solute is present and the temperature is higher. Therefore, when an experiment is performed at relatively high temperature, this would produce an energy increment per pulse and also an increment of the energy input.

To compare two experiments it is important to maintain the energy input constant. This can be achieved by varying the frequency or pulse width. In the following table the used parameters are summarized.

**Table 4.5** Parameter used to study the effect of the temperature on ALP activity.

flow [l/h]	5	5	5	5	5
T input [°C]	10	12	20	37	39
T output [°C]	31	34	44	60	62.9
Electric field strength [kV/cm]	38.25	38.25	38.25	38.25	38.25
Freq [Hz]	35	40	35	27	27
Epuls [J/puls]	4.2	3.68	427	5.5	5.5
Energy input [kJ/kg]					
1st cycle	105.84	105.984	107.604	106.92	106.92
2nd cycle	211.68	211.968	215.208	213.84	213.84
3th cycle	317.52	317.952	322.812	320.76	320.76

The pulse repetition frequency was modified in order to obtain the same energy input levels for all the used temperatures for a determined cycle. The used range for frequency values is not considered important, because for 27, 35 and 40 Hz, respectively 2.15, 2.17 and 3.38 pulses receive the volume of liquid food (see Figure 4.6).

**Figure 4.6** Pulse number per volume in treatment zone for a mass flow of 5 kg/h and conductivity of media of 4.6 mS/cm.

The pulse number per volume in the treatment zone was calculated considering the zones that corresponded to the two insulators (each insulator 4 mm in diameter and 4 mm in length) and 1 mm before and after each insulator (6 mm in diameter and 1 mm in length) and the residence time that results of the flow velocity.

Figure 4.17 shows the effect of temperature on the PEF treatment.

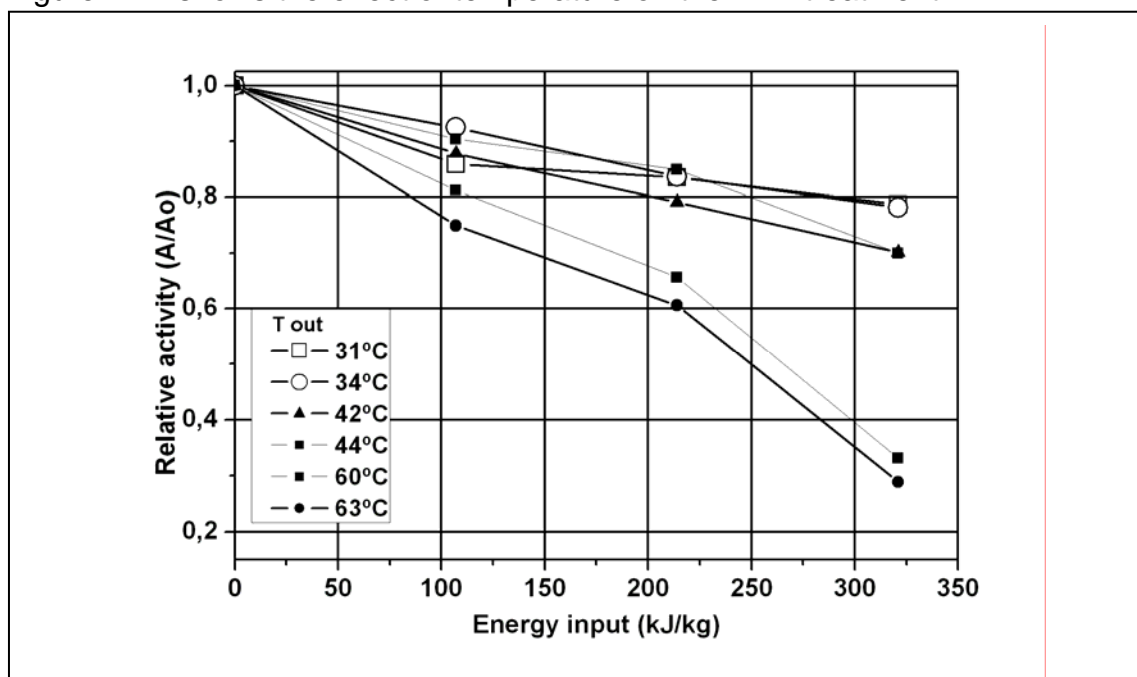


**Figure 4.7** Impact of the temperature treatment on the ALP activity.

As can be observed, the main inactivation difference existed when the treatment was performed at higher temperature levels. But no significant difference was found on the first cycle (energy input 105 kJ/kg) at a 95% confidence with  $p = 0.1195$ . On the second and third cycles (energy input of 211 and 317 kJ/kg respectively) a significant difference was found at a 95% confidence with  $p = 0.0001$ , only among the two samples that were exposed at 60 and 63 °C, showing a noticeable difference when compared with the remaining samples.

With these results, it could be said that temperature has a strong impact on the enzyme inactivation by PEF treatments. It must be considered that before the PEF treatment the inlet temperature range did not cause inactivation. After PEF treatment, the temperature increase was in the range of thermal inactivation especially when considering holding times between treatment chamber and cooling device.

For this reason, it is important to know exactly how the PEF – cooling equipment is constructed, in order to calculate the temperature and time, in which the sample is exposed.

#### 4.1.2 Temperature – time profile of Milk in PEF Equipment

The temperature profile in each section of the PEF equipment was determined with raw milk.

In the equipment used, there are five zones with different temperature profiles. These zones are summarized below in the Time-Temperature diagram:



**Figure 4.8** Time-Temperature diagram in PEF system.

Zone A is a heating coil made of stainless steel with 2 mm inner diameter and 2.34 m length, with a volume of 7.3 ml for pre-heating to the desired operating temperature with a flow rate of 5 l/h. For calculation of the temperature distribution in the coil, a finite element method was used, based on the classical laws of thermodynamics and appropriate CFD equations, as described in section 3.7.2 (Governing equations). As already mentioned, it was necessary to calculate experimentally the heat transfer coefficient  $\alpha$  in  $\text{W/m}^2\text{K}$ , using the method described in the same section 3.7.2.

The following table shows the results for the heat transfer coefficient and the temperature profile:

**Table 4.6** Parameters for heat exchanger (heating).

Temperature inlet (°C)	Temperature outlet (°C)	T water bath (°C)
13	44	46
heat transfer coefficient ( $\text{W/m}^2\text{K}$ )	average heat capacity (kJ/kgK)	mass flow (kg/h)
1132	3.98	5

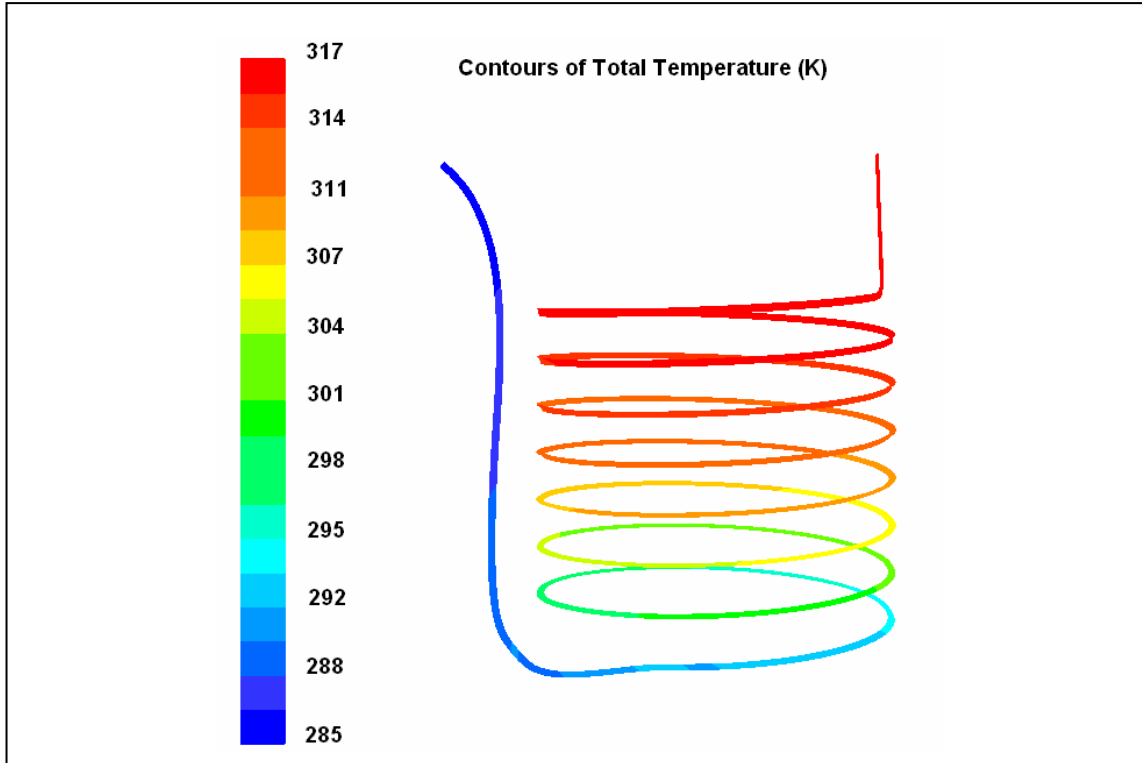


**Figure 4.9** Temperature contours for the spiral heat exchanger.

Zone B is just a tube that connects the heating coil with the treatment chamber. The temperature here is assumed constant.

Zone C is the treatment chamber. This is a very important zone, because there the maximum temperature in the process is achieved.

The bulk temperature in the treatment chamber can be calculated grouping equations (9) and (13).

$$\Delta T = \frac{W_{puls} \cdot f}{m \cdot Cp} \quad (4.1)$$

In order to obtain just the delivered energy, the residence time  $t_{res}$  can also be aggregated. Therefore, it can be obtained as follows:

$$T_2 = \frac{W_{puls}}{m \cdot Cp} \cdot f \cdot t_{res} + T_1 \quad (4.2)$$

In our case, this equation takes the following value:

$$T_2 = 0,559 \cdot f \cdot t_{res} + T_1 \quad (4.3)$$

It is important to emphasize that the bulk temperature is the average value of all the generated temperatures by Ohmic heating on the electrodes and insulators. The following figure shows the temperature distribution in the treatment chamber. In chapter 4.1.7 more information about the Ohmic's heating in the treatment chamber is given. The temperature increment in the treatment chamber is produced for a very short time interval (0.15 s), which is not enough to produce thermal phosphatase inactivation. For this reason, only the final temperature achieved in the PEF treatment is considered, in order to study the thermal phosphatase inactivation.

Zone D is a tube which connects the treatment chamber with the cooling system. In this section, the temperature is assumed constant.

Zone E is the cooling coil, with 2 mm in diameter and 2.34 m in length, with a volume of 7.3 ml of milk, operated at a flow rate of 5 kg/h, to cool the medium to the desired temperature. In some PEF equipment, the coil system is connected to another treatment chamber, and in this case it is important to control the cooling capacity. Also in our situation, this control is important in order to know how long the enzyme is exposed to the temperature achieved in the treatment chamber.

The procedure to calculate the cooling rate is similar to the one described for zone A. The results are summarized below:

**Table 4.7** Parameters for heat exchanger (cooling).

Temperature inlet (°C)	Temperature outlet (°C)	T cooling media (°C)
63	20	10
Heat transfer coefficient (W/m <sup>2</sup> K)	average heat capacity (kJ/kgK)	mass flow (kg/h)
613	3.98	5

To validate the mathematical model the experiment was made with raw milk. The input and output temperatures were measured and the output temperature was compared with the mathematical model.

The parameters used are as follows:

**Table 4.8** Experimental and modeled temperatures and the prediction error.

Experimental data				Model results	Predicted error $100 \times (T_{\text{exp}} - T_{\text{simulated}})/T_{\text{exp}}$
$T_{\text{inlet}}$	$T_{\text{outlet}}$	$T_{\text{cooling medium}}$ (10% glycerol)	$\alpha$ (W/m <sup>2</sup> K)	$T_{\text{outlet}}$	Error %
°C	°C	°C		°C	
50.1	16.5	9.8	674.92	17.0	3.03
55.5	18.2	10.0	673.16	18.8	3.29
58.6	18.9	11.0	675.58	19.2	1.58
60.7	19.6	11.0	659.87	20.5	4.59
61.3	20.0	11.0	647.29	21.0	5.00
64.9	21.5	11.0	612.51	21.9	1.86

#### 4.1.2 Thermal Inactivation of Phosphatase

As described, the PEF treatment chamber is connected with the cooling system with a tube. In this tube the temperature stays constant for approximately 9 s, depending on flow velocity. Therefore it is important to determine thermal phosphatase inactivation behavior in the range of seconds, in order to relate it with the temperature – time diagram described above.

Glass capillary method was used for this aim. The thin wall and the small diameter of the glass capillary ensure a quick heat transfer between the

tempered water and the milk in the capillary (Jaeger, 2006, Hass *et al.*, 1996a, Haas *et al.*, 1996b)

The determination of phosphatase activity was performed in a range of temperatures between 60 – 70°C and 2 – 18 sec. The phosphatase has not shown an inactivation below 60 °C for the used time range.

Below the results of phosphatase inactivation are summarized in Figure 4.10:

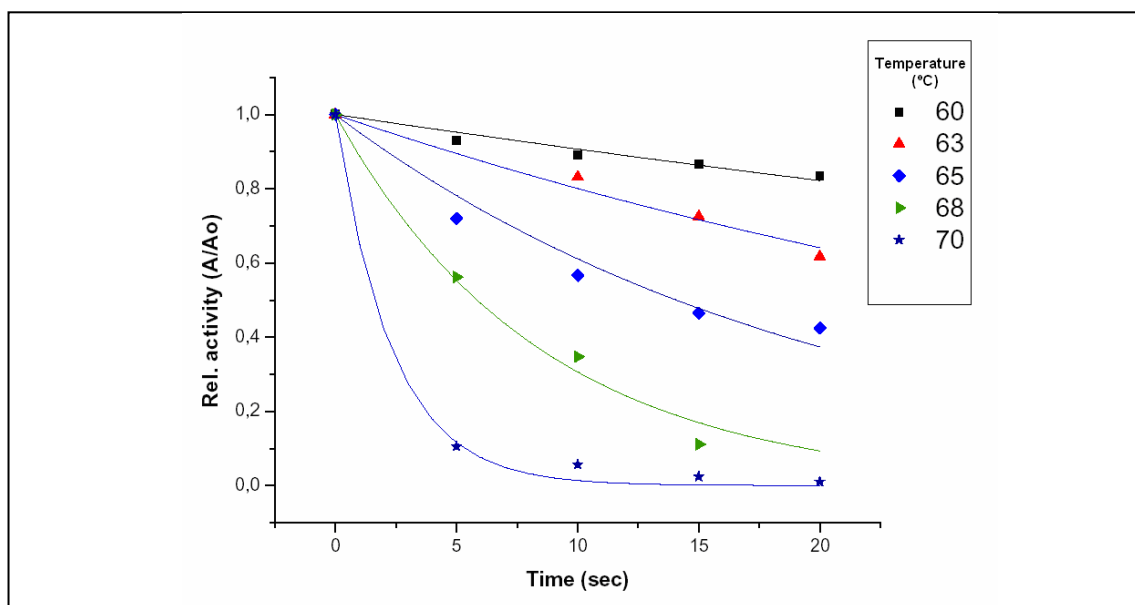


**Figure 4.10** Thermal inactivation of ALP in raw milk at different temperatures and residence time determined using a glass capillary method.

Linear regression at each temperature level was performed and first order equations were obtained. These equations give relative activity depending on inactivation time and an inactivation constant  $k$  which is different for different temperatures.

$$relA = e^{-k \cdot t} \quad (4.4)$$

It is possible to obtain a  $k$  value for each temperature, and therefore an equation that relates between temperature and the inactivation constant  $k$ :

$$k = e^{(-a+b \cdot T)} \quad (4.5)$$

The equation 3.3 can be inserted in the equation 3.2 obtaining a description of the relative enzyme activity  $A$ , depending on temperature  $T$  and treatment time  $t$  as shown on the right side of Figure 3.2.

$$relA = e^{-e^{(-a+bT)} \cdot t} \quad (4.6)$$

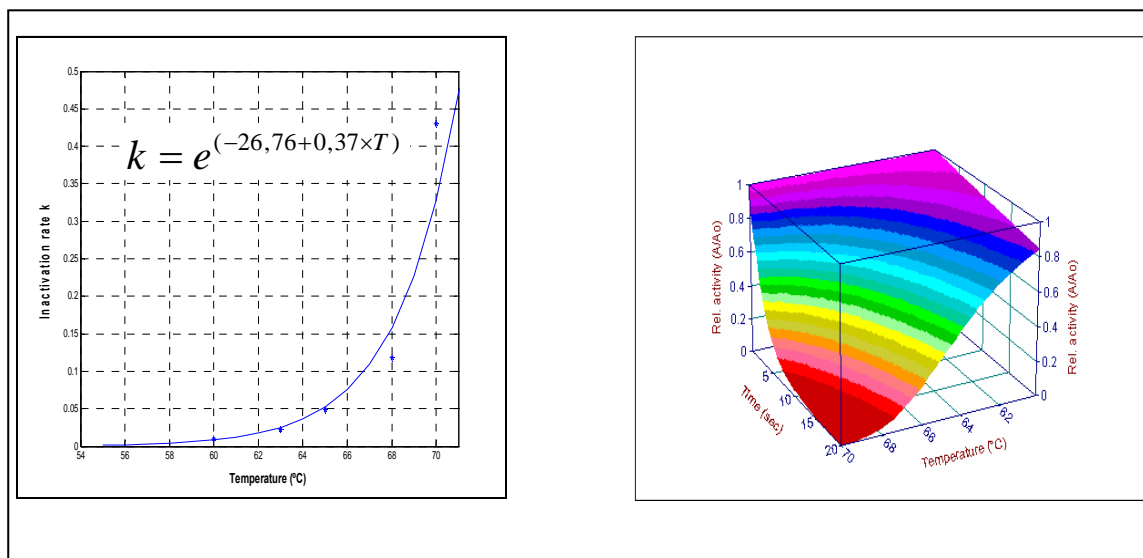


**Figure 4.11** Inactivation rate constant  $k$  of thermal ALP inactivation in milk dependent on temperature (left). Inactivation of ALP dependent on temperature-time (right).

Based on these results, the thermal phosphatase inactivation was calculated during the PEF treatment. It is possible to integrate the equation 4.5 in function of the time and temperature during the total process (Figure 4.10 left), then the following graphics can be obtained:

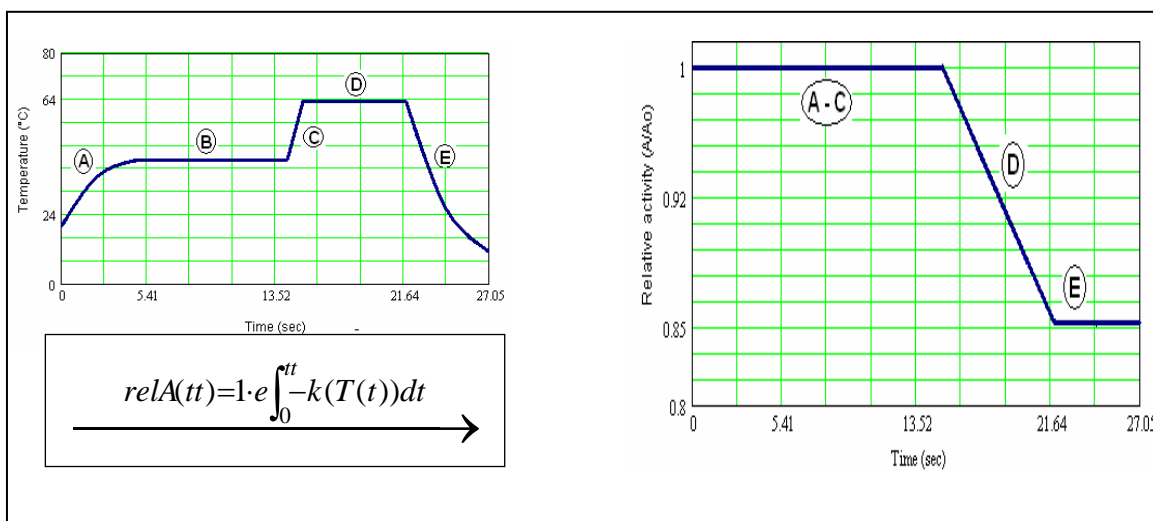


**Figure 4.12** Diagram temperature-time during the PEF treatment (left). The figure (right) shows the phosphatase inactivation according to the temperature- time presented in the diagram of left side. This example was performed with an inlet temperature of 23 °C, energy input of 120 kJ/kg, energy per pulse of 4,1 J and a frequency of 35 Hz.

As observed, there is no phosphatase inactivation in the zone between A and C, because the temperature achieved here for the zones A and B is under 40°C, and in the zone C (treatment chamber) the residence time is too short to produce enzyme inactivation, therefore the inactivation begins when the milk sample leaves the treatment chamber and flows in the tube where the temperature is constant (zone D) for 7.5 sec. The inactivation continues until the milk sample enters in the cooling coil (zone E), where nearly no inactivation exists because of very rapid cooling

#### 4.1.4 Comparison between PEF and Thermal – effect in Phosphatase inactivation

In a PEF treatment there are many factors which have an impact on the enzyme inactivation, such as: Temperature, pH, electrochemical reaction, and the PEF

treatment itself. The temperature is considered one of the major factors that results in enzyme inactivation, therefore in the present work the thermal effect was separated from the PEF effect, both occurring at the same time during PEF-processing.

With this purpose, an experiment with rising temperatures and energy input was performed, and then, the thermal enzyme inactivation was subtracted from the total inactivation, in order to obtain just the remaining enzyme inactivation which would come from the PEF treatment itself.

Summarized are the parameters below:

**Table 4.9** Parameters used to study the temperature and PEF effect on ALP.

Parameter	1	2	3	4
flow [l/h]	5 L/h	5 L/h	5 L/h	5 L/h
T inlet [°C]	20	20	20	20
T outlet [°C]	42	60	63.8	66.7
voltage [kV]	22.5 kV	22.5 kV	22.5 kV	22.5 kV
Freq [Hz]	28	47	49	51
Epuls [J/puls]	4.8	5.37	5.45	5.5
Energy input [kJ/kg]	96.768	181.7208	192.276	201.96

The following figures show the thermal and PEF effect on the enzyme inactivation.

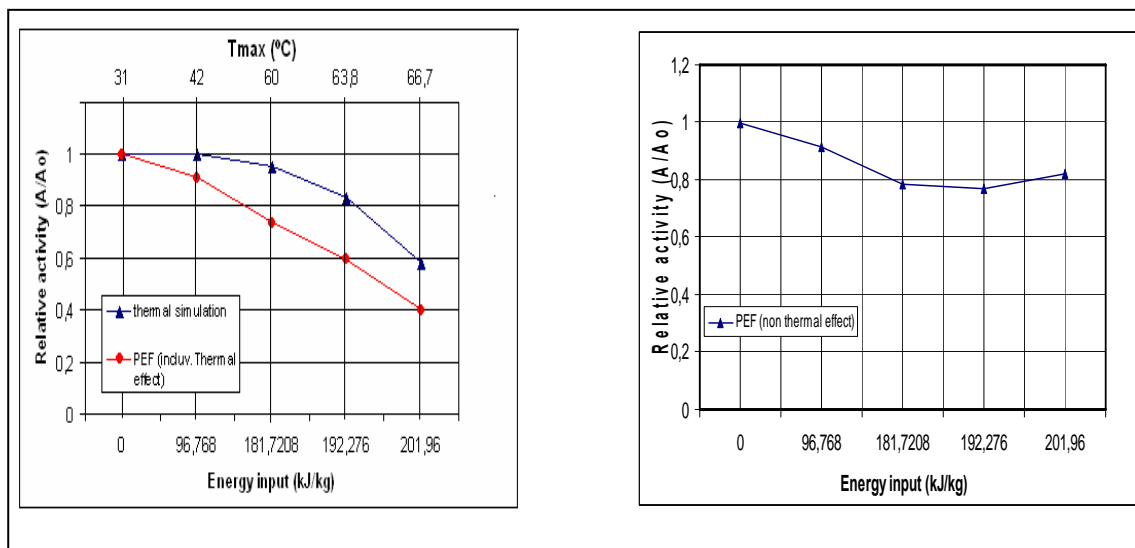


**Figure 4.13** Simulation of thermal phosphatase inactivation and PEF treatment (left) and PEF treatment without thermal inactivation (right)

As observed, the maximum enzyme inactivation is found in the PEF treatments where the energy input is higher; there the temperature is also higher (Figure 4.11 left). At 96 kJ/kg a maximum temperature of 42 °C is achieved, and there is no inactivation due to thermal effect, so the inactivation corresponds only to PEF treatment. When the temperature effect is subtracted from the PEF treatment, the graphic on the right side is obtained. It is also noticeable that this inactivation achieves a maximum value of 20 %, these results fit with all the results obtained in the present work obtained during treatment in cuvettes or continuous treatment in multi pass system, where no critical temperature was exceeded.

## 4.2 Effect of chamber geometry in PEF treatments

The PEF treatment chamber has a strong impact on the process. It mainly affects the electric field strength distribution and therefore the microbial inactivation. The electric field produced in a food processing treatment chamber must satisfy minimum requirements, such as:

- It must provide average electric field strength, high enough to produce a lethal effect on the microorganisms.
- The electric field strength must be homogeneous, whereby all the food receives the same treatment.

In the next section, two different geometries of treatment chambers are described, both of co-linear type, in which food is processed as continuous system by square-wave pulses.

#### 4.2.1 Treatment chamber geometry

The main difference between both treatment chambers is the insulator geometry and therefore the electric field strength intensity and distribution, as shown in the following figure.

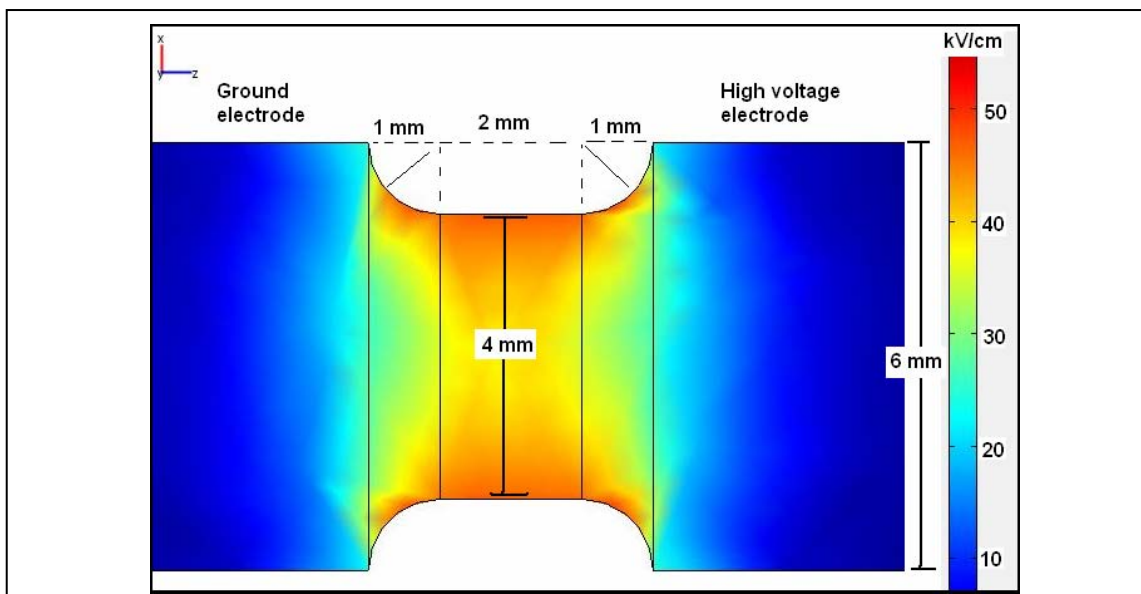


**Figure 4.14** Electric field strength distribution in treatment chamber with insulators with rounded edges, denominated G1.

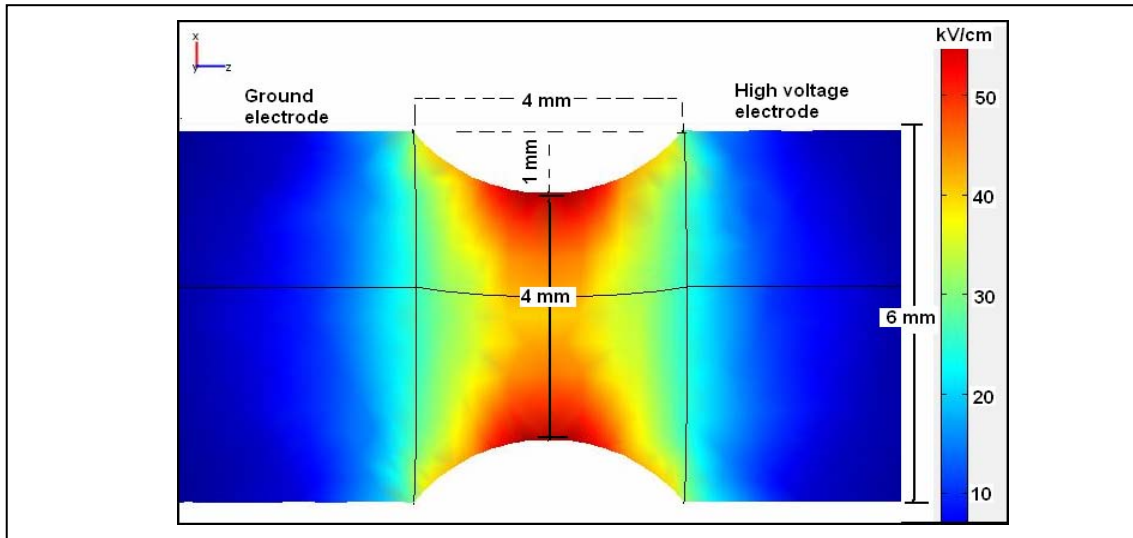


**Figure 4.15** Electric field distribution in treatment chamber with convex insulators, denominated G2.

### 4.2.2 Effect of insulator geometry on the electric field strength

A description of the generated electric field strength in both treatment chambers is presented here.

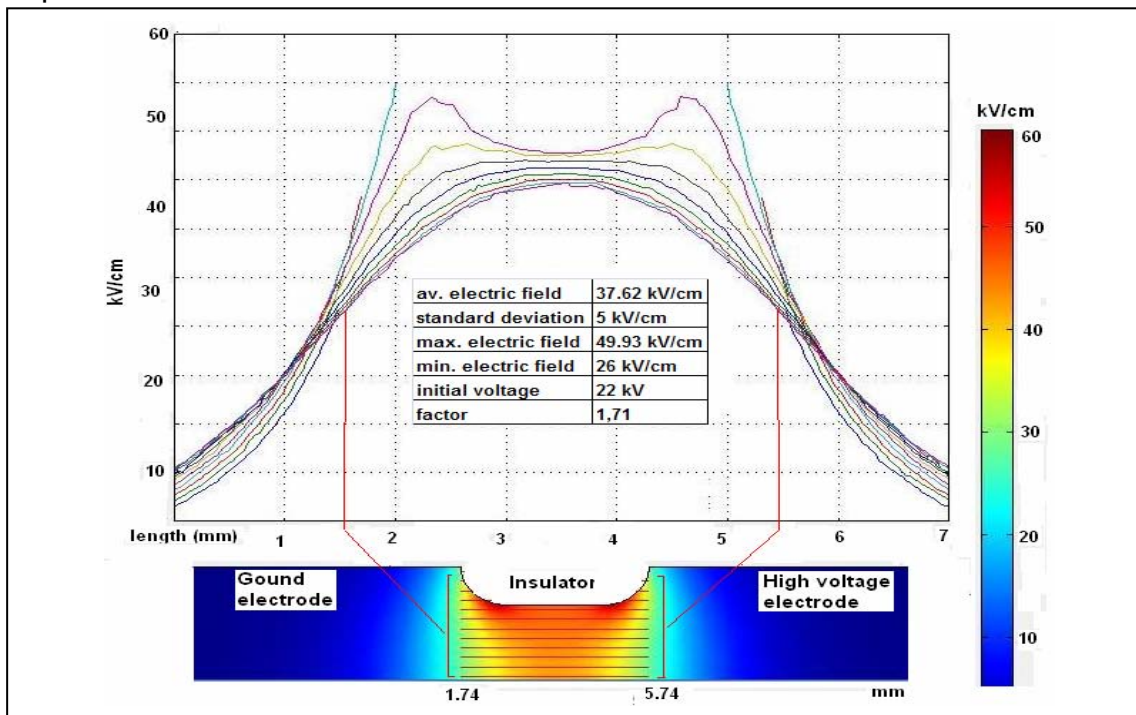


**Figure 4.16** Surface diagram of the electric field strength in treatment chamber G1.

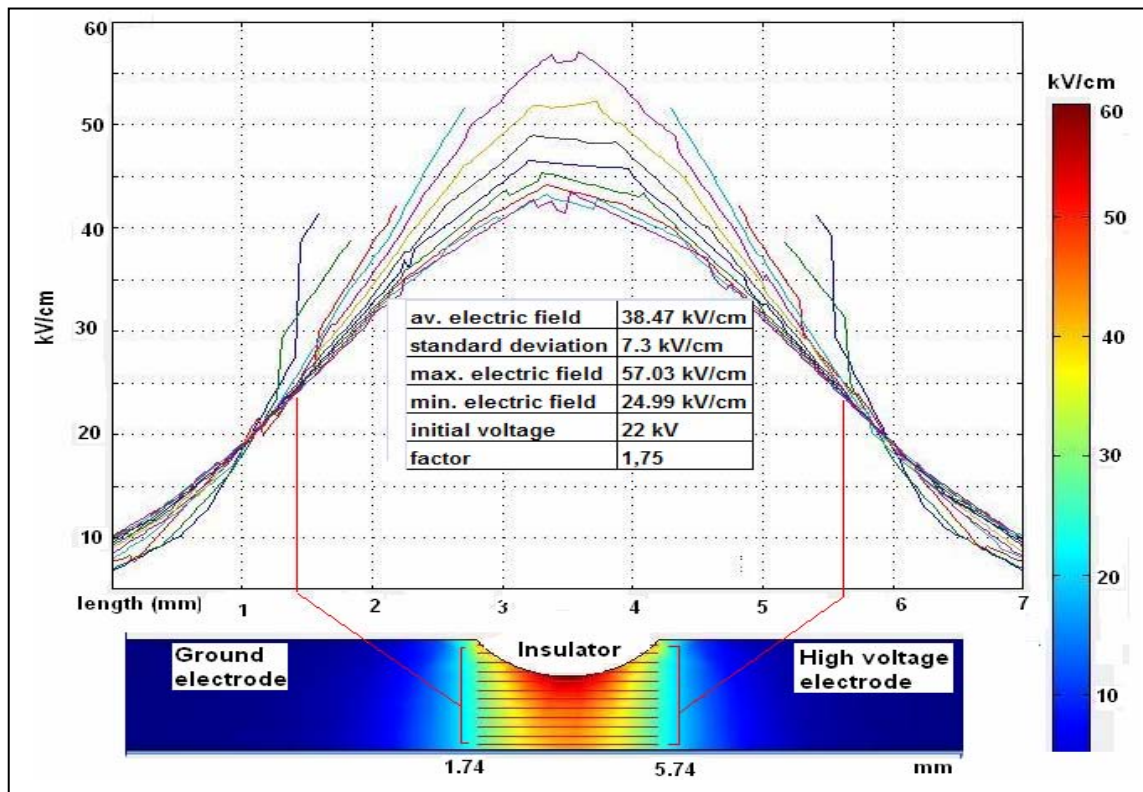


**Figure 4.17** Surface diagram of the electric field strength in treatment chamber G2.

The lines on the graphic show the profile of electric field intensity. The statistical value was obtained from the zone, corresponding to the red lines shown on the lower side of the figure; the average electric field strength is the average of all the values of the red lines, which is the zone where the main electric field is located.

As observed, the generated electric field strength in the geometry G2 is more intense; nevertheless, this chamber has an electric field distribution, that is less homogeneous.

#### 4.2.3 Effect of insulator geometry on the microbiological inactivation

The experiment to study the effect produced by geometry on the microbiological inactivation was performed in Ringer solution, adjusted at a conductivity of

4.7 mS/cm. A first experiment was made using *Lactobacillus rhamnosus*. The inactivation rate is described by the following graph:

**Table 4.10** Parameters used to study the effect on G1 and G2 at 4.7 mS/cm on *Lactobacillus rhamnosus*.

pulse width [ $\mu$ s]	3.6 for G1 and 3 for G2		
flow [L/h]	4.90		
Electric field strength [kV/cm]	30.78 for G1 and 31.5 for G2		
T inlet [ $^{\circ}$ C]	20		
T outlet [ $^{\circ}$ C]	32.91	35.74	38.52
Freq [Hz]	20	24	3.42
Epuls [J/puls]	3.22	3.38	3.42
Energie input [kJ/kg]	48.8	59.5	70

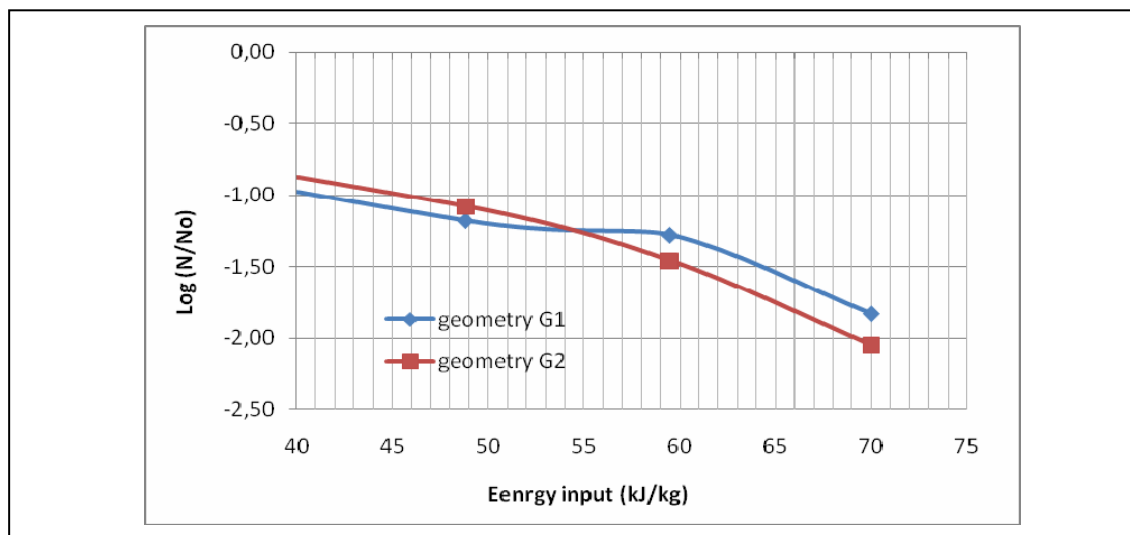


**Figure 4.18** Inactivation of *Lactobacillus rhamnosus* in Ringer solution adjusted at a conductivity of 4.7 mS/cm in G1 and G2 geometries.

A second experiment was performed using *Escherichia coli*, because this microorganism is more resistant to the electrical field treatments, because of its smaller size in comparison to *Lactobacillus* and it is possible to use a greater range of energy input.

**Table 4.11** Parameters used to study the effect of G1 and G2 at 4.7 mS/cm on *Escherichia coli*.

pulse width [ $\mu$ s]	3.6 for G1 and 3 for G2		
flow [L/h]	4.9		
Electric field strength [kV/cm]	30.78 for G1 and 31.5 for G2		
T inlet [ $^{\circ}$ C]	30		
T outlet [ $^{\circ}$ C]	51.16	56.46	61.48
Freq [Hz]	31	38	44
Epuls [J/puls]	3.57	3.68	3.73
Energie input [kJ/kg]	80	100	119

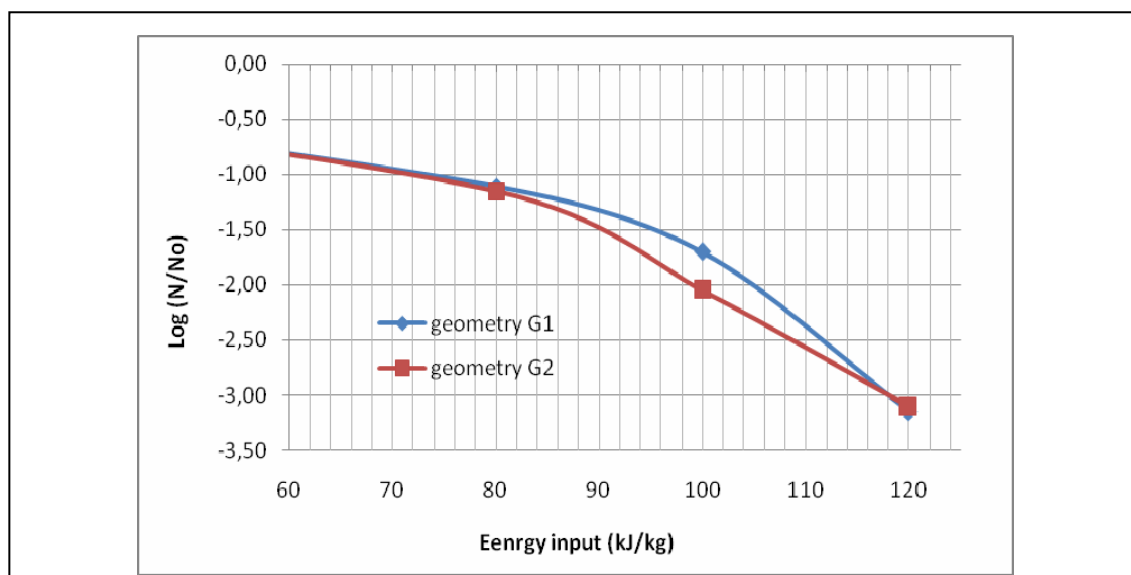


**Figure 4.19** Inactivation of *Escherichia coli* in Ringer solution adjusted at a conductivity of 4.7 mS/cm in G1 and G2 geometries.

Even though, the G2 geometry has zones, where the electric field is stronger, there is no significant difference in the microbiological inactivation between the two chambers under the treatment conditions used. The following chapter describes the evaluation of process conditions, which were more suitable for the utilization of the geometry.

#### 4.2.4 Effect of pulse frequency on the microbiological inactivation in G1 and G2

PEF treatment for low conductivity liquids in comparison to a PEF treatment for higher conductivity liquids needs a higher pulse frequency to achieve the same energy input. Nevertheless, less current flows through the liquid, due to the low solute concentration, and a better microbiological inactivation is achieved in comparison with higher conductivity liquids.

The following graphic presents a comparison between the needed frequency to achieve the same energy input in the case of a conductivity of 2.3 and 4.6 mS/cm.

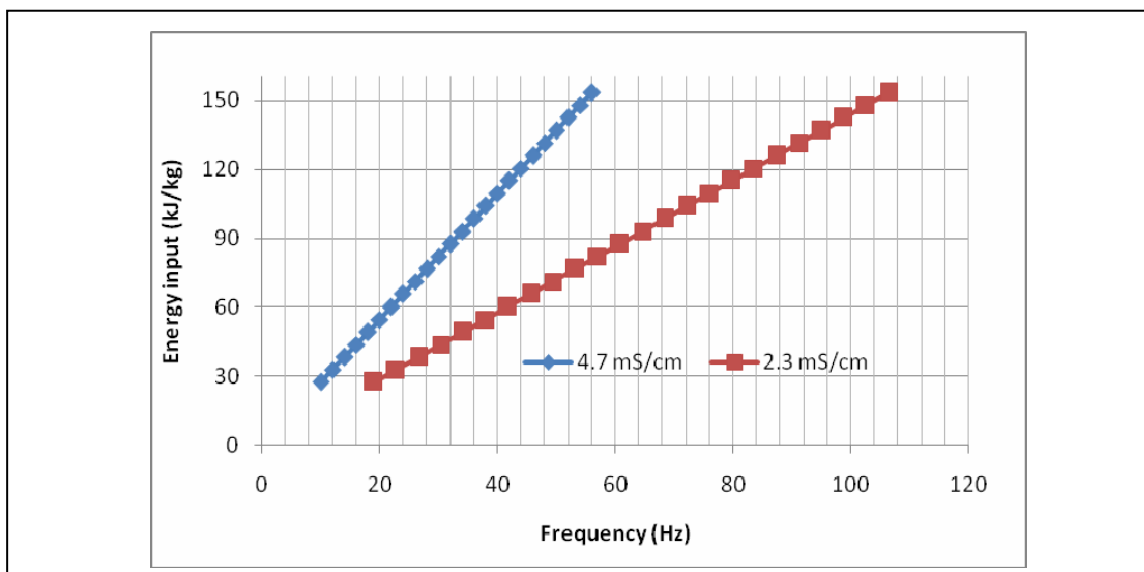


**Figure 4.20** Needed frequency and energy input in a liquid of 2.4 and 4.7 mS/cm.

As described above, the major difference that exists between the G1 and G2 geometry is that in the G2 geometry there are zones where the electric field strength is more intense, but there are not any noticeable differences in the microbial inactivation so far. This is because the pulse frequency was not high

enough to guarantee a pulse event for every volume element when flowing through the zones of high field intensity. The following figure shows how the electric field strength proportion in the G1 and G2 geometry is.

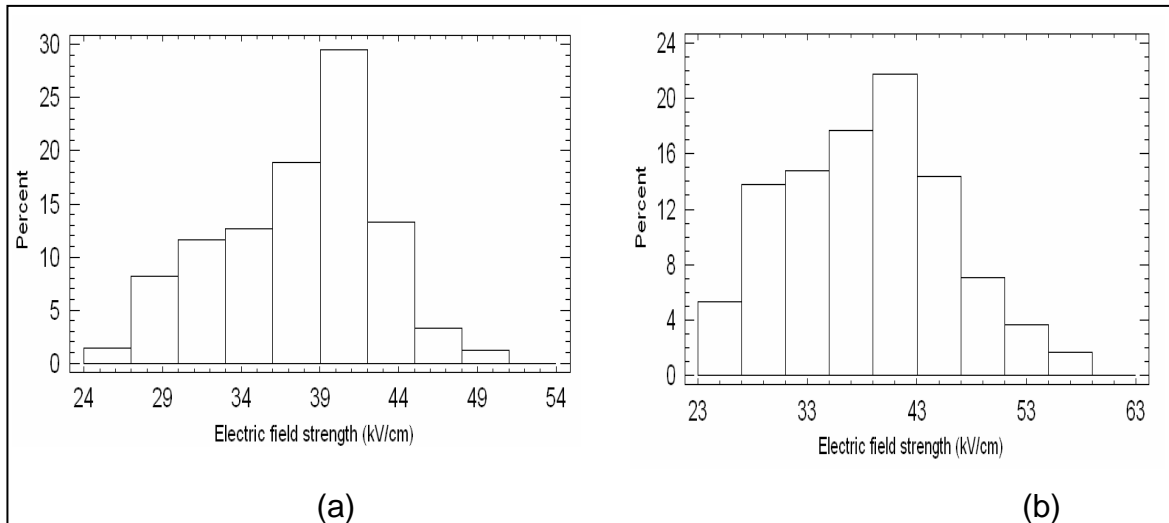


**Figure 4.21** Frequency Histogram in the G1 chamber (a) and G2 chamber (b).

These graphs relate the percentage or proportion, in which the electric field intensity in the zone covered by the insulators is present. This zone was chosen in order to compare the two geometries and to calculate a more representative average electric field strength .

It is possible to observe that the zones with higher electric field strength in the G2 chamber are in a greater proportion than in the one with G1 geometry. In the G1 geometry, the electric field strength over 43 kV/cm is in a proportion of 12 % and in the G2 geometry this proportion is of 18% existing in this latter a 5 % zone where the electric field strength is 54 kV/cm, which does not exist in geometry G1(see Figure 4.22)

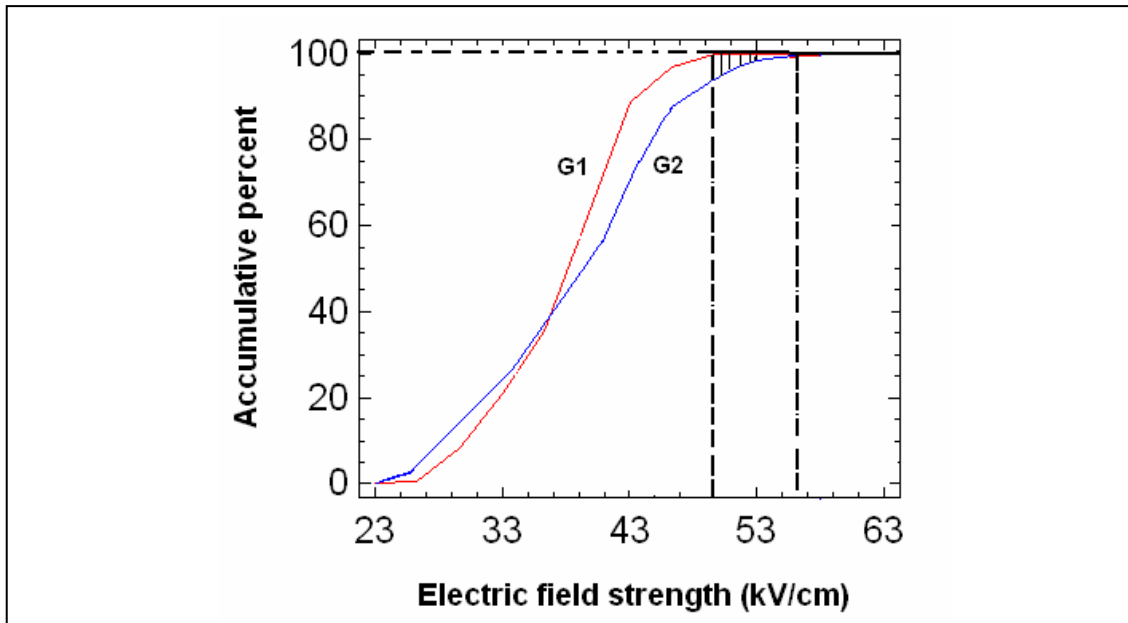


**Figure 4.22** Histogram of accumulative percent for G1 and G2.

The reason for using a liquid with a low conductivity is to achieve a higher pulse number and therefore to increase the probability for a pulse event to happen for a microorganism when flowing through zones of high intensity. Further, the results obtained by processing a fluid with conductivity 2.3 mS/cm are shown (applying a higher pulse frequency for the same energy input), for *Lactobacillus rhamnosus* and *Escherichia coli* for the geometries G1 and G2.

**Table 4.12** Parameters used to study the effect of G1 and G2 at 2.3 mS/cm on *Lactobacillus rhamnosus*.

pulse width [ $\mu$ s]	3.8 for G1 and 3.0 for G2		
Electric field strength [kV/cm]	30.78 for G1 and 31.5 for G2		
T inlet [ $^{\circ}$ C]	20		
T outlet [ $^{\circ}$ C]	35.87	37.99	39.05
Freq [Hz]	52	58	62
Epuls [J/puls]	1.58	1.6	1.58
Energie input [kJ/kg]	60	68	72

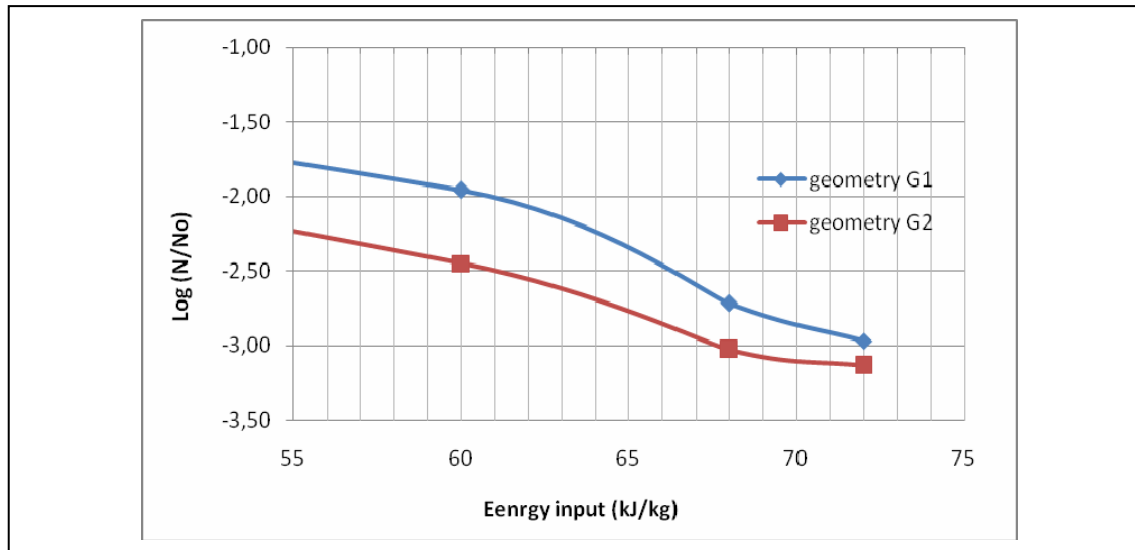


**Figure 4.23** Inactivation rates of *Lactobacillus rhamnosus* by PEF treatment in Ringer solution at 2.3 mS/cm with a flow rate of 4.9 l/h.

**Table 4.13** Parameters used to study the effect of G1 and G2 at 2.3 mS/cm on *Escherichia coli*.

pulse width [ $\mu$ s]	3.7 for G1 and 3 for G2		
Electric field strength [kV/cm]	30.78 for G1 and 31.5 for G2		
T inlet [ $^{\circ}$ C]	30		
T outlet [ $^{\circ}$ C]	51.16	56.46	61.48
Freq [Hz]	49	60	70
Epuls [J/puls]	2.26	2.3	2.36
Energie input [kJ/kg]	80	100	119

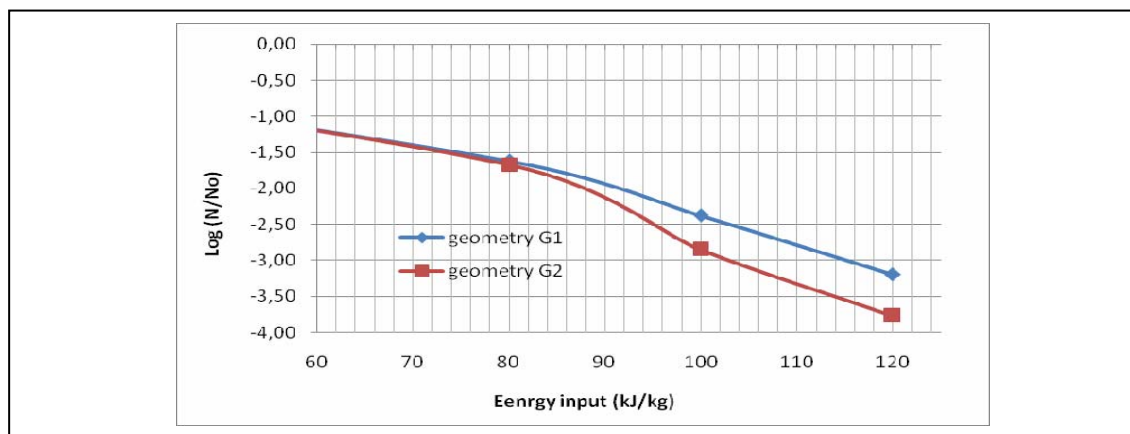


**Figure 4.24** Inactivation rates of *Escherichia coli* by PEF treatment in Ringer solution at 2.3 mS/cm with a flow rate of 4.9 l/h.

As we can observe, there is a better microbiological inactivation in the G2 geometry. This is because of the increment in the pulse frequency and the probability is increased for a microorganism to receive a pulse when located in the zones of higher field strength. On the other hand, it is also possible to observe an improvement in microbiological inactivation, when a lower conductivity medium is used, as shown in the following figure:

**Table 4.14** Parameters used to study the difference between 4.7 and 2.3 mS/cm on *Lactobacillus rhamnosus* using the G1 geometry.

pulse width [ $\mu$ s]	3					
Electric field strength [kV/cm]	30.1					
T inlet [ $^{\circ}$ C]	20					
T outlet [ $^{\circ}$ C]	35.87		37.99		39.05	
conductivity [mS/cm]	2.3	4.7	2.3	4.7	2,3	4,7
Freq [Hz]	52	20	58	24	62	28
Epuls (J/puls)	1.58	3.28	1.6	3.38	1.58	3.42
Energie input (kJ/kg)	60		68		72	

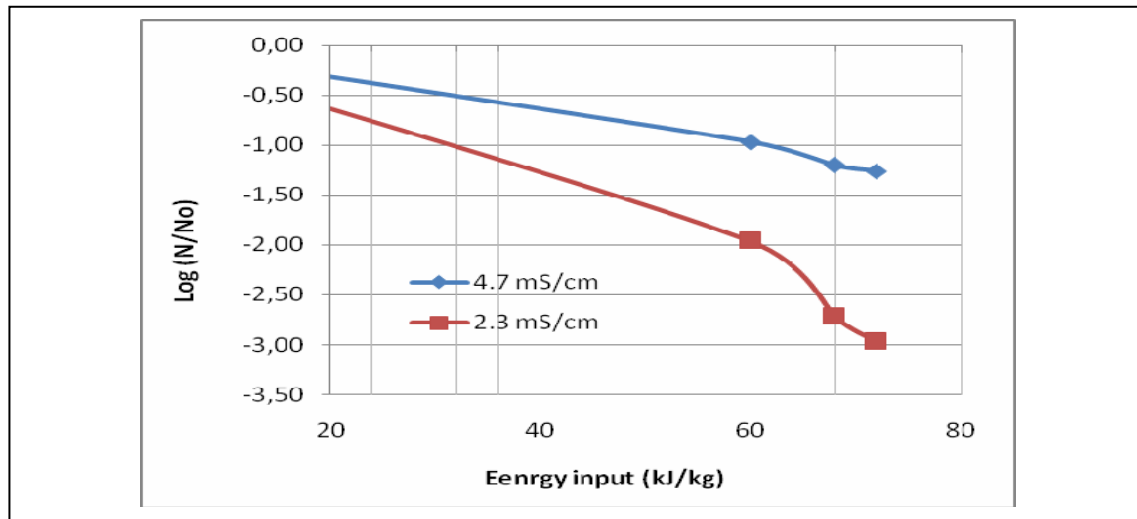


**Figure 4.25** Inactivation of *Lactobacillus rhamnosus* by PEF treatment in Ringer solution at 2.3 and 4.7 mS/cm with a flow rate of 4.9 l/h. Geometry G1 was used.

#### 4.2.5 Flow velocity in treatment chambers

The reason for increasing the flow velocity is to produce turbulence and to mix the fluid, which produces a more homogeneous treatment and also increases microbial inactivation. Furthermore, the generated turbulence produces a more homogeneous temperature distribution into the treatment chamber.

The effect of processing at high flow velocity in a PEF treatment chamber could also have a similar impact as the one produced by bipolar pulses, which avoids accumulation of charged particles on the electrode surface, and therefore reduces electrochemical reactions. The accumulation of charged particles on the electrode surface behaves as capacitor (Morren *et al.*, 2003) and this could lower the microbiological inactivation.

The velocity distribution in a treatment chamber is similar to the velocity distribution that exists in an electrostatic precipitator. The fluid flow in a precipitator may be divided into primary and secondary flows. The primary flow

is the flow field that exists in the precipitator in the absence of an imposed electric field and is known as “cross flow”. The secondary flow is the flow field caused by the electrical discharge due to the presence of the electric field, and is known as “electric wind” (Zamankhan *et al.*, 2004). The cross flow velocity is typically much smaller than the electric wind velocity. This principle is used in an electrostatic precipitator to separate charged particles due to the accumulation on a plate of such particles with opposite charges. This process could also happen in a PEF treatment chamber when an electric field is imposed. If it is possible to achieve an increase in cross flow velocity, migration of charged particles towards the electrodes due to turbulence could partly be avoided, and this would also produce a more homogenous treatment.

#### **4.2.5.1 Experimental velocity limitations**

In our case, a peristaltic pump was used able to achieve 600 rpm and the treatment zone, through which the liquid food flows, has a diameter of 4 mm; this means that it is possible to achieve velocities up to  $\approx 2.2$  m/s (Reynolds number  $\approx 8800$ ). The limitation is that, the pump produces a peristaltic movement on the fluid, which is not adequate for the experiments, since there is no control of the residence time in the electric field zone. The peristaltic movement can be easily avoided through a liquid compression, which can be generated circulating the liquid through a lower diameter tube. This procedure restricts to work with lower mass flow, because otherwise an undesired pressure drop is generated. Furthermore, in our experiments a spiral capillary was used as heat exchanger, causing the maximum velocity to get even more restricted, allowing for sufficient heat transfer. Due to these reasons, it was possible to obtain a maximum flow rate of 20 l/h at 4 mm diameter with a flow velocity of 0.44 m/s and Reynolds number  $\approx 1800$ .

### 4.2.5.2 Velocity profile in the treatment chamber.

The following figures show the velocity profile on the center line of the two treatment chamber geometries. Fluent<sup>®</sup> was used to perform the simulations. The boundary conditions are described in section 3.7.4. The results of velocity were converged using a mesh with 34.000 cells in both cases. Results remained unchanged with more cells.

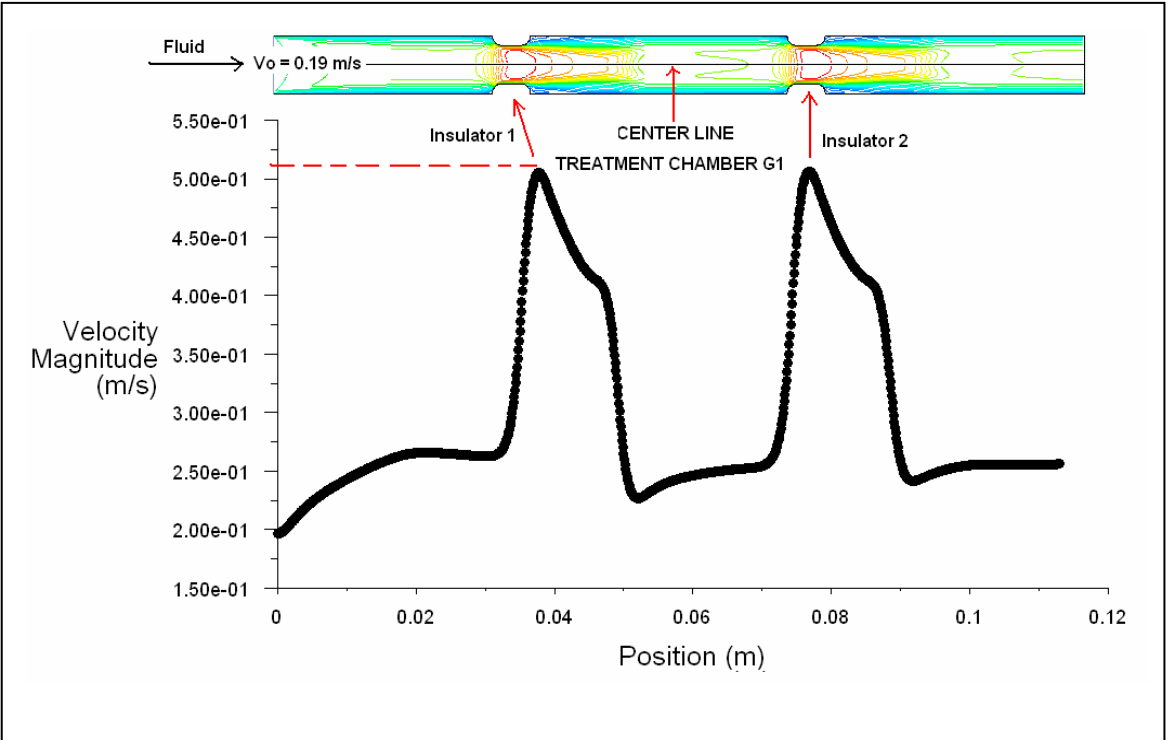


**Figure 4.26** Velocity profile on the center line of the treatment chamber G1 at a flow rate of 20 l/h.

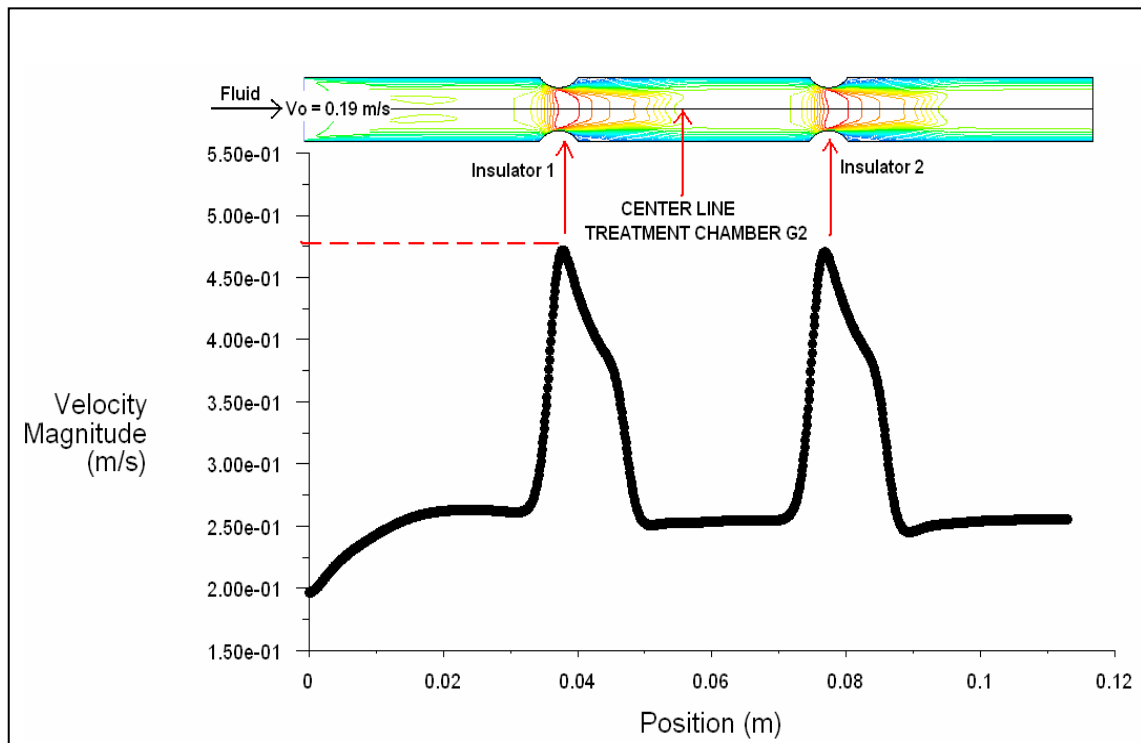


**Figure 4.27** Velocity profile on the center line of the treatment chamber G2 at a flow rate of 20 l/h.

The velocity in the center line of the pipe is higher for the G1 geometry. The peak velocity in G1 is 0.518 m/s and in the geometry G2 only 0.475 m/s. Due to the insulator geometry in G1 (insulator with corned edges) there is more fluid recirculation. This is not appropriate, because the fluid food will then be over processed due to a longer residence time.

The following figures show velocity of the turbulence intensity in the treatment chambers, exactly in the insulator zone, where the electric field is located. The graphics are based on the intensity of turbulence measured in the centre of the 2nd insulator in the radial coordinate.

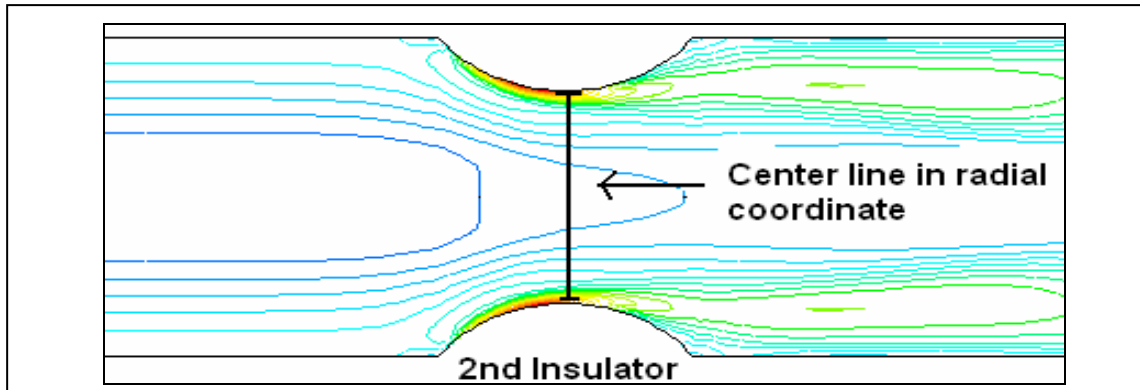


**Figure 4.28** Zone of the treatment chamber where intensity of turbulence is computationally estimated.

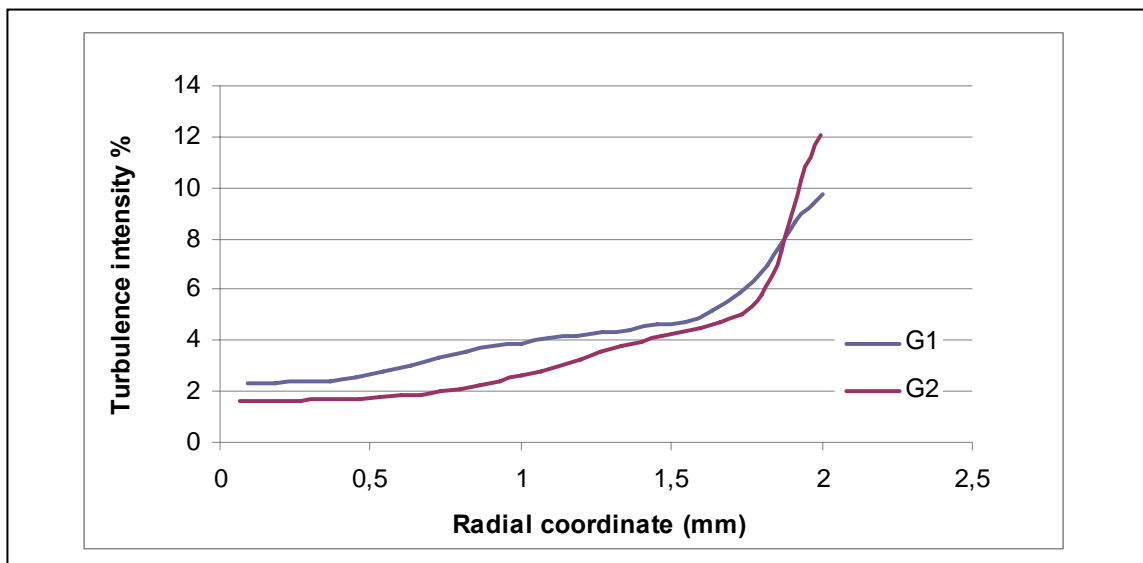


**Figure 4.29** Turbulence Intensity in insulator zone for geometries G1 and G2 at a flow rate of 20 l/h and a Reynolds number of 1763.

No noticeable differences were found in both chambers due to the turbulence intensity. A high level of turbulence intensity is a good indicator when intentional mixing is desirable.

Turbulence intensity between 5% and 20% is considered as a case of high-turbulence. Turbulence between 1% and 5% is considered as medium-turbulence case and below 1% is considered as low-turbulence case (FLUENT, 2003). Due to this definition, the flow in our case is considered as a low to

medium turbulence case. Nevertheless, the maximum Reynolds number is 1763.

In the following figure the influence of the mass flow velocity on the turbulence is shown.

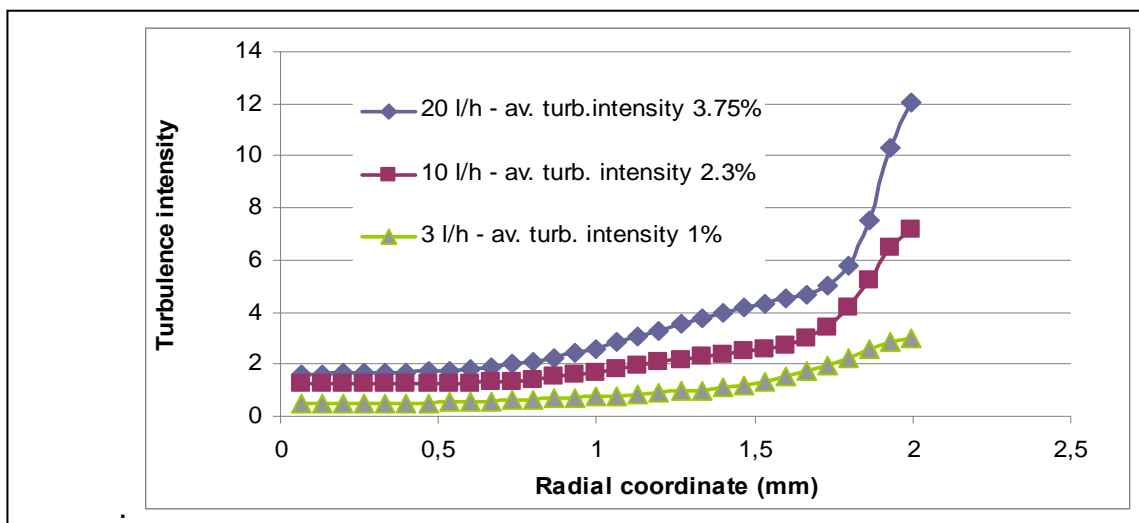


**Figure 4.30** Comparison of turbulence intensity generated in the insulator zone at 3, 10 and 20 l/h in G2 geometry.

The average turbulence intensity for the flow rates of 3, 10 and 20 l/h in the insulator zone are 1%, 2.3% and 3.75% respectively. This means, that all the flows are medium turbulent flows. It is possible to observe that the turbulence intensity for the flow at 20 l/h is greater than the others, but between 0 and 1.5 mm radial coordinate there is no significant difference between 10 and 20 l/h. The difference is only present in comparison to the flow at 3 l/h. Between 3 l/h to 20 l/h the turbulence intensity is 2.75% greater. Based on this turbulence levels experiments were performed to analyze if the velocity has any effect on microbiological inactivation.

#### 4.2.5.3 Effect of the flow velocity on microbiological inactivation

Experiments were realized at flow rates of 3, 5, 10 and 20 l/h using *E. coli* and *L. rhamnosus* suspended in Ringer solutions at conductivity of 2.3 and 4.7 mS/cm.

**Table 4.15** Parameters used to study the effect of flow velocity at 4.65 mS/cm on *Escherichia coli* using the G1 geometry.

Pulse width [ $\mu$ s]	3.5								
Electric field strength [kV/cm]	30.78								
Energy input [kJ/kg]	80			100		94	119		110
Liquid flow [l/h]	3	10	20	3	10	20	3	10	20
Frecuence [Hz]	18	60	125	22	75	150	27	89	175
T outlet [ $^{\circ}$ C]	51.16			56.46		54	61.48		59
Epulse [J/pulse]	3.38 - 3.7								

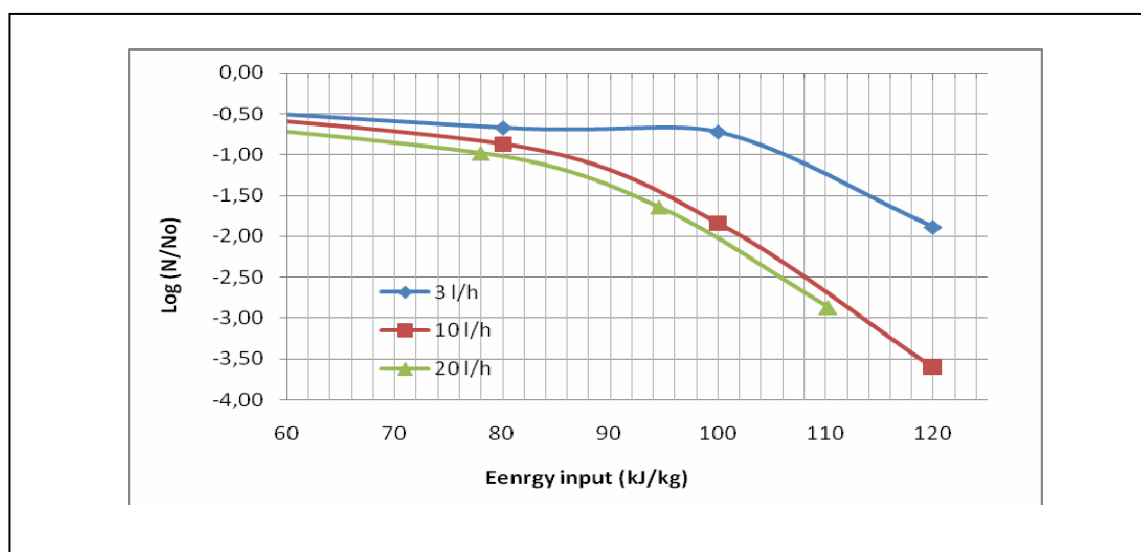


**Figure 4.31** Inactivation of *Escherichia coli* in G1 geometry at 3, 10 and 20 l/h in Ringer solution adjusted to 4.65 mS/cm and inlet temperature of 30  $^{\circ}$ C.

As observed, a noticeable difference was found when the PEF treatment was performed at higher flow velocities. Nonetheless no difference was found between the PEF treatment performed at 10 and 20 l/h. A reason could be that between 10 and 20 l/h there is no significant difference in the turbulence level. The difference is just noticeable between 3 l/h and 10 or 20 l/h.

The results were similar when the geometry G2 was used:

**Table 4.16** Parameters used to study the effect of flow velocity at 4.65 mS/cm on *Escherichia coli* using the G2 geometry.

Pulse width [ $\mu$ s]	3.5								
Electric field strength [kV/cm]	30.78								
Energie input [kJ/kg]	80		74	100		90	119		107
Liquid flow [l/h]	3	10	20	3	10	20	3	10	20
Frequence [Hz]	18	60	125	22	75	150	27	89	175
T outlet [ $^{\circ}$ C]	51.16		49	56.46		54	61.48		58
Epuls [J/puls]	3.38 - 3.7								

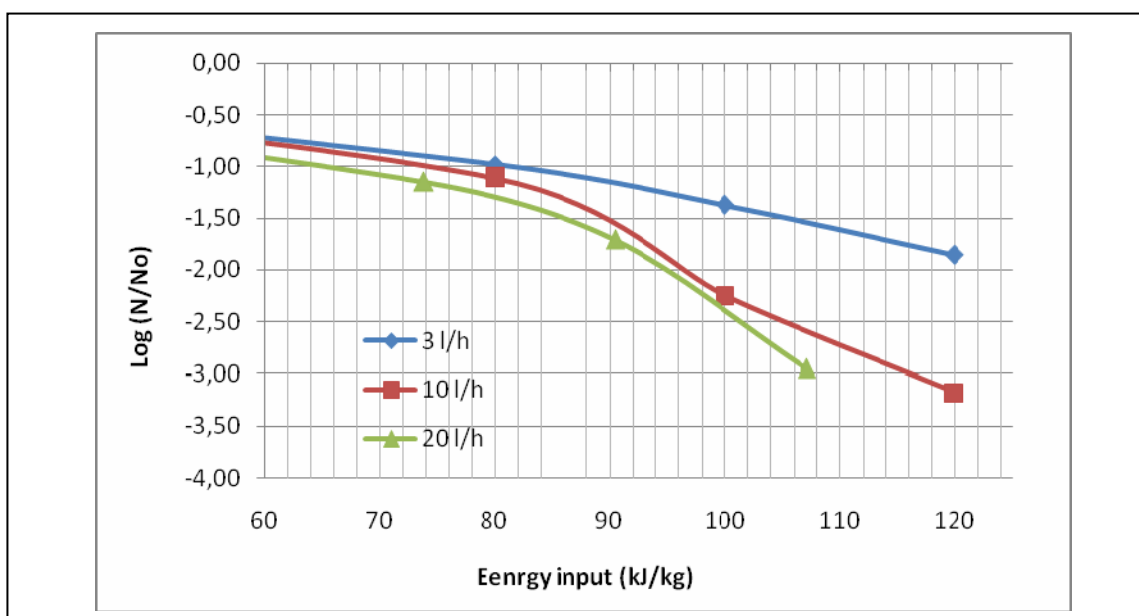


**Figure 4.32** Inactivation of *Escherichia coli* in G2 geometry at 3, 10 and 20 l/h in Ringer solution adjusted to 4.65 mS/cm and inlet temperature of 30  $^{\circ}$ C.

The graphics also show that the inactivation was better for the G2 geometry. It fits with the previously obtained results on microbial inactivation due to geometry effect; an improvement in the geometry G2. In the G2 geometry there is a nonuniform electric field distribution with high maximum zones and only at high

flow rates (generation of turbulence) or higher pulse frequency allow that different volume elements can come in these zones.

The results were better when the experiment was performed with *Lactobacillus rhamnosus* suspended in Ringer solution at 2.3 mS/cm:

**Table 4.17** Parameters used to study the effect of flow velocity at 2.3 mS/cm on *Lactobacillus rhamnosus* using the geometries G1 and G2.

Electric field strength [kV/cm]	30.78 for G1 and 31.5 for G2					
Pulse width [ $\mu$ s]	3.6 for G1 and 3 for G2					
liquid flow [l/h]	4.90			16		
Energie input [kJ/kg]	60	68	72	60	68	72
Freq [Hz]	52	58	62	175	192	205
T outlet [°C]	38	40	41	38	40	41
Epuls [J/puls]	1.48 - 1.58					

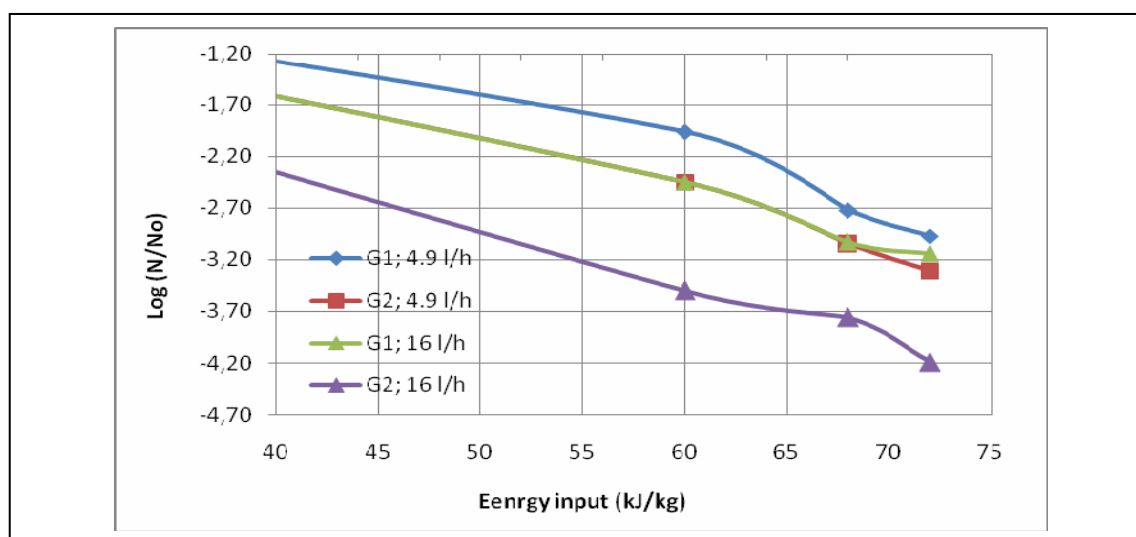


**Figure 4.33** Inactivation of *Lactobacillus rhamnosus* in G1 and G2 geometries at 4.9 and 16 l/h, using Ringer solution adjusted at 2.3 mS/cm.

For the experiments with *Lactobacillus rhamnosus*, an improvement in the microbial inactivation is also generated at higher treatment velocities, revealing

a great difference in the inactivation with a flow rate of 16 l/h for the G2 geometry.

In the following Figure 4.34 effects of conductivity on the microbiological inactivation is shown again, but this time, coupled with velocity experiments.

**Table 4.18** Parameters used to study the effect of flow velocity at 2.3 and 4.7 mS/cm on *Escherichia coli* using the geometries G1 and G2.

Electric field strength [kV/cm]	31.5											
Pulse width [ $\mu$ s]	3											
Liquid flow [l/h]	3						10					
Energie input [kJ/kg]	80		100		120		80		100		120	
conductivity [mS/cm]	2.3	4.7	2.3	4.7	2.3	4.7	2.3	4.7	2.3	4.7	2.3	4.7
Freq [Hz]	29	18	35	22	42	27	100	60	122	75	141	89
T outlet [°C]	51		56		62		51		56		62	
Epuls [J/puls] for 2.3 mS/cm	2.2 - 2.4											
Epuls [J/puls] for 4.7 mS/cm	3.38 - 3.7											

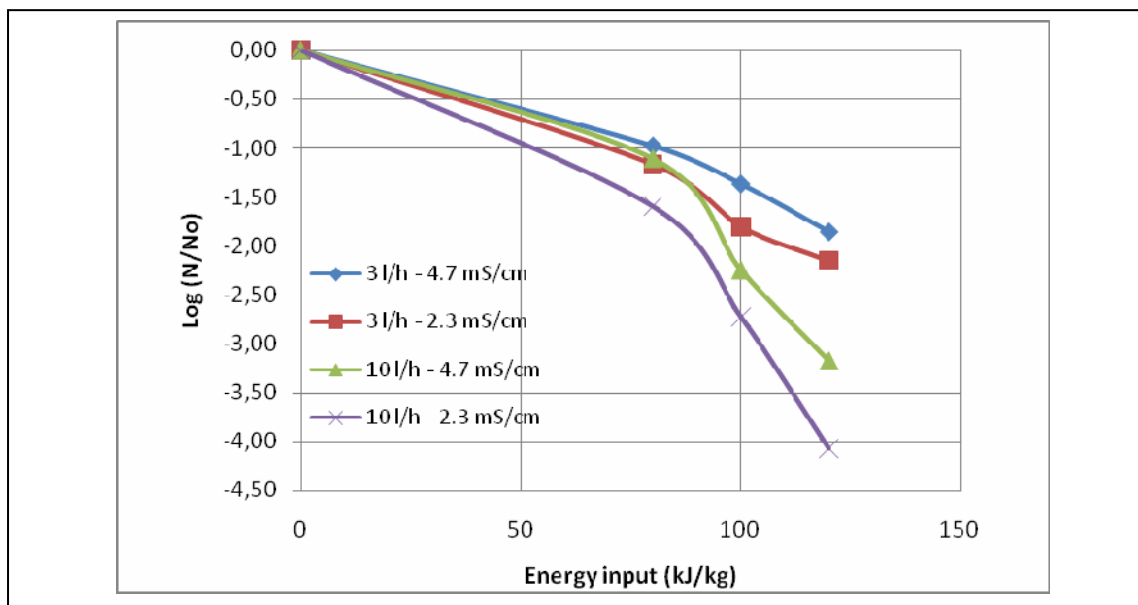


**Figure 4.34** Inactivation of *Escherichia coli* in geometry G2 at 3 and 10 l/h utilizing Ringer solutions adjusted to 2.3 and 4.7 mS/cm at an inlet temperature of 30°C.

As observed, the conductivity and velocity have helped to improve the microbial inactivation. This finding is based on the following effects:

- High flow rate: There is a higher probability for the microorganisms to be transported in high field areas due to mixing/turbulence.
- Conductivity: Low conductivity liquid needs a higher frequency, this increases the probability for the microorganisms to be affected by a pulse when located in higher field strength areas.

#### **4.2.6 Homogenous PEF treatment**

The objective of a higher velocity treatment was also to produce a more homogenous treatment. But it is not always easy to process at high velocities, since there are technical limitations, for example, in an industrial processing with a flow rate of 100 l/h, a treatment chamber with a greater diameter is generally used, whereby the generated velocity in the chamber will not be high enough to produce turbulence. For this reason, it is necessary to design a system that generates turbulence when the PEF treatment is performed at low velocities.

Turbulence generation methods in a tube may be manifold, e.g. with insertion of devices, by using expansions, compressions, vortex, curved pipes, etc., but not all of them are suitable in our case.

The following requirements are very important for turbulence generation in a PEF treatment chamber

- Generated turbulence must be homogenous and constant in a desired time interval.
- Liquid recirculation must be avoided, since this will produce an over processing of the liquid food.
- System to generate turbulence must not alter the electric field distribution, and when it is altered, it must be kept under control.

- Insertion of air has to be avoided.

#### 4.2.6.1 Insertion of devices in the treatment chamber

A possible system to produce turbulence considering the previously named requirements is the insertion of a grid in the treatment chamber. Such device was used by Cook (1973, 1978) to generate turbulence in a wind tube. He advertized that this method is not suitable for the high turbulence level production.

It is demonstrated that a grid helps to make the velocity profile more homogenous and produces greater turbulence intensity (Castro *et al.*, 2003).

In our case, the grid must be inserted exactly before the electric field zone, that is, before the insulators, because the flow velocity could not produce a great turbulence and the generated turbulence will not continue for much time. The grid can be made of insulator material or made of metal, such that it works as an electrode. The three models used are the following:

- **Model A:** Two grids made of insulated material, located each one before each insulator.
- **Model B:** Two grids made of metal, located each one before each insulator
- **Model C:** Four grids made of metal, two located before and two located after each insulator.

The models of the grid insertion in the treatment chamber and the electric field strength distribution are shown in Figures 4.35 and 4.36:

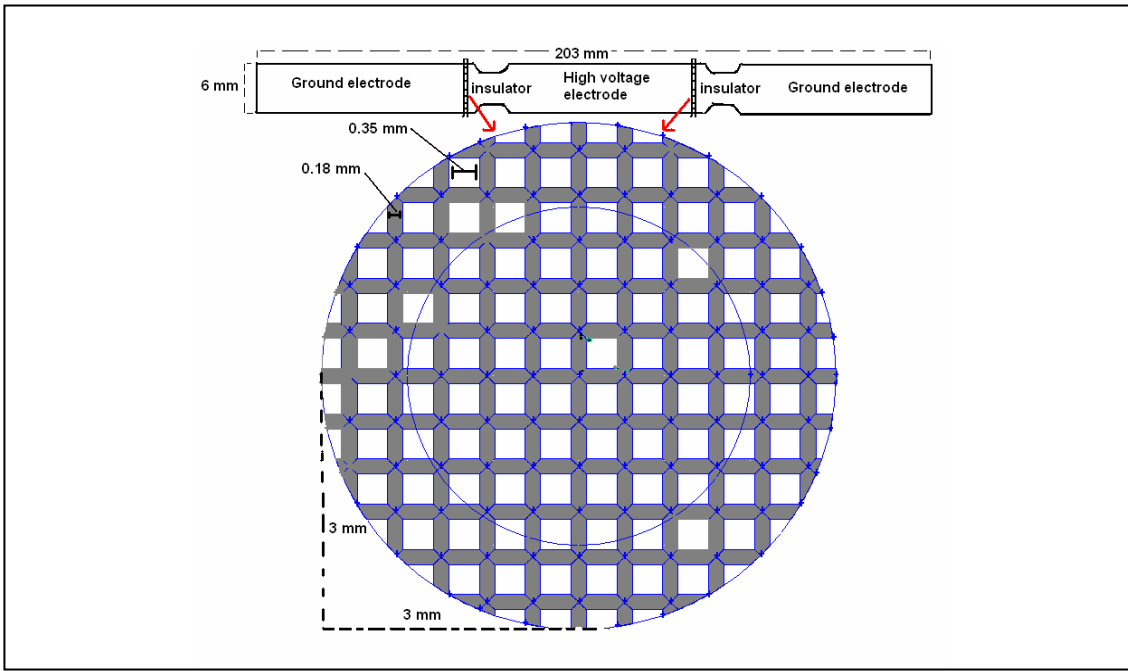


Figure 4.35 Grid dimensions and location for models A and B.

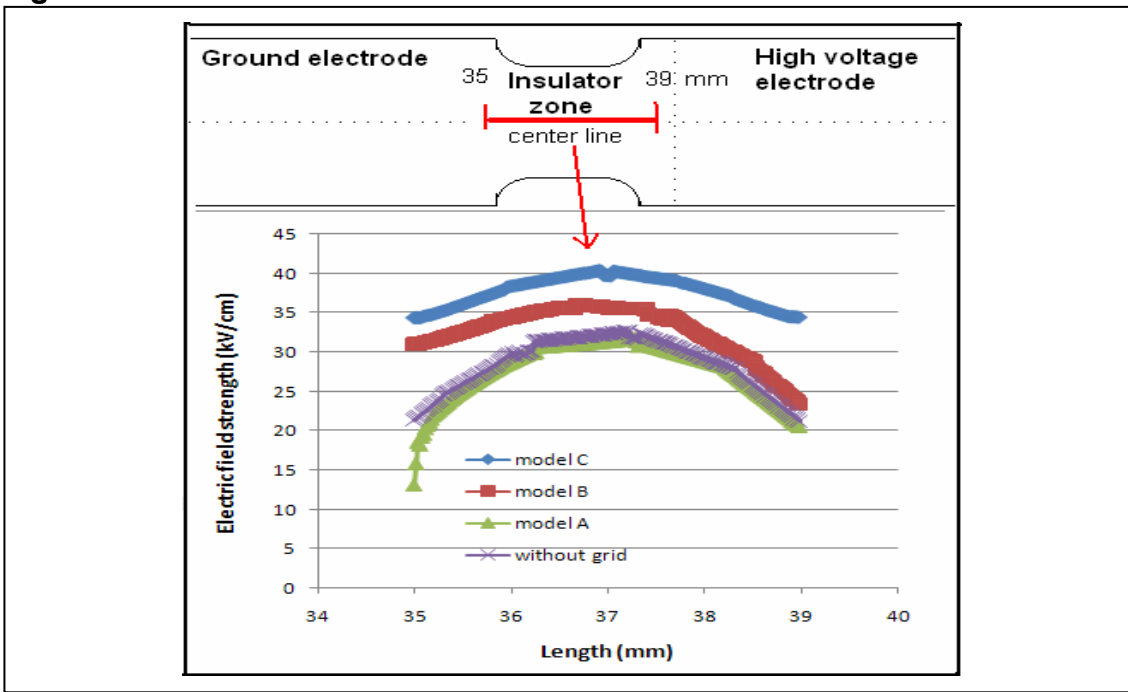


Figure 4.36 Comparison of the electric field strength on center line of insulator zone for the three models and the treatment chamber without grid.

Previous simulations have shown that a grid with these dimensions produces a more intensive turbulence and has no big impact on the electric field distribution (data not shown).

The following table shows the average electric field strength and its standard deviation, calculated from the values of the center line.

**Table 4.19** Average electric field strength.

	average electric field strength [kV/cm]	standard deviation [kV/cm]
without grid	28.6	3.4
case A	27.7	3.7
case B	32.6	3.2
case C	37.6	1.9

The following figure shows a comparison between the electric field strength generated in case C (two grids in each insulator) and an insulator without grid.

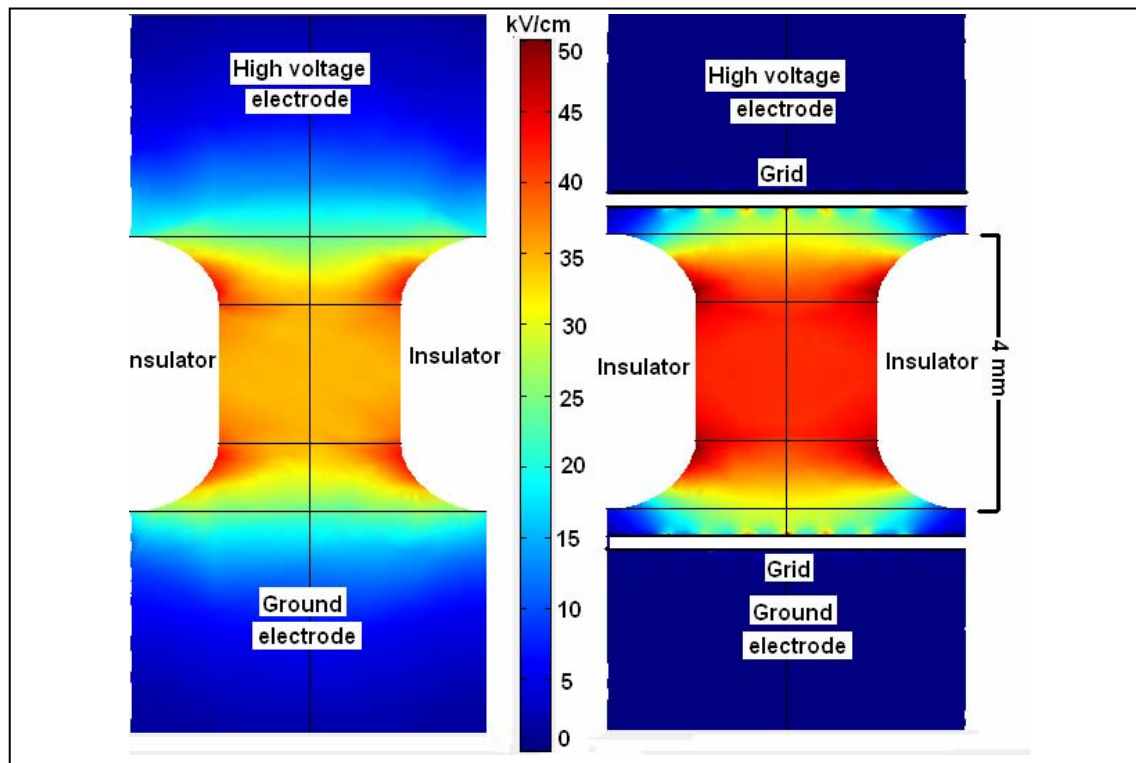


**Figure 4.37** Comparison between the electric field strength generated in the case C (right) and an insulator without grid (left).

The following figure shows how the turbulence intensity in the 2<sup>nd</sup> insulator at a distance of 1 mm from the grid for the treatment chamber with 2 inserted grids is altered in comparison to a normal treatment chamber without grid.

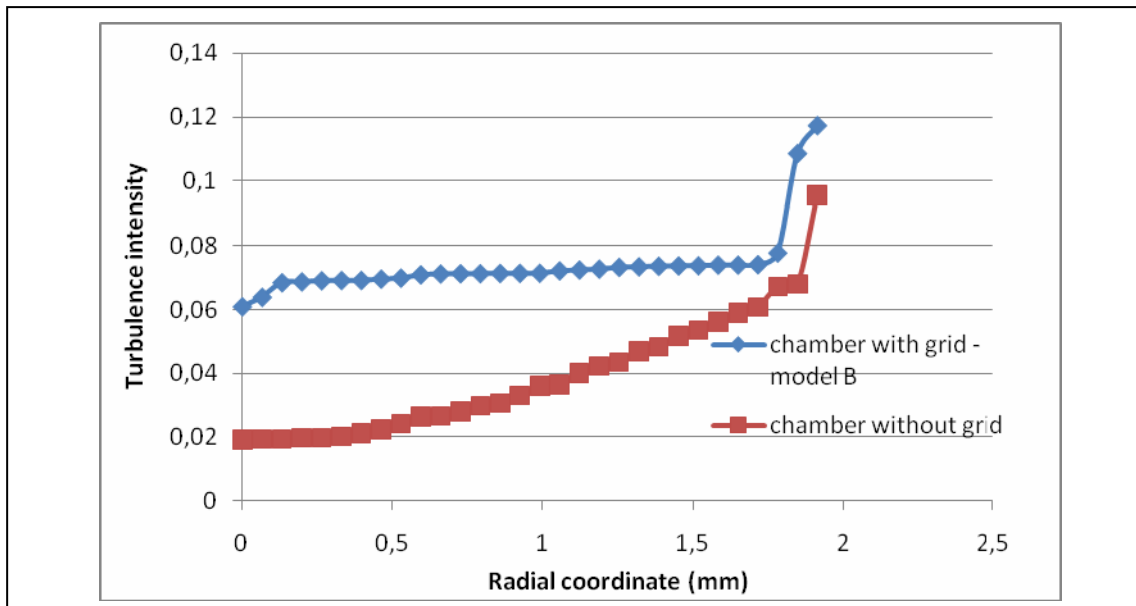


**Figure 4.38** Turbulence intensity on center line of the insulator zone for model B in comparison to a treatment chamber without grid.

As observed, the electric field strength and turbulence intensity in presence of two metal grids in each insulator is much higher, and also more homogenous, which means that all particles will receive the same treatment.

The insulator grid has the function of producing turbulence and decreasing electric field strength. Therefore, it makes it possible to analyze how the turbulence effect behaves at low electric field intensity.

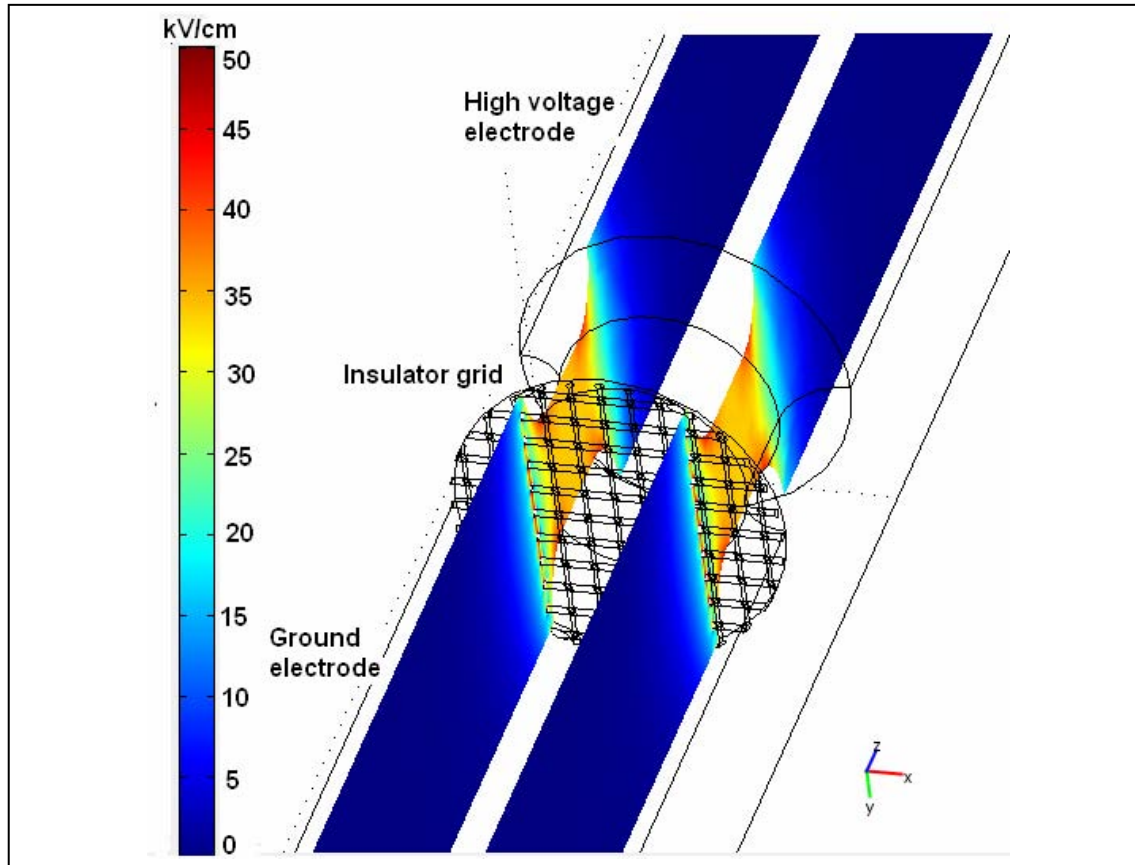


**Figure 4.39** Electric field strength in treatment chamber for model A; insulator grid.

#### 4.2.6.2 Impact on microbial inactivation due to the insertion of grids in the treatment chamber

A first experiment was performed pumping fluid at 16 l/h using Ringer solution adjusted to 2.3 mS/cm.

The following graphics show the microbial inactivation for the treatment chamber with grids in comparison to a treatment chamber without grid

**Table 4.20** Parameter used study the impact of grids on *E. coli* using G1 and G2 at 2.3 mS/cm.

	without grid	model A	model B	model B with G2
Pulse width [ $\mu$ s]	3.8	4.2	3.5	3
Electric field strength [kV/cm]	28.6	27.7	32.2	32.2
Flow [L/h]	16			
T inlet [ $^{\circ}$ C]	30			
T outlet [ $^{\circ}$ C]	51.16	56.98	61.75	61.75
Frequency [Hz]	156	189	219	219
Epulse [J/pulse]	2.3	2.35	2.45	2.45
Energie input [kJ/kg]	80	102	120	120

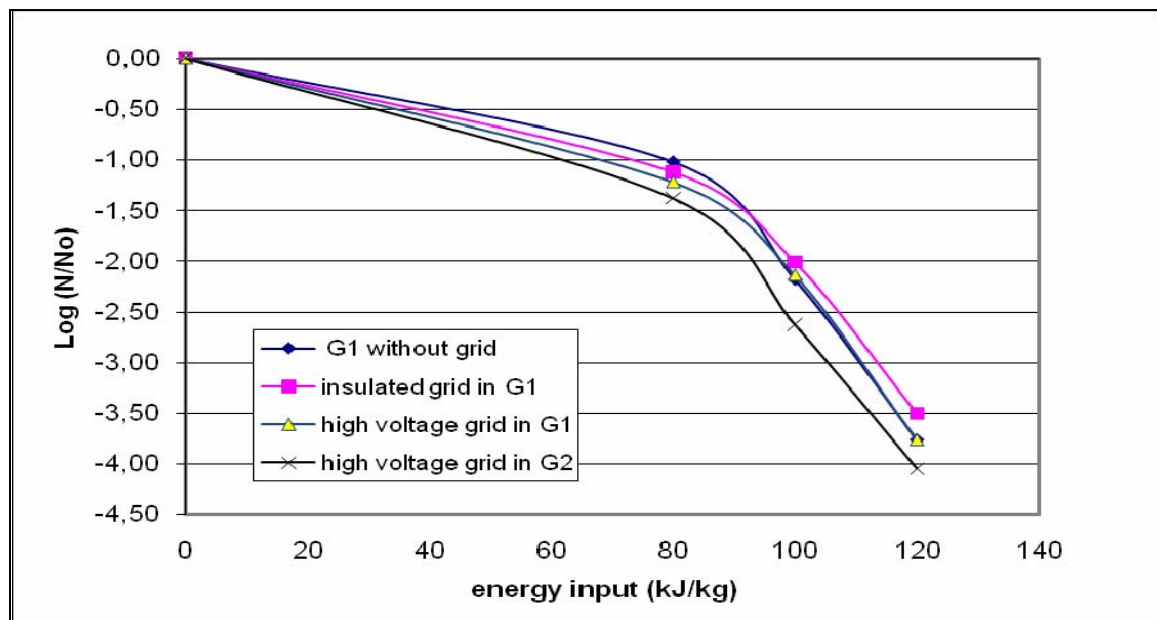


**Figure 4.40** Impact of grids on the inactivation of *E. coli* in Ringer solution at 2.3 mS/cm in comparison to a treatment chamber without grid.

The average electric field was obtained from Table 4.1.

As observed, there is no difference in the microbial inactivation among all the cases, where the G1 geometry was used. There is only a slight difference in the

treatment chamber G2 geometry in comparison to the rest, but this difference results from the chamber geometry (insulator) and not from the insertion of the grid. As observed, the turbulence intensity has no effect on the microbial inactivation in all the cases. In other words, the insertion of two grids made of metal or insulated material has no impact on the microbial inactivation under these conditions (16 l/h, 18 kV/cm).

A second experiment was performed using four grids. In this case, the grids have an important impact on the electric field strength distribution and also on the velocity profile.

The following figure shows the microbial inactivation using an initial voltage of 15 and 18 kV with a flow rate of 10 l/h. The microorganisms used were *E. coli* and *L. rhamnosus* suspended in Ringer solutions adjusted to 2.3 mS/cm.

**Table 4.21** Parameter used for a treatment chamber with four inserted grids in comparison with a treatment chamber without grid.

	treatment at 18 kV			treatment at 15 kV		
T outlet [°C]	50.00	57.20	62.00	51.00	55.00	62.00
Frequency [Hz]	48	59	68	65	77	90
Epuls [J/puls]	2.3	2.35	2.45	1.72	1.82	1.83
Energie input [kJ/kg]	80.73	102	120	80.73	102	120
treatment chamber	without grids	four grids		without grids	four grids	
pulse width [µs]	3.7	3		3.7	3	

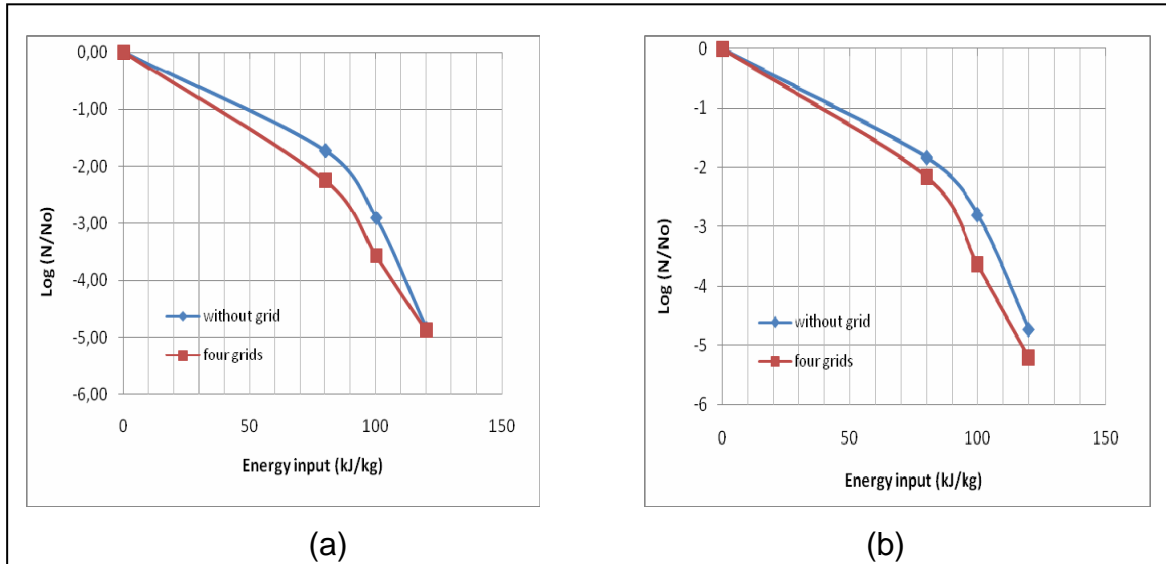


**Figure 4.41** Inactivation of *E.coli* using a treatment chamber with four inserted grids in comparison with a treatment chamber without grid. Initial voltage of 15 (a) and 18 (b) kV. Ringer solutions at 2.3 mS/cm at a inlet temperature of 30°C.

As observed, the four grids have put the inactivation forward, but there is not much difference in the treatment performed at 130 kJ/kg. Also, there is no difference in the inactivation rate between the treatment performed at 15 and 18 kV. This may be within voltage ranges where there is no difference in the impact on the microbial inactivation. For the treatment chamber without grid at 15 kV, the average electric field strength is 25.65 kV/cm, whereas with an initial voltage of 18 kV, the average electric field strength is 30.78 kV/cm. In other words between 25.65 and 30.78 kV/cm there is no difference in the microbial inactivation. On the other hand it is possible that other variables have had an influence in this experiment. For example, the frequency for the experiment at 15 kV has been 90 Hz and for the experiment at 18 kV only 50 Hz (for 130 kJ/kg).

Under these conditions it is difficult to set standards to compare between the experiments, as frequency influence eventually superposes other effects (see Table 4.3 where the parameters are presented).

The following graphics (Figure 4.42) show the same experiment using *L. rhamnosus*.

**Table 4.22** Parameter used for a treatment chamber with four inserted grids in comparison with a treatment chamber without grid.

	treatment at 18 kV			treatment at 15 kV		
T outlet [°C]	33	35	39	33	35	39
Frequency [Hz]	41	45	49	55	61	65
Epulse [J/pulse]	2.06	2.08	2.1	1.54	1.54	1.59
Energie input [kJ/kg]	60	68	74	60	68	74
treatment chamber	without grids	four grids		without grid	four grids	
pulse width [ $\mu$ s]	3.7	3		3.7	3	

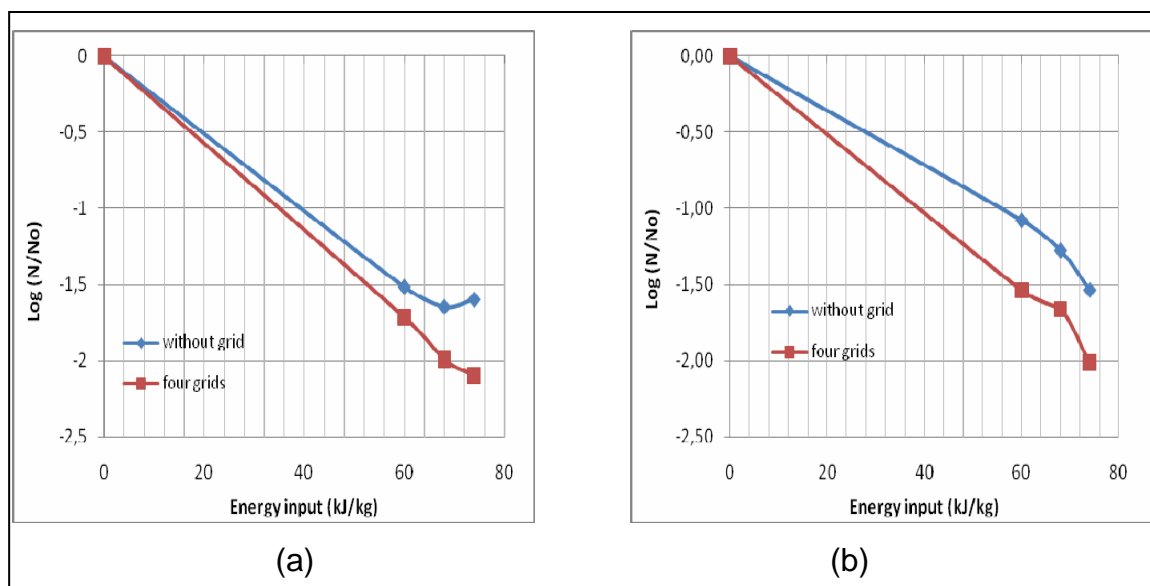


**Figure 4.42** Inactivation of *L. rhamnosus* using a treatment chamber with four inserted grids in comparison to a treatment chamber without grid.

Initial voltage of 15 (a) and 18 (b) kV. Ringer solution at 2.3 mS/cm and inlet temperature 20°C.

As observed, the four grids impact appears to be better for the inactivation. There is a noticeable difference in the voltage range between 15 and 18 kV/cm. This means, that *L. rhamnosus* is more sensible to the voltage changes in this range.

#### 4.2.6.3 Impact on enzyme inactivation due to the insertion of grids in the treatment chamber

The insertion of grids in the treatment chamber under well defined conditions has an impact on the microbial inactivation. The reason for this success is possibly due to the electric field strength increment and/or due to fluid mixture that is generated. As a further step, it is interesting to study the impact of the grids insertion on the enzyme inactivation.

The experiments of inactivation of phosphatase in row milk were performed using a treatment chamber with two grids made of insulated material and four grids made of metal in comparison to a treatment chamber without grids. The following graphic shows the enzyme inactivation.

**Table 4.23** Parameter used for a treatment chamber with four inserted grids, two insulator grids and a treatment chamber without grid.

	treatment at 18 kV		
T outlet (°C)	52	56.7	61.2
Frequency (Hz)	68	82	96
Epulse (J/pulse)	3.67	3.73	3.79
Energie input (kJ/kg)	90	110	130
treatment chamber	without grid	Insulator grid	four grids
pulse width (µs)	2.4	3.5	3

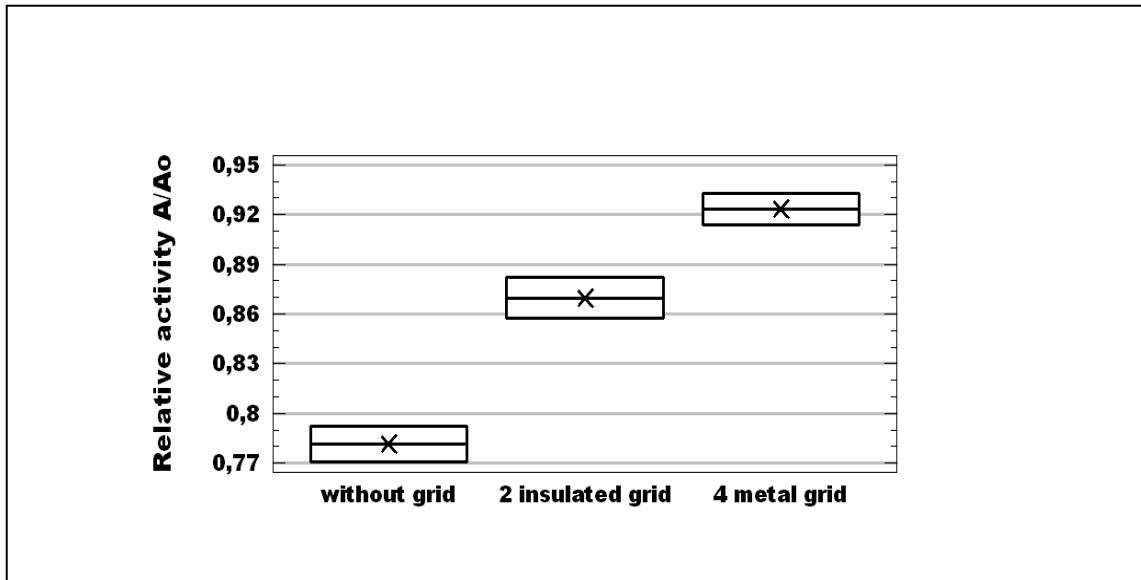


**Figure 4.43** Impact of the grids insertion on the enzyme inactivation. Experiment performed in raw milk at an inlet temperature of 30 °C.

As observed, there is a noticeable difference in the enzyme inactivation (95 % confidence with  $p = 0.0063$ ). The grids insertion improved the conservation of the enzyme activity. This is possible because the grids produced turbulences and a better mixing of the fluid. Therefore the enzymes exposed usually to high local temperature are less affected as mixing provides rapid reduction of high local temperature. In the vicinity of the insulator zone the temperature is locally very high (local maximum temperatures of 100°C are reached in many cases), and this can be avoided by a better fluid mixing.

#### 4.2.7 Temperature distribution in the PEF treatment chamber

Although the PEF treatment is a non-thermal food processing technology, there is a significant temperature increase during PEF treatment due to Ohmic heating. Many authors, Bosch *et al.*, 2002, , Fiala *et al.*, 2001, Gerlach *et al.*, 2008, Lindgred *et al.*, 2002, have described the temperature distribution in a PEF treatment chamber. They acknowledged that during PEF treatment, it is

possible to reach temperatures of 100 – 120 °C in zones near to the insulators; these temperatures are only detected through mathematical calculations. It is almost impossible to measure the temperature exactly in the small zones where the peak electric field is, because any measuring devices would interfere in the flow regime, so that it is only possible to measure overall temperature at a definite distance. Many authors use “virtual temperatures” of up to 100 °C as a limit to perform their experiments. However, these local temperatures only exist for a very short period of time of less than 2 seconds.

The increment of temperature in the treatment chamber used in this work is described in the following section.

In the present work two different conductivity values have been used. The temperature increment due to Ohmic’s heating is strongly related to conductivity. A graphic is shown that describes temperature increment due to fluid conductivity.

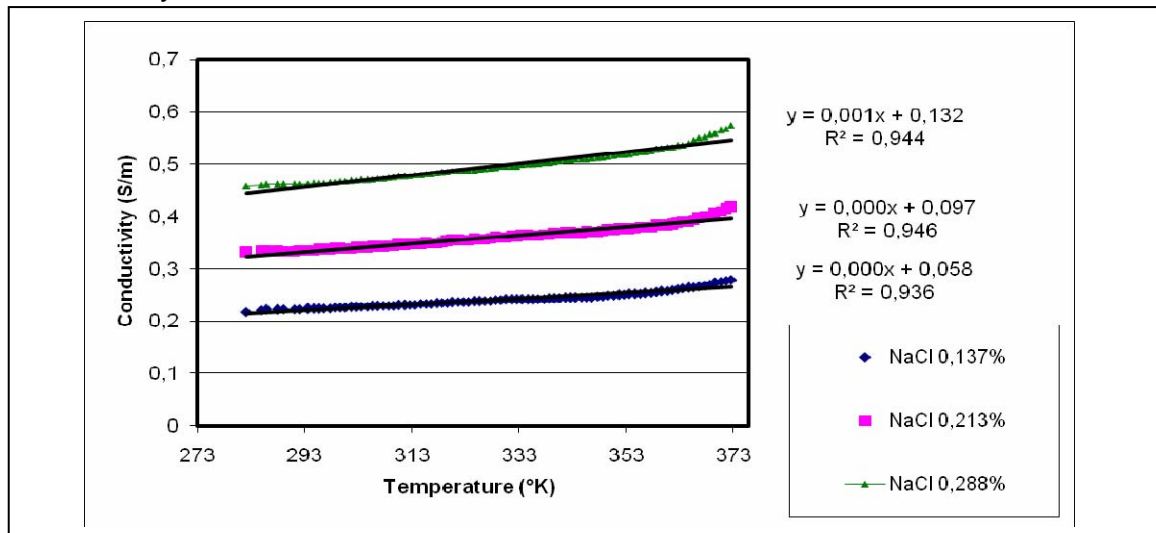


**Figure 4.44** Electrical conductivity as function of the temperature.

The following graphic shows the temperature increment in a PEF treatment as a function of the pulse frequency and conductivity, the latter as a function of temperature.

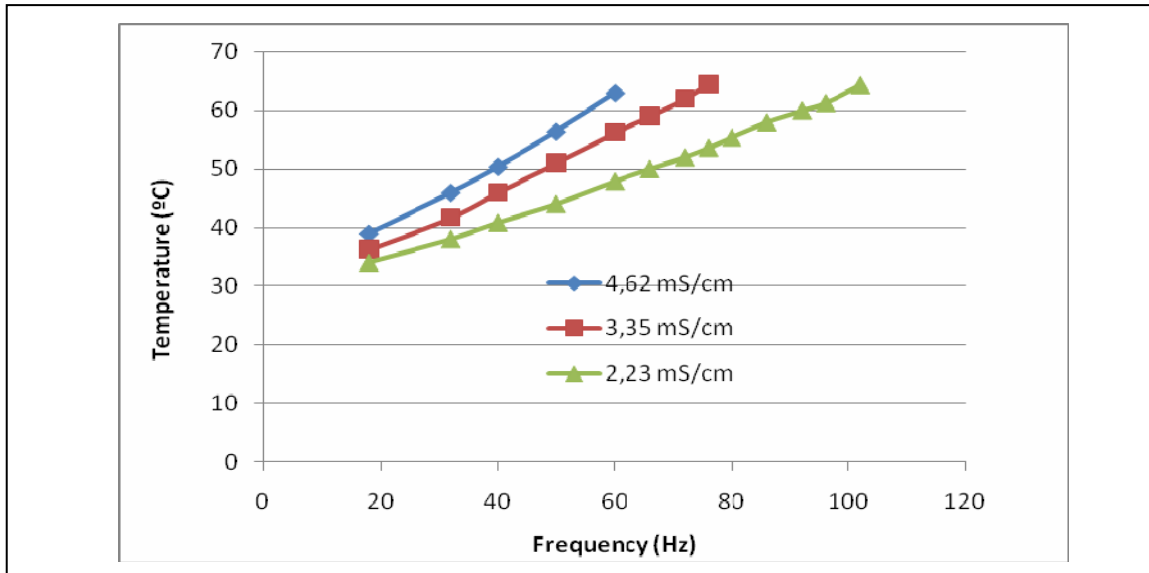


**Figure 4.45** Temperature increment as function of frequency and conductivity. Average temperature measured at 3.5 cm after the 2<sup>nd</sup> insulator.

As expected, the maximum temperature increase is achieved at higher conductivity. This is because at higher conductivity a higher quantity of current can flow and therefore the energy per pulse is increased and more energy is dissipated as heat into the liquid.

The following graphic shows the temperature profile as function of radial coordinate, as obtained by mathematical simulation.

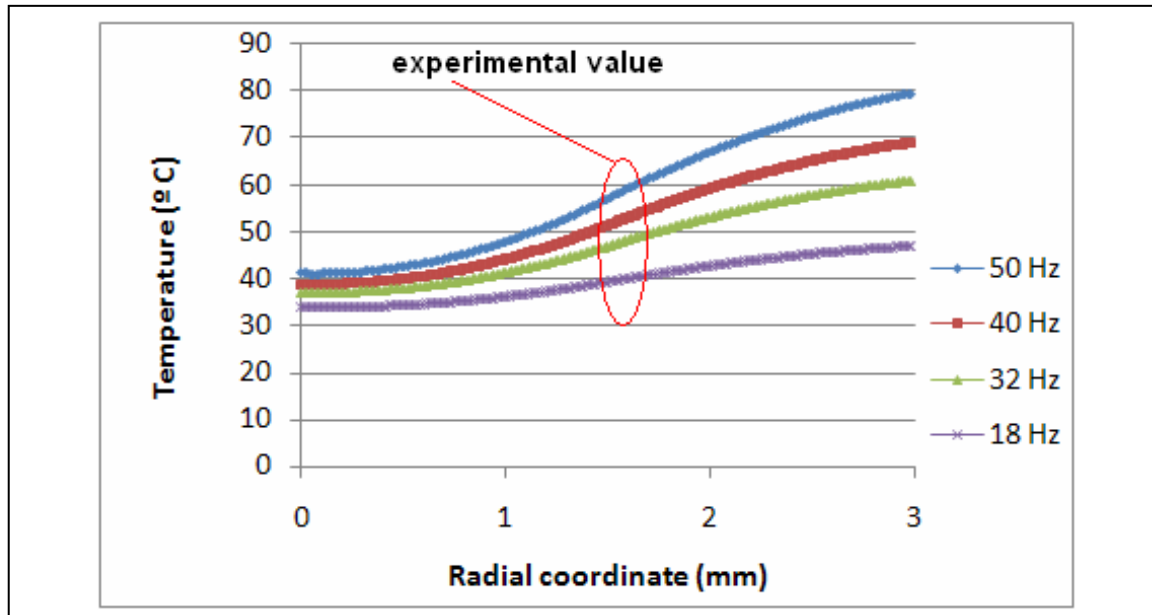


**Figure 4.46** Temperature as a function of radial coordinate at 3.5 cm after the 2<sup>nd</sup> insulator. Experiment with an initial voltage of 18 kV and a conductivity of 4.62 mS/cm as a function of the temperature.

The temperature was measured with an optic fiber thermometer inserted into the treatment chamber. It was located 1.45 mm from the electrode wall and 3.5 cm after the 2<sup>nd</sup> insulator. The simulated temperature corresponded to the same coordinate in all of the cases.

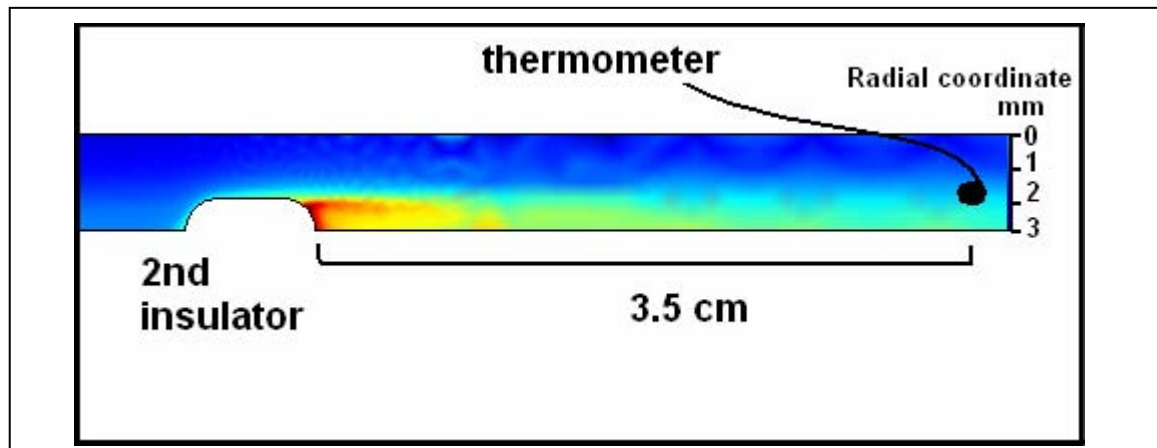


**Figure 4.47** Position of thermometer in treatment chamber.

As observed, the average temperature is 50 °C, but there exists a maximum temperature of 80 °C. In the following figure the temperature profile on the 2<sup>nd</sup> insulator is shown.

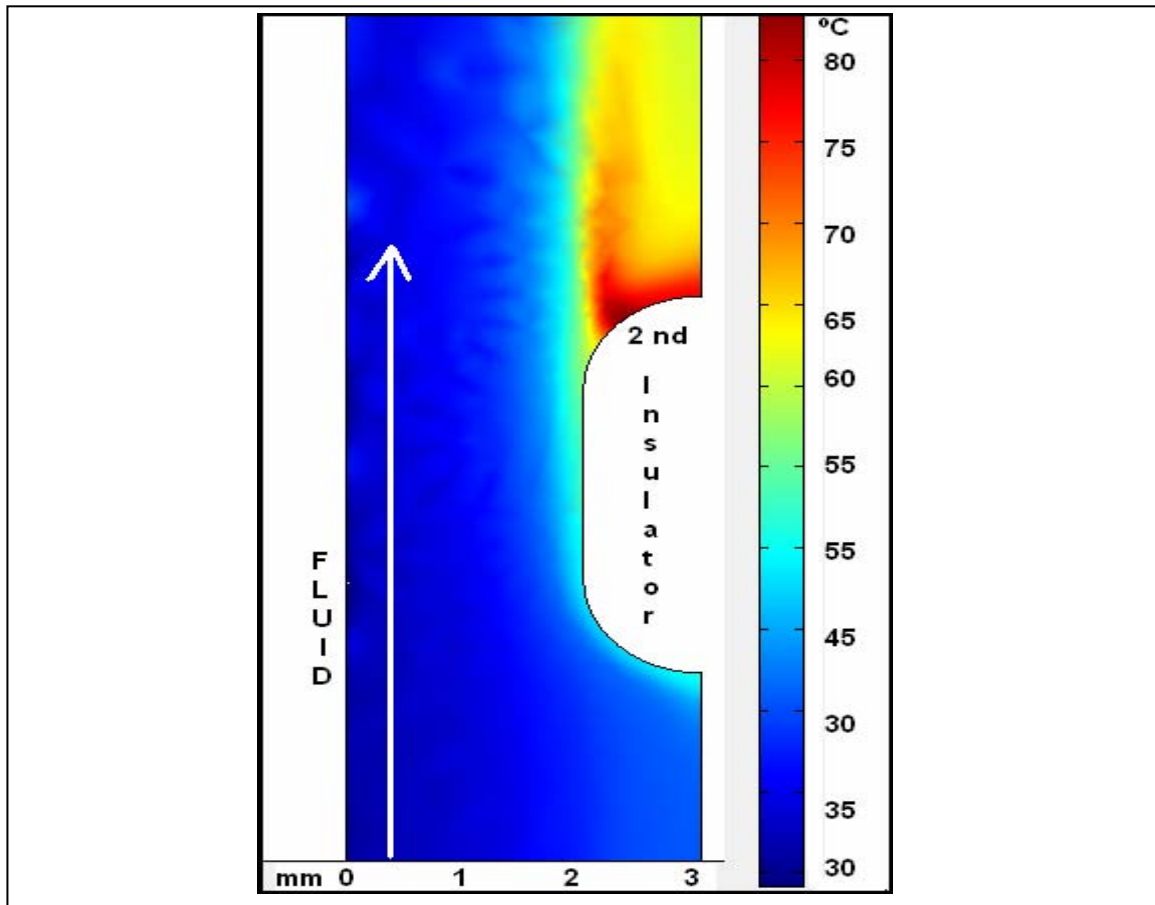


**Figure 4.48** Temperature contour along the 2<sup>nd</sup> insulator. Experiment with an initial voltage of 18 kV, frequency of 32 Hz and a conductivity (T) of 4.6 mS/cm.

As observed, the maximum temperatures are reached at the wall, there exists a long residence time due to the slowly moving fluid and therefore more energy dissipation takes place in a volume of product, thus a higher product temperature near the wall results.

These temperature peaks can be avoided through the presence of devices, as shown in the following figure.

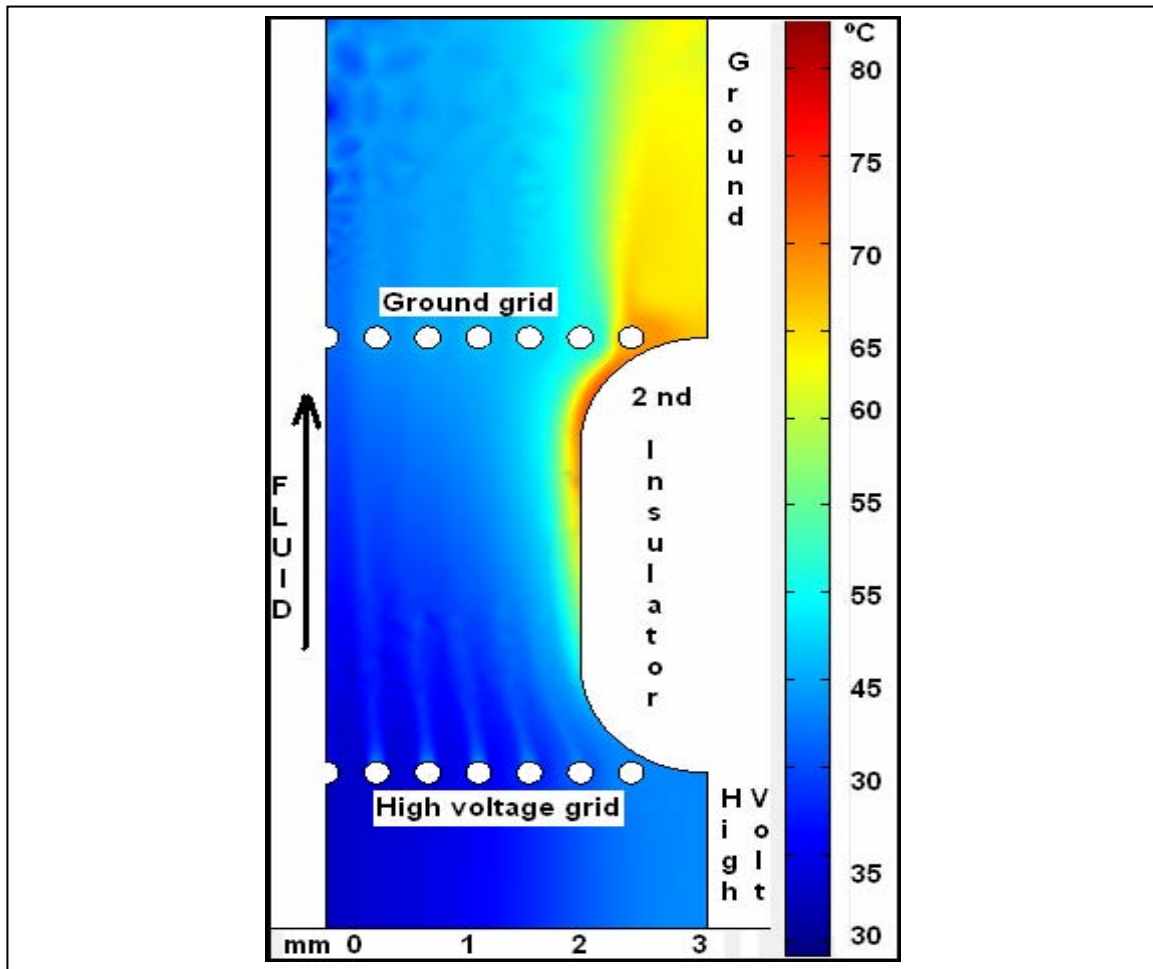


**Figure 4.49** Temperature contour along the 2<sup>nd</sup> insulator of the treatment chamber with inserted grids. Experiment with an initial voltage of 18 kV, frequency of 32 Hz and a conductivity (T) of 4.6 mS/cm.

The temperature distribution is altered by the presence of devices, as observed; the distribution is more homogenous and the maximal temperature is lower, but the average temperature at 3.4 cm after the 2<sup>nd</sup> insulator is the same. This has a significant impact on the conservation of the enzyme activity and this can explain why the enzyme inactivation in previous experiments was lower in presence of grids.

## 5 Conclusions and Outlook

The simulation of PEF process with computational tools allows the design of adequate treatment chamber and serves to improve the efficacy of microbial inactivation and to avoid food over-processing.

The results of modelling show how an adequate treatment chamber design can increase the electric field strength, resulting in an increase of microbial inactivation. The gained improvement of microbial inactivation was in the range of one log cycle under the operating conditions.

The microbial inactivation due to increment of flow velocity shows that it is advisable to perform experiments at high flow rates with created turbulences.

Important factors to achieve an increment in microbial inactivation are the number of pulses that each liquid volume receives and the medium conductivity; obtaining higher microbial inactivation when the frequency of the pulses is high and the medium conductivity is low, considering the same energy input.

The insertion of grids in the electric field zone produces a homogeneous and more intense electric field. On the other hand, the insertion of grids produces turbulences at relative low flow velocities, which produces a more homogeneous treatment and also increases the microbial inactivation. Furthermore, the generated turbulence produces a fluid mixing, avoiding the high temperatures generated in the zone near the insulators and leads to a more homogeneous temperature distribution in the treatment chamber. The latter has an important impact on the enzyme activity conservation, for example, alkaline phosphatase inactivation is reduced from 20% to 5%. It could be shown that higher activation of up to 65% only occurs when treatment temperature is not kept under control or cooling system is inappropriate.

A more detailed study about the PEF impact on alkaline phosphatase to extend the work would include: To perform experiments in continuous system with exponential pulses and in batch system with square pulses to exclude

possible pulse shape effects when comparing batch and continuous system as done in this work. To measure the local pH change that exists near the electrodes during a PEF treatment. In the case of temperature model it would be ideal to measure the temperature distribution in the treatment chamber, thereby an optimal phosphatase thermal inactivation model could be developed. And it is also necessary to develop an Ohmic heating model in batch system with exponential decay pulse which could not be accomplished in this work.

The microbial inactivation in the treatment chamber, was studied under inhomogeneous electric field distribution at low and relative high frequency. It is recommended to study the impact of high frequency also in homogeneous electric field.

Due to the treatments performed at high flow velocity it is of certain interest to study the following:

- The impact of higher flow velocities on the microbial inactivation.
- Determination of the exact velocity in which the charged particles flow to the electrode surface, to study the influence of higher flow rates superimposing this particle movement, and finally determine the effect of a probably lower accumulation of charged particles on the electrode surface.

Due to the study of the grids insertion in the treatment chamber, it is still necessary to analyse the effect on microbial inactivation, temperature distribution and electric field strength distribution when the following factors are changed:

- Density of grids, place of the grid in the treatment chamber, and the use of other materials (for example: semiconductors). In the case of a grid made of metal it is necessary to measure the metal release in the liquid sample as this might increase in comparison to traditional electrode configuration.

## SUMMARY

High intensity pulsed electric field (PEF) treatment was investigated with focus on the effectiveness of microbial inactivation and on the impact on milk alkaline phosphatase (ALP) activity.

Experiments were made in a laboratory scale, square wave pulse, co-linear treatment chamber configuration using a continuous flow-through PEF unit and a parallel plate batch system with exponentially decaying pulses.

The main focus of this work was to design a PEF treatment chamber that operates at high and homogeneous electric field strength intensities with limited increase in liquid temperature. The co-linear treatment chambers used have been modified by insertion of grids (made of metal or plastic) resulting in the formation of turbulences and in changes of the electric field strength distribution. The Finite Element Method (FEM) analysis showed that the electric field strength has been increased and was more homogeneous after the insertion of grids. Also the velocity profile improved and turbulence was more intense, which produces uniform treatment of each volume element. As result of this modification, the liquid temperature was decreased, the microbial inactivation was increased and the inactivation of heat sensitive alkaline phosphatase (ALP) was reduced.

A mathematical comparison of the thermal exposure during PEF treatment and the thermal stability of the enzyme was used as a capable tool to distinguish between pulsed electric field and thermal effects on the ALP activity. It was observed that only a minor part of the inactivation was related to electric field effects.

Finally, a model was developed that couples the electric field, heat transfer and fluid dynamics analysis. The predicted product temperatures downstream of the treatment chamber were in good agreement with the observed temperature for a range of conditions considered.

## RESUMEN

En el presente trabajo se estudiaron Tratamientos de Campos de Pulsos Eléctricos de Alta Intensidad (PEF) enfocado en la efectividad de la inactivación de microorganismos y el impacto sobre la actividad de la fosfatasa alcalina (ALP).

Los experimentos fueron realizados a escala de laboratorio, utilizando una cámara de tratamientos continua, co-linear de pulsos cuadráticas y una cámara de placas paralelas batch de pulsos exponencial.

El objetivo principal de este trabajo fue diseñar una cámara de tratamientos PEF capaz de producir intensidades de fuerza de campo eléctrico altas y homogéneas y reducir el incremento de temperatura en el líquido. La cámara de tratamientos co-linear usada fue modificada mediante la inserción de grillas, lo cual produjo la formación de turbulencias y cambios en la fuerza del campo eléctrico. Análisis de Elementos Finitos (FEM) mostraron que la fuerza del campo eléctrico ha sido incrementada y más homogénea al insertar las grillas. Además, el perfil de velocidades mejoró y la turbulencia más intensa, lo cual permite un tratamiento más uniforme para el alimento. Como resultado de esta modificación, la temperatura del líquido disminuyó, aumentó la inactivación microbiana y disminuyó la inactivación de la fosfatasa alcalina.

Se utilizó una comparación matemática entre la exposición térmica durante el tratamiento PEF y la estabilidad térmica enzimática como una herramienta para distinguir entre el efecto producido por el campo de pulsos eléctricos y la temperatura en la actividad de ALP. Se observó que solo una menor parte de la inactivación se relaciona al efecto de los campos de pulsos eléctricos.

Finalmente, se desarrolló un modelo para acoplar análisis de campo eléctrico, transferencia de calor y dinámica de fluidos. Las temperaturas predichas por el modelo y las experimentales concordaron estrechamente en un rango de condiciones determinadas.

## REFERENCES

- Alkhafaji, S.R. and Farid, M. 2006. An investigation on pulsed electric fields technology using new treatment chamber design. *Innovative Food Science and Emerging Technologies*, doi:10.1016/j.ifset.2006.11.001
- Barbosa-Cánovas, G.V., Góngora-Nieto, M.M., Pothakamury, U.R. and Swanson, B.G. 1999. *Preservation of foods with pulsed electric fields. Food science and technology*. San Diego: Academic Press.
- Barsotti, L., Merle, P., & Cheftel, J.C. 1999a. Food processing by pulsed electric fields:1. Physical effects. *Food Reviews International*, 15(2), 163 – 180.
- Barsotti, L., Merle, P. and Cheftel, J. C. 1999b. Food processing by pulsed electric fields: 2. Biological effects. *Food Reviews International* 15(2): 181 – 213.
- Bendicho, S., Barbosa-Cánovas, G. V. and Martín, O. 2003. Reduction of Protease Activity in Milk by Continuous Flow High- Intensity Pulsed Electric Field Treatments. *Journal Dairy Science* 86: 697 – 703.
- Bertsch, A. J. 1983. Surface tension of whole and skim-milk between 18 and 135°C. *Journal of Dairy Research*, 50:259 – 267.
- Bosch, E. v.d., Morshuis, P., Smit, J. 2002. Temperature distribution in fluids treated by Pulsed Electric Fields. 14<sup>th</sup> International Conference on Dielectric Liquids. Graz, Austria.

- Bruhn, P.D. Pedrow, R.G. Olsen, G.V. Barbosa-Canovas, and B.G. Swanson. 1998. Heat conduction in microbes exposed to pulsed electric fields. *IEEE Trans. On Dielectrics and Electrical Insulation*, Vol. 5, No. 6:878 – 885.
- Bushnell, A.H., J.E. Dunn, R.W. Clark, and J.S. Pearlman. 1993. High pulsed voltage system for extending the shelf life of pumpable food products. U.S. patent 5,235,905.
- BVL (Bundesamt für Verbraucherschutz und Lebensmittelsicherheit). 1980. Amtliche Sammlung von Untersuchungsverfahren nach: 64 LFGB. Beuth Verlag GmbH. Berlin. Germany
- Castro, A. J., Barbosa-Cánovas, G. V. and Swanson B.G. 1993. Microbial inactivation of foods by pulsed electric fields. *J. Food Process. Preserv.* 17(1):47 – 73.
- Castro A. J, Swanson B G, Barbosa-Cánovas G V, Zhang Q H 2001a. “Pulsed electric field denaturation of bovine milk alkaline phosphatase activity”, in Barbosa-Cánovas G V and Zhang Q H, *Pulsed Electric Fields in Food Processing. Fundamental Aspects and Applications*, Lancaster, USA, Technomic Publishing Company Inc., 83 – 103.
- Castro A., Swanson B., Barbosa-Cánovas G. and Zhang Q.. 2001b. ‘Pulsed electric field modification of milk alkaline phosphatase activity’, in Barbosa-Cánovas G V and Zhang Q H, *Pulsed Electric Fields in Food Processing. Fundamental Aspects and Applications*, Lancaster, USA, Technomic Publishing Company Inc., 65-82.

- Castro, H., Marighetti, J., De Bortoli, M., Natalini, M. 2003. Modificación de la intensidad de turbulencia en el canal de aire de la UNNE. Argentina. Universidad Nacional del Nordeste.
- Chang, D. C., Chassy, B. M., Saunders, J. A. and Sower, A. E. 1992. Guide to electroporation and electrofusion. San Diego, Academic Press.
- Chen, W., and Lee, R. (1994). Altered ion channel conductance and ionic selectivity induced by large imposed membrane potential pulse. *Biophysics Journal*, 67, 603-612.
- Dimitrov, D.S. 1995. Electroporation and Electrofusion of Membranes. *Handbook of Biological Physics*, vol. 1. Elsevier Science B.V.
- COMSOL. 2005. COMSOL User`s Guide. COMSOL, Inc.
- Cook, N. 1973. On simulating the lower third of the urban adiabatic boundary layer in a wind túnel. *Atmos. Environ* 7:691 – 705.
- Cook, N. 1978. Wind Tunnel simulation of the adiabatic atmospheric boundary layer in a wind tunnel. *Amos. Environ* 3:197 – 214.
- Fiala, A., Wouters, P. C., van den Bosch, E. and Creyghton, Y. L. M. 2001. Coupled electrical-fluid model of pulsed electric field treatment in a model food system. *Innovative Food Science and Emerging Technologies* 2: 229 – 238.
- FLUENT. 2003. FLUENT User`s Guide. FLUENT, Inc.

- Fosset M., Chappelet-Tordo, D., Lazdunski, M. 1974. Intestinal alkaline phosphatase. Physical properties and quaternary structure. *Biochemistry* 13:1783 – 1788.
- Gerlach, D., Alleborn, N., Baars, A., Delgado, A., Moritz, J. & Knorr, D. 2008 Numerical simulations of pulsed electric fields for food preservation: A review. *Innovative Food Science and Emerging Technologies*, doi: 10.1016/j.ifset.2008.02.001
- Grahl T. and Märkl, H. 1996. Killing of microorganisms by pulsed electric fields. *Appl Microbiol Biotechnol.* 45:148 – 157.
- Hämäläinen, V. 2001. Implementing an explicit algebraic Reynolds stress model into the three-dimensional finflo flow solver. Helsinki University of Technology., Finland.
- Hass J., Behnlian, D. and Schubert , H.1996a. Determination of the Heat Resistance of Bacterial Spores by the Capillary Tube Method. I. Calculation of Two Borderline Cases Describing Quasi-isothermal Conditions. *Lebensm.-Wiss. u.-Technol.* 29:197 – 202.
- Hass J., Behnlian, D. and Schubert , H.1996a. Determination of the Heat Resistance of Bacterial Spores by the Capillary Tube Method. II — Kinetic Parameters of *Bacillus stearothermophilus* Spores. *Lebensm.-Wiss. u.-Technol.* 29:299 – 303.
- Heinz, V. and Knorr, D. 2000. Effect of pH, ethanol addition and high hydrostatic pressure on the inactivation of *Bacillus subtilis* by pulsed

electric fields. *Innovative Food Science and Emerging Technologies* 1: 151 – 159.

Heinz, V., Alvarez, I., Angersbach, A. und Knorr, D. 2002. Preservation of liquid foods by high intensity pulsed electric fields-basic concepts for process design. *Trends in Food Science and Technology*, Band 12, 103 – 111.

Hetrick, H., Tracy, P. 1990. Effect of High-Temperature Short-Time Heat Treatments on some properties of milk. University of Illinois, USA.

Ho, S. Y., Mittal, G. S., Cross, J. D., Griffiths, M. W. 1995. Inactivation of *Pseudomonas fluorescens* by high voltage electric pulses. *J. Food Sci.*60:1337 – 1340.

Ho, S., and Mittal, G. S. 2000. High voltage pulsed electrical field for liquid food pasteurization. *Food Reviews International*, 16(4):395 – 434.

Hofmann, G. A. and Evans, G. A. 1986. Electric genetic-physical and biological aspects of cellular electromanipulation. *IEEE Eng. Med. Biol.* 5:6 – 25.

Hsu, H. Muñoz, P., Barr, J., Oppliger, I., Morris, D., Vaananen, H., Tarkenton, N., Anderson, H. 1985. Purification and partial characterization of alkaline phosphatase of matrix vesicles from fetal bovine epiphyseal cartilage. Purification by monoclonal antibody affinity chromatography *J. Biol. Chem.* 260:1826 – 1831.

- Hülshager, H., Potel, J. and Niemann, E. G. 1981. Killing of bacteria with electric pulses of high field strength. *Radiation and Environmental Biophysics* 20:53 – 65.
- Hülshager, H., Potel, J. and Niemann, E. G. 1983. Electric field effects on bacteria and yeast cells. *Radiation and Environmental Biophysics* 22:149 – 162.
- Jacob, H. E., Förster, W. and Berg, H. 1981. Microbiological Implications of electric field effects. II. Inactivation of yeast cells and repair of their envelope. *Zeitschrift für Allgemeine Mikrobiologie* 21(3): 225-233.
- Jayaram, S., and Castle, G. S. P. 1992. Kinetics of sterilization of *Lactobacillus brevis* cells by the application of high voltage pulses. *Biotechnology and Bioengineering*, 40:1412 – 1420.
- Jayaram, S., Castle, G. S. P. and Magaritis, A. 1993. The effect of high field DC pulse and liquid medium conductivity on survivability of *L. brevis*. *Applied Microbiology and Biotechnology*. 40: 117 – 122.
- Jeanet., R., Baron, F., Nau, F., Roignant, M., and Brule, G. 1999. High intensity pulsed electric fields applied to egg white: effect on *Salmonella enteritidis* inactivation and protein denaturation. *J. Food Protect.* 62:1088 – 1096.
- Jeyamkondan, S., Jayas, D. S. and Holley, R. A. 1999. Pulsed electric field processing of foods: a review. *Journal of Food Protection* 62(9): 1088 – 1096.

- Kinosita, K. J. and Tsong, T. Y. 1979. Voltage- induced conductance in human erythrocyte membranes. *Biochim. Biophys. Acta.* 554:479 – 497.
- Latner A., Parsons M. and Skillen AW. 1971. Isoelectric focusing of alkaline phosphatases from human kidney and calf intestine. *Enzymologia.* 31;40(1):1 – 7.
- Lelieveld H. L. M., Notermans, S. and de Haan S. W. H. 2007. Food preservation by pulsed electric fields. Cambridge, Woodhear Publishing.
- Lindgren, M., Aronsson, K., Galt, S. And Ohlsson, T. 2002. Simulation of the temperature increase in pulsed electric field (PEF) continuous flow treatment chambers. *Innovative Food Science & Emerging Technologies*, 3:233 – 245.
- Martín, O., Vega-Mercado, H., Qin, B. L., Chang, F. J., Barbosa-Cánovas, G. V. and Swanson, B. G. 1997. Inactivation of *Escherichia coli* suspended in liquid egg using pulsed electric fields. *Journal of Food Processing and Preservation.* 21:193 – 203.
- Martín, O., Zhang, Q., Castro, A. J., Barbosa-Cánovas, G. V., and Swanson, B. G. 1994. Pulsed electric fields of high voltage to preserve foods. Microbiological and engineering aspects of the process. *Spanish J. Food Science Technology*, 34:1 – 3.

- Mertens, B., & Knorr, D. 1992. Developments of non-thermal processes for food preservation. *Food technology*, 46:124 – 133.
- Mizuno, A. and Hori, Y. 1988. Destruction of living cells by pulsed high-voltage application. *IEEE Trans. Ind. Appl.* 24(3): 387 – 394.
- Morren, J., Roodenburg, B., and Han, S. W. H. D. 2003. Electrochemical reactions and electrode corrosion in pulsed electric field (PEF) treatment chambers. *Innovative Food Science & Emerging Technologies*, 4(3):285 – 295.
- Ohshima, T., Tamura, T. and Sato, M. 2006. Influence of electric field on various enzyme activities. *Journal of Electrostatics* 65: 156 – 161.
- Pataro, G. 2004. The utilization of pulsed electric fields in food stabilization. University of Salerno. Salerno, Italy.
- Peleg, M. 1995. A model of microbial survival after exposure to pulsed electric fields. *Journal of Science of Food and Agriculture* 67: 93 – 99.
- Perez, O. E. and Pilosof, A. M.R. 2004. Pulsed electric fields effects on the molecular structure and gelation of  $\beta$ -lactoglobulin concentrate and egg white. *Food Res Int.* 37:102 – 110.
- Pothakamury, U. R., Vega Mercado, H., Zhang, Q. H., Barbosa-Cánovas, G. V. and Swanson, B. G. 1996. Effect of growth stage and processing temperature on the inactivation of e-coli by pulsed electric fields. *Journal of Food Protection*, 59(11):1167 – 1171.

- Qin, B.-L., Zhang, Q., Barbosa-Cánovas, G. V., Swanson, B. G. and Pedrow, P. D. 1994. Inactivation of microorganisms by pulsed electric fields of different voltage waveforms. *IEEE Transactions on Dielectrics and Electrical Insulation* 1(6): 1047 – 1057.
- Rogers, H. J., Perkins, H. R. and Ward, J. B. 1980. *Microbial Cell Walls and Membranes*. London, Chapman&Hall.
- Sale, A. J. and Hamilton, W. A. 1967. Effect of high electric fields on microorganisms. I. Killing of bacteria and yeast. II. Mechanism of action of the lethal effect. *Biochimica Biophysica Acta* 148: 781 – 800.
- Sanders, G., and Sagem, O. 1947. Phosphatase Test for Various Dairy Products. *J.Dairy Sei.*, 30: 909 – 920.
- Schoenbach, K. H., Peterkin, F. E., Alden III, R. W., and Beebe, S. J. 1997. The effect of pulsed electric fields on biological cells: Experiments and applications. *IEEE Transactions on Plasma Science*, 25, 284 – 292.
- Sitzmann, W. 1995. High voltage pulse techniques. New methods for food preservation. G. W. Gould. London, Graham & Hill.
- Smith, E. A., Zhang, Z., Thomas, C.R., Moaxam, K.E., and Middelberg, A.P.J. 2000. The mechanical properties of *Saccharomyces cerevisiae*. *PNAS*, 97:9871 – 9874.
- Stanley, D. W. 1991. Biological membrane deterioration and associated quality losses in food tissues. *Critical Reviews in Food Science and Nutrition*. F. M. Clydesdale. New York, CRC Press.

- Tiaab, W., Smith, L. 1980. Some properties of Alkaline Phosphatase of milk. University of Alberta. Edmonton, Canada.
- Toepfl, S., 2006 Pulsed Electric Fields (PEF) for Permeabilization of Cell Membranes in Food and Bioprocessing - Applications, Process and Equipment Design and Cost Analysis. Dissertation, Technical University of Berlin. Germany.
- Tsong, T. Y. 1990a. Voltage modulation of membrane permeability and energy utilization in cell. *Biosci. Rep.* 3:487 – 505.
- Tsong, T. Y. 1990b. Electrical modulation of membrane proteins: Enforced conformational oscillations and biological energy and signal transductions. *Annu. Rev. Biophys. & Chem.* 19:83 – 106.
- Van Loey A., Verachtert B. and Hendrickx M. 2002. Effect of high electric field pulses on enzymes. *Trends Food Sci Technol*, 12:94 – 102.
- Vassilev, P. M. and Tien, H.T. 1985. Planar lipid bilayer in relation to biomembranes. En: Benga, G. (ed.), *Structure and properties of cell membranes. Vol. III Methodology and properties of membranes.* Boca Raton: CRC Press. 64 – 94.
- Vega-Mercado, H., O. Martín-Belloso, B.L. Chang, A.J. Castro, G.V., Barbosa-Cánovas, and B.G. Swanson, 1996a. Inactivation of

*Escherichia coli* and *Bacillus subtilis* suspended in pea soup using pulsed electric fields. J. Food Proc. Pres. 20:501 – 510.

Vega-Mercado, H., Pothakamury, U. R., Chang, F.-J., Barbosa-Cánovas, G. V. and Swanson, B. G. 1996b. Inactivation of *Escherichia coli* by combining pH, ionic strength and pulsed electric field hurdles. Food Research International 29(2):117 – 121.

Vega-Mercado, H. 1996c. Inactivation of proteolytic enzymes and selected microorganisms in foods using pulsed electric field. Biological Systems Engineering. Pullman, WA. Washington State University. USA.

Waschipky, H., & Zschörnig, O. 2005. Electroporation of human erythrocytes and erythrocyte ghosts. Leipzig University. Germany.

Weaver, J.C. 2000. Electroporation of cells and tissues. IEEE Transactions on Plasma Science, 28(1):24 – 33.

Wilinska, A., Bryjak, J., Illeová, V. and Polakovic, M. 2007. Kinetics of thermal inactivation of alkaline phosphatase in bovine and caprine milk and buffer. International Dairy Journal 17:579 – 586.

Wouters, P. 2001. Pulsed Electric Field Inactivation of Microorganisms. Berlin University of Technology. Germany.

Wouters, P.C., Bos, A.P. and Ueckert, J. 2001. Membrane permeabilization in relation to inactivation kinetics of *Lactobacillus* species due to pulsed electric fields. Applied and Environmental Microbiology, 67:3092 – 3101.

- Zamankhan, P., Ahmadi., G., Fan., F. 2004. Coupling effects of the flor and electric fields in electrostatic precipitators. *Journal Applied Physics* 96(12).
- Zhang, Q., Barbosa-Cánovas, G. V. and Swanson, B. G. 1995. Engineering aspects of pulsed electric field pasteurization. *Journal of Food Engineering* 25:261 – 281.
- Zimmermann, U., Pilwat, G. and Riemann, F. 1974. Dielectric breakdown in cell membranes. In: *Biophysical Journal.*, Band 14:881– 899.
- Zimmermann, U., Pilwat, G., Beckers, F. and Riemann, F. 1976. Effects of external electrical fields on cell membranes. *Bioelectrochemistry Bioenergetics* 3: 58 – 83.
- Zimmermann, U. 1986. Electric breakdown, electropermeabilization and electrofusion. In: *Rev. Physiol. Biochem. Pharmacol.*, Band 105:175 – 256.